Series in Plasma Physics

Reaction–Diffusion Problems in the Physics of Hot Plasmas

Hans Wilhelmsson

Chalmers University of Technology, Göteborg, Sweden

Enzo Lazzaro

Istituto di Fisica del Plasma ''P Caldirola'', Consiglio Nazionale delle Ricerche, Milan, Italy

IoP
Institute of Physics Publishing
Bristol and Philadelphia

British Library Cataloguing-in-Publication Data

A catalogue record for this book is available from the British Library.

ISBN 0 7503 0615 7

Library of Congress Cataloging-in-Publication Data are available

Commissioning Editor: John Navas
Production Editor: Simon Laurenson
Production Control: Sarah Plenty
Cover Design: Frederique Swist
Marketing Executive: Colin Fenton

Published by Institute of Physics Publishing, wholly owned by
The Institute of Physics, London

Institute of Physics Publishing, Dirac House, Temple Back,
Bristol BS1 6BE, UK

US Office: Institute of Physics Publishing, The Public Ledger Building,
Suite 1035, 150 South Independence Mall West, Philadelphia, PA 19106, USA

Typeset by the Alden Group, Oxford.
Printed in the UK by Bookcraft, Midsomer Norton, Somerset

Dedication

To Mariarosa, Anna and Andrea

Enzo Lazzaro

To my wife Julie and to the future of all our children and grandchildren

Hans Wilhelmsson

Contents

Preface

The points of view and the methods developed in this book are oriented to the non-linear evolution in space and time of plasmas where diffusion and reaction processes occur simultaneously. Applications are presented for some paradigmatic problems of fusion plasmas that are examples of self-organization of a complex system. In this sense, the material presented may be interesting beyond the particular examples illustrated, encompassing phenomena met in a variety of fields, such as chemistry, biology, meteorology, economics and the evolution of populations.

The analytical results, which are often relatively simple, have been benchmarked by extensive numerical calculations. The investigations show how experience and knowledge gained from studying simple cases (exact particular solutions of non-linear equations) can be used in extended forms for describing more complicated and more realistic situations encountered in practice.

The book should be of interest to advanced undergraduate and graduate students, and teachers involved in plasma physics in university courses, as well as to scientists doing active research, with an open mind to approaching problems from often unconventional points of view.

The reader should have a basic knowledge of plasma physics and elementary electrodynamics.

Early phases of this work started at Chalmers University of Technology, Göteborg, in Sweden. The most extensive parts of the research on which the book is based were, however, developed at the École Polytechnique at Palaiseau (Paris) and at the Université de Paris 7 when one of the authors (HW) held a visiting professorship, co-sponsored by the Fondation de France. Finally the concepts, based on the previous work, matured through a collaboration between the authors at the Istituto di Fisica del Plasma ''P Caldirola'' in Milan. Our most sincere thanks are due to the Director of the institute, Professor Giampietro Lampis, for his continuous encouragement and support.

The very generous and skilful help of Professor Marie-Noel LeRoux at the University of Bordeaux, Talence, with the numerical simulations is gratefully acknowledged, as well as the contributions of calculations by Drs B Etlicher

(Éc. Pol., Paris), H-G Gustavsson (Chalmers) and for the early phases of the work, M Benda (Chalmers).

Drs S N Dimova and D P Vasileva (Sofia, Bulgaria) kindly allowed us to use the results of their research on spiral waves in chapter 4.

It is also a pleasure for us to thank Dr Paola Mantica (IFP, Milan) for allowing us to include new experimental results on the propagation of a temperature pulse that changes sign (chapter 10).

In the text, a section on travelling wave solutions of non-linear diffusion equations (chapter 10) owes much to recent interesting investigations by Dr Julio Herrera (Mexico City) and co-authors.

The collaboration with Professor R Jancel (Univ. de Paris VII), especially on fundamental aspects related to the ''Painleve' test'' has been a great stimulation and is gratefully acknowledged.

Professor J Weiland (Chalmers) has provided throughout the work unfailing support and encouragement which has always been greatly appreciated.

To all of those not mentioned here, who have contributed in various ways to the completion of this work, go our most sincere thanks.

Introduction

The physics of plasmas and thermonuclear fusion encompasses basic problems in the universe and promises applications for the production of energy on earth.

It is of overall importance and it is linked to the most fundamental problems of non-linear science. A large part of this field can be described by reaction–diffusion processes, which account for the simultaneous non-linear effects of heating, diffusion and losses. In laboratory experiments, a combination of these processes is decisive for the net behaviour of the plasma. In particular, the problems of existence, accessibility and approach to possible equilibria can be studied by means of phase space description.

The analytical and computer simulation techniques developed in this context are of great interest also in other branches of science.

A major part of this book is therefore devoted to the special characteristics of reaction–diffusion processes, which may occur in space plasmas as well as in laboratory plasmas.

The reaction process is always a non-linear process involving at least two species. Examples are the alpha particle generation by thermonuclear reactions in a confined plasma and the loss of electrons by recombination with ions or attachment to neutrals, e.g. in ionospheric plasmas; the higher the densities are, the higher are the interaction rates.

Diffusion can occur as a fundamental transport process as a result of Coulomb collisions of magnetically confined charged particles or simply due to collisions with neutral particles. The tendency is to take particles away from regions of high concentration and a basic problem is to test and establish under which circumstances equilibrium is possible under the effect of competing processes.

The challenge and fascination of plasma physics is that it requires great insight in formulating the relevant problems and great ingenuity and flexibility in choosing the mathematical (and experimental!) tools to treat them. It is not by chance that the more significant contributions to the present status of knowledge of plasma physics has been given by scientists who coupled a very solid formal background education to great ingenuity in approaching problems often from unconventional points of view.

This appears all the more unavoidable since even the simplest model of plasma is that of a non-linear dynamical system with far too many degrees of freedom to be treated exactly. Naturally the reliability of a model and of its techniques is judged on the score of its success in its interpretative and predictive ability. Feedback improves the model and therefore the understanding.

The robustness of the models and the methods obtained could be measured, according to some procedure. Essentially it means that the dependent (response) variables of the model have bounded variation for bounded variation of the physical data and bounded variation for changes of accuracy of the numerical technique (e.g. stability with respect to changes of integration step size). These obvious requirements are not so often guaranteed over wide parameter ranges, even with modern numerical methods and powerful computers.

The evolution and thermal equilibrium of a thermonuclear plasma assumed to be in a successfully controlled confinement condition is formally considered here within the framework of a reaction–diffusion process, albeit with important peculiarities.

The basic elements for the description of such an evolution would, in fact, be a non-linear source term accounting for heating by, e.g., alpha particles, neutral beams or HF radiation. The diffusion would, in this case, correspond to the temperature conduction, in a broad sense. In more realistic situations, the diffusion of particles and temperature are coupled processes and even the crudest model consists of a problem of coupled partial differential equations (PDE). The theoretical and experimental research in plasma physics still falls somewhat short of providing the ultimate formulation of the transport processes, but it is worthwhile taking advantage of interdisciplinary know-how to procure the methods to analyse the fundamental effects, which at least should be expected *also* in a reacting plasma environment.

In this text, we examine a number of techniques which have proved useful in addressing problems with many degrees of freedom and reduce them to a tractable number of 'global' variables of direct physical significance. Their dynamics is ruled by coupled non-linear ordinary differential equations (ODE), obtained by transformation from the original PDE. To help the reader to become familiar with the particular examples presented here, which are taken from a wide range of physical problems, introductory sections on the basic derivation of the relevant equations are given, in chapters 1–3. Also succinct but hopefully useful summaries of the relevant mathematical procedures are given to make the presentation self-sufficient. Of course, the interested reader is referred to specialized texts for more rigorous and in-depth treatment. In particular, the material presented in chapter 2 is meant to provide a link between the derivation of fluid plasma description and the form of evolution equations with strong non-linear sources and sinks, which is the focus of a large part of this book.

A reduced variable technique, the central expansion method, which has strong links with similarity transformation techniques, has been introduced and

applied to many cases of interest and supplemented by computer simulations that validate it.

This description, when possible, presents the advantage of a direct analysis with phase space methods, similarity transformations and other useful algebraic manipulations. We select a number of demonstrative problems of mathematical physics that can be related to plasma phenomena, with some original results of interest *per se* and for the methods used.

An interesting example of its possibilities is presented, almost as a corollary, in chapter 6 where scaling laws are obtained for the energy confinement time in a magnetically confined plasma with additional (non-Ohmic) heating. The degradation of confinement with input power, in convincing agreement with experimental findings, turns out to be a simple property of the solutions of the power balance equation with non-linear sources and sinks.

To appreciate the material collected and presented here, it is necessary to recall that the *formulation* and the *solution* of a sensible physical problem rest in an essential way on *ordering* of the physical effects, represented by suitably weighted terms in the describing equations. Therefore, often, *approximate* solutions (to some order in a relevant parameter) of a realistic problem are better and more sensible than exact mathematical solutions that are out of physical ordering. This leads many physicists to get into the habit of looking for approximate solutions sometimes even when exact ones are at hand, and often to limit the analysis of a phenomenon to a linear approximation. On the other hand, the knowledge of properties of exact solutions of exemplary problems are an important guide for more realistic situations. Furthermore, an important property of exact solutions is to 'attract' all approximate ones; indeed a proper approximate must 'reach' the exact one when the parameters of the approximate form take the limiting values of the exact one. In chapter 3, the most significant types of formal solutions of reaction–diffusion equations are presented and discussed.

Reduced models of complex systems presented here, motivated from a general point of view in the introductory sections, turn out to be very useful in demonstrating a number of phenomena occurring in such a very complex system as a burning plasma. The reaction–diffusion equations, which are generally non-linear, are analysed here on the basis of the important class of similarity solutions (chapter 4, section 4.2). These are connected with the method of the 'central expansion' (chapter 4), which is a version of a method of continuous scale factors, descending from the general structure of similarity solutions. This '*ad hoc*' procedure simplifies considerably the treatment of complex problems from the very beginning, leading directly to formulations in terms of a reduced number of dynamical variables. Then phase space analysis becomes applicable to illustrate the evolution of even very complex systems.

The occurrence and the characteristics of explosive solutions in problems ruled by reaction–diffusion equations is analysed and examples are reported of the same type of solutions in problems of magnetohydrodynamic (MHD), and of non-linear wave interaction.

The formalism developed for non-linear wave coupling, chapter 8, gives another example of reduction of a system to a limited number of descriptive dynamical variables. An extension of the non-linear wave coupling in the domain of resistive MHD is presented, concerning the interaction of non-linear magnetic islands. Among other examples, some attention has been paid to non-linear heat propagation and travelling wave solutions of the heat transport equation, which may be connected with the results of recent experiments in tokamak plasmas (chapter 9, section 9.1). Among the most spectacular solutions of reaction–diffusion equations, the spiral structure solutions should be mentioned (see chapter 4 and section 4.3). They also can exhibit explosive features (chapter 7).

Problems of simultaneous reaction–diffusion processes are found in many other areas of science and life, such as chemistry, biology, medicine and economics. From the many applications of reaction–diffusion models, it may seem as if the most obvious examples come from chemistry. Clearly the chemical reactions occur at a rate that depends on the product of the concentrations of the molecular species participating in the reactions. The reaction products as well as the constituent elements also take part in the diffusion processes, which could be non-linear. The biological and medical sciences offer even more complex systems of reactions than the fields of physics and chemistry. The problems involved often are related to the field of information theory.

The problems of evolution of population are obviously connected to reaction–diffusion models. The growth and emigration of population from overcrowded countries, for instance, represent a growth-dominated explosive type of evolution. The diffusion of epidemics and, as another example, the reproduction and diffusion of insects in bio-systems, can also be mentioned in this context. The growth and diffusion of forests (for example, in the Amazon) have recently been studied by means of reaction–diffusion analysis. The detailed discussion of these heterogeneous applications is not the purpose of this text, of course, but the methods developed in the particular context of physics are of general importance also in other disciplines and fields of application.

The authors hope that the survey and the treatment presented here, though by no means exhaustive, of a vast domain of interesting and unusual phenomena could serve to stimulate the readers to use the results of this work and take part in the development of a field that appears to be as fruitful as it is challenging.

Chapter 1

The Concept of Time Scale

A 'time scale' is a useful concept that separates slow and fast phenomena occurring in science, as well as in life.

The identification of different time scales in natural phenomena, from the femto-second scale of laser pulses (10^{-15} s) to the lifetime of our sun (10^{17} s) or our universe (10^{18} s), is one of the pillars on which scientific work is founded. The same could be said of space scales.

It has been said that the evolution of science in the 20th century has meant as much to our society as did the use of fire to people in ancient history.

When, and how important, could the realization of fusion energy on earth be?

The answer naturally depends not only on our ability but also on our need for fusion, which settles the support for further research [1.13]. Naturally, questions of this type are often related not only to quantity but also to quality. It took, for example, quite some time before coherent light was developed, even if light was used in science and by our society from the very beginning.

We can notice that things seem to go much faster today. What is the reason? Even if ground-breaking ideas still come from individuals, the development and exploitations depend on the environment.

As a scientist experienced in these matters said: ''if you make a discovery in Silicon Valley you find lots of interested organizations to exploit your findings, but when you do the same thing in Finland you find two meters of snow!''

From school, we remember that if things change, they usually do this in proportion to the amplitude of the force that drives the change.

If we change the voltage applied to an electrical resistor, the current changes accordingly (linearly, for ususal circuit components). But most often, this is not true when we consider a medium like a gas or a plasma. And in fusion-oriented plasma physics, phenomena that are instead characterized by non-linear effects have a strong and often dominating influence.

To illustrate a non-linear phenomenon and the associated role of time scale, let us take the growth of the population on Earth.

For centuries, the rate of change of population with time has been proportional to the square of the existing population [1.11, 1.9]. Such a dependence is on its way to causing a population explosion, growing unlimited in only a couple of decades from now, see sections 1.2.2 and 3.3.

For comparison, it should be mentioned that a theory with a linear dependence of the time rate of change on the population would not describe the *observed* evolution. It would give an exponential growth, rather than an explosive trend, see section 1.2.

This means that, in this case, the non-linear effect reduces the time scale.

In plasma physics, not only phenomena in the laboratory but also in astrophysics may have an explosive evolution as it happens, for example with solar flares, see chapter 7.

If, in the description of the plasma, one includes the effects of diffusion, which as a rule is a non-linear process, new phenomena of an explosive nature may occur.

A reaction–diffusion process in a plasma, governed by equations that include inertia, diffusion and source terms, can be shown to have explosive solutions, but of a particular type. The exploding units are finite size bell-shaped configurations that grow in amplitude in a finite time preserving their spatial shape. They have been named explosive localized solutions, ELS, or Singletons [1.12] and will be discussed explicitly in chapter 3 in connection with examples of non-linear equations separable in space and time.

Sometimes, one has the impression that plasmas, rather than being smooth and well-behaved structures, resemble something like 'magic eggs' that could either explode or collapse and also interplay with each other. The internal structure and processes remain hidden to us and cannot even be envisaged or described. At a distance, the overall picture could be reconstructed by means of average parameters that, however, rest on uncertainties and often lack solid foundations.

Looking from *our* distance, the sun seems to shine rather uniformly, whereas from a closer viewpoint (e.g. from a spacecraft, or through a telescope) we know that the solar surface exhibits lots of bubbles and holes, representing great variations of the local magnetohydrodynamic configuration and temperature distribution. Occasionally, the detailed phenomena become more visible as prominences, flares and sunspots, having various time scales and spatial structures.

It is well known that it is generally energetically favourable for a plasma to break up in separate parts (filaments and blobs) [1.3, 1.4]. Laboratory experiments as well as cosmic plasma observations of, for example, final states of cosmic jets or prominence arcs, as well as wave-breaking phenomena, witness the presence of such localized configurations [1.13].

From astrophysics, we know that the fusion burn in the centre of the sun producing alpha particles that keeps the central temperature high $(1.4 \times 10^7\ \mathrm{K})$ is very slow. The average reaction time per particle for the intermediate reaction producing deuterium (D) out of protons (H) is indeed 10^{11} years!

Therefore the solar life time is extremely long and we can rely on the solar radiation for billions of years.

In laboratory plasmas, all the different processes that may occur can be related to characteristic time scales that account for the often extremely complicated detail behind the observed data. Let us mention that time scales for the various types of instabilities, for heat and particle production, for diffusion and radiative losses, are all non-linear.

The time scale for energy confinement described by the 'energy confinement time' τ_E is an example of an averaged 'effective' time scale, see section 2 and section 6.1. It represents a measure of the balance of losses and sources in a confined plasma and it is a decisive parameter for the realization of a future fusion reactor.

1.1 Simple Linear and Non-linear Examples

In this section, we give a review of the simplest mechanisms of linear and non-linear instabilities, and the definitions and the nomenclature are indicated in the text by italics. They are meant to demonstrate some essential features of the analysis of more detailed problems presented in the text. As an illustration, we also discuss an interesting example from ionospheric plasmas.

1.2 Parametric Instabilities

Let us first discuss two coupled equations describing *parametric instability.*

Consider dynamical variables a_1 and a_2 governed by the equations

$$\begin{aligned} \frac{\mathrm{d}a_1}{\mathrm{d}t} &= c_1 a_0 a_2 \\ \frac{\mathrm{d}a_2}{\mathrm{d}t} &= c_2 a_0 a_1 \end{aligned} \tag{1.2.1}$$

where a_0 is a constant parameter and all quantities are real.

The solution for large times is

$$a_1 \approx \mathrm{e}^{a_0\sqrt{c_1 c_2}t} \quad \text{and} \quad a_2 \approx \mathrm{e}^{a_0\sqrt{c_1 c_2}t} \tag{1.2.2}$$

provided the *coupling coefficients* c_1 and c_2 are positive.

These solutions describe *exponential growth* where the *growth rate* increases with the coupling strengths and the parameter a_0.

If c_1 and c_2 are both negative, we obtain decreasing amplitudes for small times. However, except for a very special choice of initial conditions, one amplitude will, after some time, become negative while the other starts growing.

If the dynamic variables experience damping, we may rewrite the equations as:

$$\begin{aligned} \frac{\mathrm{d}a_1}{\mathrm{d}t} + b_1 a_1 &= c_1 a_0 a_2 \\ \frac{\mathrm{d}a_2}{\mathrm{d}t} + b_2 a_2 &= c_2 a_0 a_1 \end{aligned} \tag{1.2.3}$$

where $b_1 > 0$ and $b_2 > 0$ are the damping coefficients.

Assuming solutions of the type $a_{1,2} \approx \mathrm{e}^{a\lambda t}$, one obtains from equation (1.2.3) the relation

$$(\lambda + b_1)(\lambda + b_2) = c_1 c_2 a_0^2. \tag{1.2.4}$$

It can be seen that to have exponentially growing solutions ($\lambda > 0$), the condition to be fulfilled is: $b_1 b_2 \leq c_1 c_2 a_0^2$. A *threshold* value is found for the parameter a_0, which is controlling the instability onset, given by:

$$a_0 = \left(\frac{b_1 b_2}{c_1 c_2}\right)^{1/2}. \tag{1.2.5}$$

This is then the *threshold* for the *parametric instability*.

1.3 The Explosive Instability and the Problem of Saturation

Let us consider the simplest form of equation for describing an *explosive instability*, namely, for a population n

$$\frac{\mathrm{d}n}{\mathrm{d}t} = \alpha n^2 \tag{1.3.1}$$

with the solution

$$n = \frac{n_i}{1 - \alpha n_i t} \tag{1.3.2}$$

where n_i is the initial value [1.11, 1.9]. This solution blows up at $t = t_0 = 1/\alpha n_i$.

One way to limit the explosive growth would be to make α time dependent by introducing, after a certain time, a continued decrease of α.

In a crude but illustrative model, we assume that at a certain time $t = t_c < t_0$ we diminish the value of α to α/m ($m > 1$).

From an initial value n_i at $t = 0$, the population will then follow the relation (1.3.2) until $t = t_c$, after which, by simple integration of equation (1.3.1) with α substituted by α/m, $t > t_c$, we find

$$n = \frac{mn_i}{m - \alpha n_i[t - (m-1)t_c]} \tag{1.3.3}$$

that tends towards infinite values of n when t approaches t_∞, where

$$t_\infty - t = m\{1/\alpha n_i - t_c\} \tag{1.3.4}$$

or since from (1.3.1)

$$n_i = \frac{n_c}{1 + \alpha n_c t_c} \tag{1.3.5}$$

one gets

$$t_\infty - t_c = m/\alpha n_i. \tag{1.3.6}$$

The result means that, counted from the time t_c at the beginning of diminishing α by a factor $1/m$ ($m > 1$), the explosion time t_∞ increases by a factor m. It means that, if by year 2000 we could diminish α by a factor 2, we might increase the time until explosion by a factor 2, from about year 2035 to 2070, or by a decrease in α of 10% to about 2038, indeed a very minor shift worth noticing!

Another possibility to diminish the growth rate is to introduce a dependence of the derivative of density with regard to time in the effective coefficient, so that equation (1.3.1) is changed to

$$\frac{\mathrm{d}n}{\mathrm{d}t} = \alpha\left(1 - \gamma\frac{\mathrm{d}n}{\mathrm{d}t}\right)n^2 \tag{1.3.7}$$

or expressed in an equivalent form

$$\frac{\mathrm{d}n}{\mathrm{d}t} = \frac{1}{\gamma + 1/\alpha n^2}. \tag{1.3.8}$$

Assuming, quite arbitrarily, an initial density n_i that satisfies $\alpha n_i^2 = 1/\gamma$ one has

$$\left(\frac{\mathrm{d}n}{\mathrm{d}t}\right)_{n_i} = \frac{1}{2\gamma} \tag{1.3.9}$$

whereas for large values of n, for which $\alpha n^2 \gg 1/\gamma$

$$\frac{\mathrm{d}n}{\mathrm{d}t} \propto 1/\gamma \tag{1.3.10}$$

i.e. a linear growth of n with regard to time with growth rate $1/\gamma$.

Again, this is an indication of a typical non-linear effect, namely to counteract the perturbation and try to re-establish a previous trend.

The results illustrate how difficult it is to change the non-linear trend of evolution associated with an explosive instability. In the explosive type equation, the constant α accounts for an average general trend encompassing an extremely complicated internal structure in many cases of application.

One can draw parallels of the description of the overall situation with the behaviour of hot plasmas, where the parameters (e.g. the heat conductivity and the particle diffusion coefficients) cover many intrinsic 'secrets' due to complex and varying turbulent regimes.

1.4 Solar Eclipse Diagnostics of Ionospheric Plasmas

The ionospheric free electron density experiences a reduction during a solar eclipse and reaches a minimum before it returns to normal values when the eclipse is over. The time shift between the density minimum and the half-time of the entire eclipse (total or partial) is a measure of the recombination coefficient of the ionospheric plasma. The reason is that the ultraviolet (UV) radiation from the sun, which usually ionizes the atoms of the ionosphere, experiences the shadowing effect by the moon. Accordingly, the balance between the ionization and recombination, which is quadratic in the free electron density (diffusion and attachment of free electrons to neutral atoms can be neglected), will be perturbed.

The variation in density can easily be recorded by a ground-based electromagnetic radiation backscatter device.

The measurement of the *time-shift* of the plasma density minimum with reference to the time of the eclipse maximum (minimum in UV radiation) and the *minimum value of the electron density* are sufficient to determine the recombination coefficient [1.8].

Consider the equation

$$\frac{\mathrm{d}n}{\mathrm{d}t} = S(t) - \alpha n^2 \tag{1.4.1}$$

where $S(t)$ is the source term describing the variation of the ionizing influence of the solar UV radiation, and α describes the recombination coefficient of the plasma, cf. section 3.1.

To illustrate the process, we approximate the variation in n simply by a square of the cosine function, having maximum value n_0 at $t = 0$ and minimum value at $t = t_{n_{\min}}$:

$$n = n_0 - (n_0 - n_{\min})\ \cos^2\left(\frac{\pi}{2}\frac{t}{t_{n_{\min}}}\right). \tag{1.4.2}$$

From the non-linear rate equation (1.4.1), we estimate the time for the minimum of the corresponding source function $S(t)$ (that is in fact a given quantity, used here for reference) $t = t_{S_{\min}}$. Elementary calculations yield the relation

$$2\alpha \ \sin\left(\pi\frac{t_1}{t_2}\right)\left[(n_0 - n_{\min}) \ \cos^2\left(\frac{\pi}{2}\frac{t_1}{t_2}\right) - n_0\right] = \frac{\pi}{t_2} \ \cos\left(\frac{\pi}{2}\frac{t_1}{t_2}\right) \qquad (1.4.3)$$

where, for simplicity of notation, we have used $t_1 = t_{S_{\min}}$ and $t_2 = t_{n_{\min}}$, with $t_1 < t_2$.

Expanding the cosine and sine functions for $(t_2 - t_1) < 1/\pi$, one obtains the simple form

$$2\alpha(t_2 - t_1)n_{\min} \cong 1. \qquad (1.4.4)$$

We notice that to this approximation, the initial density n_0 does not enter the relation (1.4.4), a typical non-linear effect (compare the asymptotic form of the solution to (1.4.1) $n = n_0/(1 + \alpha n_0 t)$ for $S(t) = 0$ which approaches $n = 1/\alpha t$ for $t \gg 1/\alpha n_0$.

Estimated values of $t_1 \approx 1$, $h = 3600$ s, $(t_2 - t_1) \approx 900$ s, $n_{\min} \approx 10^5$ cm^{-3}, $n_0 - n_{\min} \cong 2 \times 10^{15}$ cm^{-3} give $\alpha \approx 6 \times 10^{-9}$ cm^{3}s^{-1} for the recombination coefficient.

1.5 Stationary Non-linear Longitudinal Waves in Hot Plasmas

The frequency of non-linear, one-dimensional, free oscillations of a plasma under certain assumptions coincides with the plasma frequency of the linearized theory [1.1, 1.5]. The result is strictly valid for non-relativistic oscillations of a cold plasma if the ion motion is neglected [1.2] and provided the charged sheets do not cross each other in the oscillating motion [1.6]. One wonders what happens when the plasma is no longer cold but has an average thermal energy $\propto \langle v^2 \rangle$.

Neglecting the ion motion, one finds by integrating the non-linear Boltzmann and Poisson equations the *non-linear* dispersion relation:

$$\omega^2 = \omega_p^2\left\{1 + 3\frac{k^2\langle v^2\rangle}{\omega_p^2}\left[1 + \frac{5}{2}(k_p\xi_0)^2\right]\right\} \qquad (1.5.1)$$

where ξ_0 is the amplitude of the oscillation, k the wavenumber, $k_p = \omega_p^2\langle v^2\rangle^{-1}$, and it is assumed that the non-linear effect $\frac{5}{2}(k_p\xi_0)^2 < 1$.

One notices the limits where:

(a) the temperature T $\propto \langle v^2 \rangle$ vanishes and one recovers the result for the cold case $\omega^2 = \omega_p^2$ even for large amplitudes of oscillation ξ_0,

(b) the dispersion relation assuming small oscillation ξ_0 (linear theory) but finite temperature $T \propto \langle v^2 \rangle$

$$\omega^2 = \omega_p^2\{1 + \frac{3k^2\langle v^2\rangle}{\omega_p^2}\}. \tag{1.5.2}$$

The non-linear effect described by (1.5.1) was verified experimentally on a plasma diode by Stern, shortly after the publication of the theory by Wilhelmsson [1.10].

These relations illustrate an interesting interplay between the effects of non-linearity and temperature effects and serves as simple examples of the forthcoming discussions.

References

[1.1] Akhiezer A I and Lyubarskii G Y 1951 Nonlinear theory of the oscillations of an electron plasma *Dokl. Akad. Nauk. SSSR* **80** 193

[1.2] Akhieser A I and Polovin R V 1955 On relativistic plasma oscillations *Dokl. Akad. Nauk. SSSR* **102** 119

[1.3] Alfvén H 1982 Paradigm transition in cosmic plasma physics *Phys. Scripta* **T2/1** 10

[1.4] Alfvén H 1986 The plasma universe *Physics Today* September 22

[1.5] Bernstein I B, Green J M and Kruskal M D 1957 Exact nonlinear plasma oscillations *Phys. Rev.* **108** 546

[1.6] Dawson J 1959 Nonlinear electron oscillations in a cold plasma *Phys. Rec.* **113** 383

[1.7] Polovin R V 1957 On the nonlinear theory of longitudinal plasma oscillations *Sov. Phys.-JETP* **4** 290

[1.8] Rydbeck O E H and Wilhelmsson H 1954 A theoretical investigation of the ionospheric electron density variation during a solar eclipse *CTHH 149*, *RRLE* **31** 1

[1.9] Weiland J and Wilhelmsson H 1974 On the evolution and saturation of the world population *Phys. Scripta* **10** 10

[1.10] Wilhelmsson H 1961 Stationary nonlinear plasma oscillations *Phys. Fluids* **4** 335

[1.11] Wilhelmsson H 1972 On the analysis of the population problem *Phys. Scripta* **5** 5

[1.12] Wilhelmsson 1989 Self-formation and evolution of singleton, *Int. J. Quantum Chem.* **35** 887

[1.13] Wilhelmsson H 1999 *FUSION A Voyage through the Plasma Universe* (Bristol: IOP)

Chapter 2

Description of Continuous Media

A continuous medium is an abstract model of a real physical system defined through a systematic or intuitive 'smearing' process of the distribution of physical properties (for example, mass, charge) that bypasses the difficulties connected with volumes smaller than some critical size.

A classical physical system can ultimately be considered to be composed of an extremely large but *finite* number of particles each possessing *finite* physical and geometrical properties (size, mass, charge). A continuum model of such a system consists of *infinite* material points, each possessing three degrees of freedom, which globally are therefore infinite. However, each point is paradoxically devoid of physical meaning since each geometric point is zero-dimensional, and mass and charge are meaningful quantities when associated with the integral over infinitesimal portions of the medium. Therefore the physical quantities are, in fact, somewhat abstract continuous 'field' functions of the co-ordinates and time, such as the density of mass, charge, current, momentum, force, angular momentum and energy. Each infinitesimal part of the continuum is a deformable, vanishingly small *finite* part having in an Euclidean space, in principle, twelve degrees of freedom, since the displacement vector $\vec{\xi} = \boldsymbol{x} - \boldsymbol{x}_0$ of a point of such a system, from an initial position $\boldsymbol{x}_0$, is identified by the co-ordinates of its position vector (three degrees of freedom) and its deformation tensor $(\partial \xi_k / \partial x_i^0)$, nine degrees.

However, the geometry of the problem and conditions of force balance of each infinitesimal element interacting with neighbouring elements and with external forces reduce the allowed freedom.

A continuum model is *intrinsically non-linear* and the structure of this non-linear behaviour can be understood as follows.

At an initial time $t = 0$, let C_0 be a reference configuration (domain of points in a Euclidean space) of a *classical continuum* and let $C(t)$ be the configuration at time $t > 0$. The co-ordinates x_i of any point $P(t)$ of the latter are related to the co-ordinates x_i^0 of the corresponding initial point $P_0 = P(0)$ in the same reference system, by a transformation

$$x_i = x_i(x_1^0, x_2^0, x_3^0, t) \tag{2.1}$$

assumed to be continuous and invertible. Following the movement of one particle of C from its initial position, its (*Lagrangian*) velocity vector components are

$$\upsilon_r = \frac{\partial x_r(x_1^0, x_2^0, x_3^0, t)}{\partial t}. \tag{2.2}$$

But if the expressions of x_i^0 obtained inverting (2.1) are substituted in (2.2) one obtains the components of the (*Eulerian*) velocity vector *field* of the element, which at time t, transits through the observation point $P(t)$:

$$u_r(\boldsymbol{x}, t) \equiv \upsilon_r(x_1^0(x_s, t), x_2^0(x_s, t), x_3^0(x_s, t), t). \tag{2.3}$$

Any differentiable function $f = f(x, t)$ of the co-ordinates and time representing a physical or geometrical property of the continuum, hereafter called 'fluid', has a rate of change expressed by the total derivative

$$\frac{\mathrm{d}f}{\mathrm{d}t} = \frac{\partial f}{\partial t} + \frac{\partial f}{\partial x_s} u_s \tag{2.4}$$

sometimes called the 'substantial' or 'convective' or 'hydrodynamic' derivative that represents the rate of change of the field $f = f(\boldsymbol{x}, t)$ at the observation point $P(t)$ and is the origin of the universal *convective non-linearity* intrinsic to the 'fluid' description.

In general, the dynamics of a continuum is constructed on the two basic principles that for *each* infinitesimal element of the continuum (i) the resultant of all forces external to it must balance the rate of change of momentum and that (ii) the resultant external torque must balance the rate of change of angular momentum.

From the constraints of generalized conservation or exchange with the external world of basic *extensive* quantities $Q_\alpha(t)$ (e.g. mass, charge, energy) of a bounded system as a whole, supplemented by constitutive relations, using the basic transformations (2.1–2.4) one obtains systems of coupled non-linear evolution equations for *intensive* variables $q_\alpha(\boldsymbol{x}, t)$ describing local properties and related to the extensive variables by $Q_\alpha(t) = \int_v q_\alpha(\boldsymbol{x}, t)\,\mathrm{d}V$. The intensive quantities are space- and time-dependent *fields, which* can, in principle, be related to the microscopic dynamics of the individual particles.

The fundamental structure of conservation theorems leading to fluid equations is that of Reynolds lemma. The total rate of change of an extensive quantity associated to a time varying volume $V(t)$ bounded by a smooth surface

$S(t)$ is given by:

$$\frac{\mathrm{d}Q_\alpha(t)}{\mathrm{d}t} = \int_{v(t)} \mathrm{d}V \left(\frac{\partial q_\alpha}{\partial t} + \nabla \cdot (\boldsymbol{u} q_\alpha) \right). \tag{2.5}$$

The continuous system of interest here is a fluid model of plasma. A plasma macroscopically can be considered a globally electrically neutral gas of charged particles (electrons and ions) interacting through long-range Coulomb electrostatic forces. An exact description of the dynamics of the system based on the study of the phase space trajectories of all its constituent particles, subject to the effect of self-consistent local electromagnetic fields, is impossible analytically, but might, however, be simulated by computer calculations.

The electrodynamic fields responsible for the charged particle's interaction are described in terms of Maxwell's equations for which there is the key *closure* problem of specifying the sources of the electric field $\boldsymbol{E}(\boldsymbol{x}, t)$ and the magnetic induction field $\boldsymbol{B}(\boldsymbol{x}, t)$, consisting of charge and current density distributions. The latter may be defined summing the contributions of all α species:

$$\rho(\boldsymbol{x}, t) = \sum_\alpha e_\alpha n_\alpha(\boldsymbol{x}, t) \tag{2.6}$$

$$\boldsymbol{J}(\boldsymbol{x}, t) = \sum_\alpha e_\alpha n_\alpha \boldsymbol{u}_\alpha(\boldsymbol{x}, t). \tag{2.7}$$

Here $n_\alpha(\boldsymbol{x}, t)$ is the average number per unit volume of particles α that at time t are near the point $\boldsymbol{x}$ and $\boldsymbol{u}_\alpha(\boldsymbol{x}, t)$ is the Eulerian velocity field of the 'fluid' of species α.

So the medium need be described by *only two* macroscopic fields, a scalar one $n_\alpha(\boldsymbol{x}, t)$ and a vectorial one $\boldsymbol{u}_\alpha(\boldsymbol{x}, t)$, and the problem of microscopic mechanics of the interacting charged particles is transformed to the problem of evolution equations of the 'macro' variables $n_\alpha(\boldsymbol{x}, t)$ and $\boldsymbol{u}_\alpha(\boldsymbol{x}, t)$ coupled to Maxwell's equations.

The local density of the particles and their mean velocity (Eulerian) are the lowest order physically meaningful 'moments' of the kinetic distribution function of the particles, which gives a statistical mechanics description of the medium 'bridging' the gap between the (untreatable) single particle model and the macroscopic fluid model.

A short summary of the basic concepts of the fluid plasma models used in the particular problems addressed in this text is given here. Appropriate references on the full theoretical foundations of plasma kinetic theory and magnetized plasma transport theory are provided and should be consulted for a rigorous description, and to frame correctly the picture of linear and non-linear plasma response in special problems presented in this text.

When dimensional quantities are used, we use Gaussian cgs units, as is customary in plasma physics theory.

The behaviour of a plasma is substantially more complicated than that of a neutral gas because the motion of the charged particles of which it consists is affected by externally applied electromagnetic fields and in its turn it produces local space charge and current fluctuations, which are sources of electromagnetic fields. Furthermore, the long-range Coulomb interaction among particles dominates the short-range interactions that can be described as a sudden variation of the velocity vector and are similar to collisions between neutral particles.

The kinetic description of a plasma of, say, two species α of non-relativistic particles (ions and electrons) is based on the determination of a function $F_\alpha(\boldsymbol{v},\boldsymbol{x},t)$ of co-ordinates and velocity (momenta) with the meaning that $F_\alpha(\boldsymbol{v},\boldsymbol{x},t)\Delta\boldsymbol{v}\Delta x$ is the number of particles, which at time t, are near the phase space co-ordinates $(\boldsymbol{v},\boldsymbol{x})$, within the volume $\Delta V = \Delta\boldsymbol{v}\Delta x \equiv \mathrm{d}x\,\mathrm{d}y\,\mathrm{d}z\,\mathrm{d}v_x\,\mathrm{d}v_y\,\mathrm{d}v_z$.

The task of a basic 'microscopic' kinetic theory is to provide and solve an equation for $F_\alpha(\boldsymbol{v},\boldsymbol{x},t)$ related to the dynamics of each individual particle. We assume for the moment that atomic and nuclear reactions are absent and therefore the number of particles of each species $N_\alpha(t) = N_\alpha^0 \int_{V(t)} \mathrm{d}V F(\boldsymbol{x},\boldsymbol{v},t)$, in a given region $V(t)$ of phase space at time t, is conserved. Then the equation for $F_\alpha(\boldsymbol{v},\boldsymbol{x},t)$ (normalized to one) must express conservation along particles' trajectories, according to Reynolds lemma:

$$\frac{\partial F_\alpha}{\partial t} + \nabla\cdot(\boldsymbol{v}F_\alpha) + \frac{\partial}{\partial\boldsymbol{v}}\cdot\left(\frac{\mathrm{d}\boldsymbol{v}}{\mathrm{d}t}F_\alpha\right) = 0. \tag{2.8}$$

The acceleration field $\boldsymbol{a}(\boldsymbol{x},\boldsymbol{v},t) = (\mathrm{d}\boldsymbol{v}/\mathrm{d}t)$ depends on *all* the forces applied, including the external forces and the full electromagnetic interaction between particles, deterministic but macroscopically indeterminate as it involves all possible classical time and space scales. To obtain a useful description, it is necessary to smear out all the microscopic space and time variations conceiving a suitable ensemble average operation and splitting both the applied forces and the response distribution function into an 'average' part smoothly varying on macroscopically observable (in principle) time and space scales describing the external and 'collective' effect on any given test particle plus a zero average irregular fluctuation, which represents the irreducible individual particle interaction:

$$F_\alpha(\boldsymbol{v},\boldsymbol{x},t) = \langle F_\alpha(\boldsymbol{v},\boldsymbol{x},t)\rangle + \delta F_\alpha(\boldsymbol{v},\boldsymbol{x},t) \tag{2.9}$$

$$\boldsymbol{a}_\alpha(\boldsymbol{x},\boldsymbol{v},t) = \langle \boldsymbol{a}_\alpha(\boldsymbol{v},\boldsymbol{x},t)\rangle + \delta\boldsymbol{a}_\alpha(\boldsymbol{v},\boldsymbol{x},t) \tag{2.10}$$

with $\langle\delta F_\alpha(\boldsymbol{v},\boldsymbol{x},t)\rangle = \langle\delta\boldsymbol{a}_\alpha(\boldsymbol{v},\boldsymbol{x},t)\rangle \equiv 0$.

Substituting $f_\alpha(\boldsymbol{v},\boldsymbol{x},t) = \langle F_\alpha(\boldsymbol{v},\boldsymbol{x},t)\rangle$, expressing the acceleration in terms of the electromagnetic field and applying the $\langle\cdots\rangle$ operator to the kinetic equation one obtains, with straightforward algebra, the useful form:

$$\frac{\partial f_\alpha}{\partial t} + \nabla \cdot \boldsymbol{v} f_\alpha + \left(\frac{e_\alpha}{m_\alpha}\right) \nabla_{\boldsymbol{v}} \cdot [(\boldsymbol{E} + \boldsymbol{v} \times \boldsymbol{B}) f_\alpha] = \left(\frac{\partial f_\alpha}{\partial t}\right)_{\mathrm{C}} \tag{2.11}$$

or the more common form

$$\frac{\partial f_\alpha}{\partial t} + \boldsymbol{v} \cdot \nabla f_\alpha + \left(\frac{e_\alpha}{m_\alpha}\right) (\boldsymbol{E} + \boldsymbol{v} \times \boldsymbol{B}) \cdot \frac{\partial f_\alpha}{\partial \boldsymbol{v}} = \left(\frac{\partial f_\alpha}{\partial t}\right)_{\mathrm{C}} \tag{2.12}$$

where the right hand side (r.h.s) 'collision' term embodies the contributions of the correlated fluctuations and may include the possible inelastic atomic processes of ionization, recombination and nuclear fusion.

The solution of the kinetic problem (2.11) complete of initial and boundary conditions and specified structure of the external magnetic field is in general a formidable work and the systematic approaches are based on the ordering of the terms driving the perturbation from the equilibrium distribution (e.g. Maxwellian) and subsequent expansion of the perturbation of $f_\alpha(\boldsymbol{x}, \boldsymbol{v}, t)$ in terms of a complete set of functions. The reader should consult [2.2, 2.4, 2.22, 2.23] for exhaustive description of the appropriate methods.

But to respond to the basic need of providing a closure to the Maxwell system by specifying the sources, it would then appear sufficient to deduce from the full kinetic problem, a subset of equations for the two lowest order velocity space moments of $f_\alpha(\boldsymbol{x}, \boldsymbol{v}, t)$

$$n_\alpha(\boldsymbol{x}, t) = N_\alpha^0 \int \mathrm{d}^3 v' f_\alpha(\boldsymbol{x}, \boldsymbol{v}', t) \tag{2.13}$$

$$\boldsymbol{u}_\alpha(\boldsymbol{x}, t) = \int \mathrm{d}^3 v' \boldsymbol{v}' f_\alpha(\boldsymbol{x}, \boldsymbol{v}', t). \tag{2.14}$$

The system of equations for Nth order physical moments of $f_\alpha(\boldsymbol{x}, \boldsymbol{v}, t)$, defined in general as $\mathscr{M}^{N,\alpha}_{ijk\ldots r}(\boldsymbol{x}, t) = N_\alpha^0 \int \mathrm{d}^3 v' v_i v_j v_k \ldots v_r|_N f_\alpha(\boldsymbol{x}, \boldsymbol{v}', t)$ may be deduced formally performing the corresponding weighted integrations over velocity space of equation (2.11). However, as expected, the system of coupled equations obtained is infinite and to achieve a 'fluid' closure, it is necessary to truncate at some order the next higher order moment, on the basis of physical justifications or rigorous asymptotic expansion in some small parameter.

To establish the notation most appropriate for the applications to follow, and to conform with the best known literature, we add to the list of standard definitions of other important fluid moments for a magnetically confined plasma and their evolution equations governing the thermal energy and heat flux balance.

The stress tensor in the laboratory frame is

$$\overleftrightarrow{\Pi}_\alpha = m_\alpha N_\alpha \int \mathrm{d}^3 v' \boldsymbol{v}' \boldsymbol{v}' f_\alpha \tag{2.15}$$

while the pressure tensor, in the rest frame of species α is defined as

$$\overleftrightarrow{\boldsymbol{p}}_\alpha = m_\alpha N_\alpha \int \mathrm{d}^3 v'(\boldsymbol{v}' - \boldsymbol{u})(\boldsymbol{v}' - \boldsymbol{u}) f_\alpha. \tag{2.16}$$

The energy flux vector in the laboratory frame is

$$\boldsymbol{Q}_\alpha(\boldsymbol{x}, t) = \tfrac{1}{2} m_\alpha^2 N_\alpha^0 \int \mathrm{d}^3 v' \boldsymbol{v}' v'^2 f_\alpha(\boldsymbol{x}, \boldsymbol{v}', t) \tag{2.17}$$

and the heat flux vector in the rest frame of species α is

$$\boldsymbol{q}_\alpha(\boldsymbol{x}, t) = \tfrac{1}{2} m_\alpha^2 N_\alpha^0 \int \mathrm{d}^3 v' |\boldsymbol{v}' - \boldsymbol{u}_\alpha|^2 (\boldsymbol{v}' - \boldsymbol{u}_\alpha) f_\alpha(\boldsymbol{x}, \boldsymbol{v}', t). \tag{2.18}$$

The collision momentum transfer

$$\boldsymbol{R}_\alpha(\boldsymbol{x}, t) = m_\alpha \int \mathrm{d}^3 v' (\boldsymbol{v}' - \boldsymbol{u}) \left(\frac{\partial f_\alpha(\boldsymbol{x}, \boldsymbol{v}', t)}{\partial t} \right)_{\alpha\beta}. \tag{2.19}$$

The above definitions are consistent with the relations:

$$\overleftrightarrow{\Pi}_\alpha = \overleftrightarrow{\boldsymbol{p}}_\alpha + m_\alpha n_\alpha \boldsymbol{u}_\alpha \boldsymbol{u} \tag{2.20}$$

$$\boldsymbol{Q}_\alpha = \boldsymbol{q}_\alpha + \boldsymbol{u}_\alpha \cdot \overleftrightarrow{\boldsymbol{p}}_\alpha + \tfrac{3}{2} p_\alpha \boldsymbol{u}_\alpha + \tfrac{1}{2} m_\alpha n_\alpha u_\alpha^2 \boldsymbol{u}_\alpha. \tag{2.21}$$

Furthermore, by averaging over the distribution function, one defines the thermal energy of the system in terms of the average kinetic energy of a particle:

$$W_{\mathrm{th}_\alpha} = \tfrac{1}{2} m_\alpha \langle (\boldsymbol{v} - \boldsymbol{u}_\alpha)^2 \rangle = \tfrac{1}{2} m_\alpha \langle \boldsymbol{v}^2 \rangle + \tfrac{1}{2} m_\alpha \boldsymbol{u}_\alpha^2. \tag{2.22}$$

By definition, the *temperature and the thermal velocity* of the species α are related to the thermal energy by

$$W_{\mathrm{th}_\alpha} = \tfrac{3}{2} k_\mathrm{B} T_\alpha \tag{2.23}$$

and

$$\tfrac{1}{2} m_\alpha v_{\mathrm{th}} \alpha^2 = k_\mathrm{B} T_\alpha.$$

This can be easily seen to be related to the trace of the pressure tensor (2.16) by

$$\tfrac{3}{2}k_{\mathrm{B}}n_\alpha T_\alpha = \tfrac{1}{2}\mathrm{Tr}(\overleftrightarrow{\boldsymbol{p}}_\alpha).$$

The procedure to obtain the fluid description from the kinetic one is then straightforward, although complexity increases with the order of the moments. For convenience, we report here the essential formal steps.

Integrating equation (2.12) over all velocity space gives

$$\frac{\partial}{\partial t}\int \mathrm{d}^3v' f_\alpha(\boldsymbol{x},\boldsymbol{v}',t) + \int \mathrm{d}^3v' \nabla\cdot\boldsymbol{v}' f_\alpha + \left(\frac{e_\alpha}{m_\alpha}\right)\int \mathrm{d}^3v' \nabla_{\boldsymbol{v}}\cdot\left[\left(\boldsymbol{E}+\frac{\boldsymbol{v}'}{c}\times\boldsymbol{B}\right)f_\alpha\right] = \int \mathrm{d}^3v'\left(\frac{\partial f_\alpha}{\partial t}\right)_{\mathrm{C}}. \tag{2.24}$$

This can be written as

$$\frac{\partial}{\partial t}\int \mathrm{d}^3v' f_\alpha(\boldsymbol{x},\boldsymbol{v}',t) + \nabla\cdot\int \mathrm{d}^3v' \boldsymbol{v}' f_\alpha + \left(\frac{e_\alpha}{m_\alpha}\right)\int_{\Sigma_\infty} \mathrm{d}^2\sigma\boldsymbol{n}\cdot\left[\left(\boldsymbol{E}+\frac{\boldsymbol{v}'}{c}\times\boldsymbol{B}\right)f_\alpha\right] = \int \mathrm{d}^3v'\left(\frac{\partial f_\alpha}{\partial t}\right)_{\mathrm{C}} \tag{2.25}$$

where Σ_∞ represents a surface at infinity in velocity space, $\boldsymbol{n}$ is its outward unit vector and naturally the surface integral vanishes as $\lim_{|\boldsymbol{v}|\to\infty} f_\alpha(\boldsymbol{x},\boldsymbol{v},t) = 0$.

Therefore using the definitions (2.13) and (2.14), the resulting equation expresses continuity of particle density in the form

$$\frac{\partial n_\alpha}{\partial t} + \nabla\cdot\boldsymbol{u}_\alpha n_\alpha = 0 \tag{2.26}$$

where account has been taken only of elastic collision processes, which conserve the number of particles.

Multiplication of equation (2.12) by $\boldsymbol{v}$ and integration over velocity space gives

$$\frac{\partial}{\partial t}\int \mathrm{d}^3v' \boldsymbol{v}' f_\alpha(\boldsymbol{x},\boldsymbol{v}',t) + \int \mathrm{d}^3v' \boldsymbol{v}'\nabla\cdot\boldsymbol{v} f_\alpha + \left(\frac{e_\alpha}{m_\alpha}\right)\int \mathrm{d}^3v' \boldsymbol{v}'\nabla_{\boldsymbol{v}}\cdot\left[\left(\boldsymbol{E}+\frac{\boldsymbol{v}'}{c}\times\boldsymbol{B}\right)f_\alpha\right] = \int \mathrm{d}^3v'\boldsymbol{v}'\left(\frac{\partial f_\alpha}{\partial t}\right)_{\mathrm{C}}.$$

Using the identities

$$\boldsymbol{v}\nabla_{\boldsymbol{v}}\cdot\boldsymbol{v}f_\alpha=\nabla_{\boldsymbol{v}}\cdot\boldsymbol{v}\boldsymbol{v}f_\alpha$$
$$\nabla_{\boldsymbol{v}}\cdot\left[\left(\boldsymbol{E}+\frac{\boldsymbol{v}}{c}\times B\right)f_\alpha\boldsymbol{v}\right]=\boldsymbol{v}\nabla_{\boldsymbol{v}}\cdot\left[\left(\boldsymbol{E}+\frac{\boldsymbol{v}}{c}\times\boldsymbol{B}\right)f_\alpha\right]+\left(\boldsymbol{E}+\frac{\boldsymbol{v}}{c}\times\boldsymbol{B}\right)f_\alpha$$

the equation can be written as:

$$\frac{\partial}{\partial t}\int \mathrm{d}^3v'\boldsymbol{v}'f_\alpha(\boldsymbol{x},\boldsymbol{v}',t)+\nabla\cdot\int \mathrm{d}^3v'\boldsymbol{v}'\boldsymbol{v}'f_\alpha$$
$$+\left(\frac{e_\alpha}{m_\alpha}\right)\left\{\int \mathrm{d}^3v'\nabla_{\boldsymbol{v}}\cdot\left[\left(\boldsymbol{E}+\frac{\boldsymbol{v}'}{c}\times\boldsymbol{B}\right)\boldsymbol{v}'f_\alpha\right]-\int \mathrm{d}^3v'\left(\boldsymbol{E}+\frac{\boldsymbol{v}'}{c}\times\boldsymbol{B}\right)f_\alpha\right\}$$
$$=\int \mathrm{d}^3v'\boldsymbol{v}'\left(\frac{\partial f_\alpha}{\partial t}\right)_{\mathrm{C}}.$$

The integral

$$\int \mathrm{d}^3v'\nabla_{\boldsymbol{v}}\cdot\left[\left(\boldsymbol{E}+\frac{\boldsymbol{v}'}{c}\times\boldsymbol{B}\right)\boldsymbol{v}'f_\alpha\right]=\int_{\Sigma_\infty}\mathrm{d}^2\sigma\boldsymbol{n}\cdot\left[\left(\boldsymbol{E}+\frac{\boldsymbol{v}'}{c}\times\boldsymbol{B}\right)\boldsymbol{v}'f_\alpha\right]$$

is obviously vanishing therefore the resulting momentum balance equation is

$$\frac{\partial n_\alpha\boldsymbol{u}_\alpha}{\partial t}+\nabla\cdot(n_\alpha\boldsymbol{u}_\alpha\boldsymbol{u}_\alpha)+\left(\frac{1}{m_\alpha}\right)\nabla\cdot\overleftrightarrow{\boldsymbol{p}}_\alpha-n_\alpha\left(\frac{e_\alpha}{m_\alpha}\right)\left(\boldsymbol{E}+\frac{\boldsymbol{u}}{c}\times\boldsymbol{B}\right)$$
$$=\int \mathrm{d}^3v'\boldsymbol{v}'\left(\frac{\partial f_\alpha}{\partial t}\right)_{\mathrm{C}}\tag{2.27}$$

where the pressure tensor $\overleftrightarrow{\boldsymbol{p}}_\alpha$ has been used and the collision process is as yet unspecified.

Summing over the species, the latter can be transformed into a useful form introducing the scalar pressure p and the stress tensor $\overleftrightarrow{\Pi}$ describing the internal tangential forces of friction, as well as the current density $\boldsymbol{J}=\sum_\alpha q_\alpha n_\alpha\boldsymbol{u}_\alpha$.

Then the net rate of change of momentum per unit volume of a fluid element is the result of the balance of the applied macroscopic forces and the force of inertia per unit volume, in an Eulerian description:

$$\sum_\alpha\left[\frac{\partial}{\partial t}m_\alpha n_\alpha\boldsymbol{u}_\alpha+\nabla\cdot(m_\alpha n_\alpha\boldsymbol{u}_\alpha\boldsymbol{u}_\alpha)\right]=-\nabla p-\nabla\cdot\overleftrightarrow{\Pi}+\frac{1}{c}\boldsymbol{J}\times\boldsymbol{B}.\tag{2.28}$$

In a similar fashion, an equation for the energy balance can be obtained.

With the ordering $\varepsilon = u/v_{\mathrm{th}_\alpha} \ll 1$, expression (2.21) is approximated by

$$\boldsymbol{Q}_\alpha = \boldsymbol{q}_\alpha + \tfrac{5}{2} p_\alpha \boldsymbol{u}_\alpha + \mathcal{O}(\varepsilon^2) \tag{2.29}$$

and a useful form of the energy equation for a single fluid model (summing over species) turns out to be:

$$\frac{3}{2}\frac{\partial}{\partial t} p = -\frac{3}{2}\nabla \cdot (\boldsymbol{u} p) - p \nabla \cdot \boldsymbol{u} - \nabla \cdot \boldsymbol{Q} - \overleftrightarrow{\Pi} : \nabla \boldsymbol{u} + \eta J^2 + P_{\mathrm{aux}} \tag{2.30}$$

where the last term is the power input due to the electromagnetic Poynting flux.

The velocity moments of the right hand side of the kinetic equation, representing the 'collisional' interaction of the particles, depend naturally on the detailed theoretical model of the interaction considered and it is a matter of considerable complexity. The physical content of the collisional terms in the moment equations amounts, however, to the rather simple concept of 'effective' frequency ν of a collision relaxation process, or dissipative ('sink') term for the evolution of each of the various physical velocity moments considered.

The evaluation of these dissipative terms is difficult as the collision operator is a complicated function of velocity. As anticipated above, a general systematic procedure of deduction of the equations for the moments of the distribution can be formulated under the assumption of small deviation of the distribution function from an equilibrium distribution $f_\alpha(\boldsymbol{v}) = f_0\{1 + \phi_1(\boldsymbol{v})\}$ and using suitable expansion of $\phi_1(\boldsymbol{v})$. The method has been developed in detail by [2.9, 2.10] and extended subsequently by many researchers for the case in which the local Maxwellian equilibrium distribution function is Maxwellian:

$$f_0 = \left(\frac{m_\alpha}{2\pi T_\alpha}\right)^{3/2} \exp[-m_\alpha (\boldsymbol{v}_\alpha - \boldsymbol{u}_\alpha)^2 / 2T_\alpha] \tag{2.31}$$

where the temperature T_α and mean velocity $\boldsymbol{u}_\alpha$ are functions of space coordinates and time.

This allows the construction of the linear transport matrix formalism, which relates a set of *thermodynamic forces* $\boldsymbol{X}_i$ that are gradients of state variables, and *fluxes* Γ_i that are 'canonically conjugate' in the sense that the (positive) rate of increase of entropy is expressed as

$$\dot{\Sigma} \equiv -\sum_\alpha \int \mathrm{d}^3 v \, \ln(f_\alpha) C_\alpha = -\sum_{i=1}^{N} \boldsymbol{X}_i \Gamma_i . \tag{2.32}$$

While there is not a unique choice and definition of the 'canonically conjugate' pairs $\boldsymbol{X}_i$ and Γ_i, the linear transport model assumes that each flux be related linearly to the combination of thermodynamic forces through a matrix of

transport coefficients L_{ij}:

$$\vec{\Gamma} = [L_{ij}] \cdot \vec{X}. \tag{2.33}$$

Diagonal coefficients relate each flux to its main driving mechanism, the gradient of a state variable, off-diagonal ones represent the cross-effect of different thermodynamic forces and according to Onsager, in a magnetized plasma, they fulfil the condition $L_{ij}(\vec{B}) = \pm L_{ij}(-\vec{B})$.

In experiments where hot plasmas are confined magnetically, the transport properties depend on the elementary collision processes as well as on the constraints imposed by the magnetic field geometry on the particles' motion. The *topological genus* of the closed surfaces suitable to keep a plasma in equilibrium by effect of the magnetic field is a *torus*, on which a point may be identified, for instance, by co-ordinates $(r, \vartheta, R\phi)$. The magnetic field is the helical resultant of a *toroidal* component $\boldsymbol{B}_\phi$ and a *poloidal* component $\boldsymbol{B}_\vartheta$, *tangent* to nested toroidal surfaces of constant pressure (magnetic surface). The magnetic field lines wind helically with pitch $q = rB_\phi/RB_\vartheta$ on surfaces of constant magnetic flux that are isobars. If the winding number q is *irrational*, the isobar–isoflux surfaces are covered *ergodically*; if q is a *rational* number, the lines of force are *closed* and the corresponding magnetic surface is 'fragile', being potentially resonant to helical field perturbations with the same pitch that grow unstable. The physics of the tokamak as a device for the confinement, in a closed volume, of the charged particles of a hot plasma by magnetostatic forces is of considerable complexity [2.1, 2.6, 2.8, 2.25, 2.27]; it is beyond the scope of this chapter and this book to describe it in just few words, but it is advised to become acquainted with it through the recent excellent review presentations by Wesson [2.31] and by Kadomtsev [2.21] and for more advanced study, the book by Hazeltine and Meiss [2.12] is very good.

The magnetic field introduces different time and space scales for the motion of each species parallel and perpendicular to it. The different transport regimes for each species can be classified in terms of the comparison of these basic scales with the collisional ones.

The conventional definition of 'classical' transport is appropriate in the case when the effective random walk step of a particle is of the order of its Larmor radius, $\Delta x \cong \rho_\alpha$ and, for instance, the classical diffusion rate for electrons is $D_{e_{\text{Class}}} \approx \rho_{\text{e}}^2 \nu_{\text{e}}$ [2.26, 2.29]. A finite value of the '*inverse aspect ratio* r/R' of the torus introduces important toroidal effects, related to the $1/R$ dependence of the magnetic field that traps a class of particles in a magnetic well on the outboard side of the magnetic equilibrium configuration. In this case, the appropriate theory is the neo-classical one based on another elementary random walk step size, related to the 'radial' width of the reflected particles' orbits, typically $\Delta x \cong \rho_{\alpha\vartheta}$, the poloidal Larmor, leading to three regimes of diffusion, according to the value of the collision frequency.

In neo-classical theory [2.14], both the thermodynamic forces $\boldsymbol{X}_i$ and fluxes Γ_i are defined as *averages* over a magnetic surface thereby forcing $\boldsymbol{X}_i$ and Γ_i to depend only on the surface label, e.g. the small radius r, making the transport problems formally one-dimensional again.

In summary, the central questions addressed by transport theory in magnetized plasmas are: (a) what are, for each species separately, the collision-induced plasma flows and currents; (b) what are the irreducible levels of the plasma transport coefficients: electrical resistivity, particle diffusion, heat conductivity, momentum relaxation time, etc; finally (c) what is the dependence of these quantities on the state variables of the plasma (density, temperature, magnetic field, aspect ratio of the magnetic configuration).

Although neo-classical theory is considered the rock-bottom theory of transport, providing the lower limit to transport effects, real experiments show largely anomalous values, attributed to different kinds of turbulence and instability regimes.

In general, this latter point leads to empirical or theory based non-linear 'scaling' of the transport coefficients that is of great interest. It is *not* the purpose of this text to address plasma transport theory but this short resumé is meant to provide the connection between the plasma transport problems and the specific problems analysed here, in which certain aspects of non-linearity in the transport coefficients and in the source terms dominate over the standard classification of the transport regimes.

In practice, the problems discussed will stem from appropriate variants of the continuity equation (2.26) and the energy balance equation (2.30). One of the key issues of thermonuclear fusion research is the attainment of long time scales of confinement of the plasma thermal energy produced by the reactions and by additional power input. A precise definition of a physically meaningful 'confinement time' is needed and we report here the derivation of such a concept from the energy balance equation relating the desired confinement time constant to that which is measurable. To be clear, we reconsider the energy balance equation (2.30) for a single fluid plasma model with the specification of the physical meaning of each term:

$$\begin{aligned}
\frac{\partial}{\partial t}\left[\tfrac{3}{2}nT\right] + \nabla\cdot\left[\tfrac{3}{2}nT\boldsymbol{u}\right] &= -nT\nabla\cdot\boldsymbol{u} - \nabla\cdot\boldsymbol{Q} + \eta J^2 + P_{\text{aux}} \\
&\quad (P_{\text{convection}} \quad P_{\text{compress}} \quad P_{\text{conduction}} \quad P_{\text{Ohm}} \quad P_{\text{aux}}) \\
&\quad - \sum \frac{T_{\text{e}} - T_{\text{i}}}{\tau_{\text{eq,i}}} - \sum \frac{T_{\text{e}} - T_{\text{n}}}{\tau_{\text{eq,n}}} \\
&\quad (P_{\text{exch e–i}} \qquad P_{\text{exch e–n}}) \\
&\quad - \sum \chi_i n_{\text{e}} n_{\text{i}-1} \langle\sigma v\rangle_{\text{I}} - \sum \tfrac{3}{2} T n_{\text{e}} n_{\text{i}} \langle\sigma v\rangle_{\text{R}} \\
&\quad (P_{\text{ioniz}}) \qquad\qquad (P_{\text{recomb}}) \\
&\quad - P(T)_{\text{rad}}.
\end{aligned}$$

To establish the energy loss per second of confined plasma, it is *convenient* to introduce the times of energy *confinement* and *recycling*

$$\tau_{\mathrm{E}} = \frac{E}{\int_S [\frac{3}{2} nTv + Q]\,\mathrm{d}S}; \quad \tau_{\mathrm{E}_{\mathrm{recycle}}} = \frac{E}{\int [\eta J^2 + P_{\mathrm{aux}}]\,\mathrm{d}V} \tag{2.35}$$

with the definitions of total thermal energy

$$E = \int_v \tfrac{3}{2} nT\,\mathrm{d}V \tag{2.36}$$

and bolometric power

$$P_{\mathrm{bolo}} = \int_v [P_{\mathrm{rad}} + P_{\mathrm{ion}} + P_{\mathrm{e}-i} + P_{\mathrm{compr}}]\,\mathrm{d}V. \tag{2.37}$$

One obtains the global power balance

$$\frac{1}{E}\frac{\mathrm{d}E}{\mathrm{d}t} = \frac{1}{\tau_{\mathrm{E}_{\mathrm{recycle}}}} - \left\{\frac{1}{\tau_{\mathrm{E}}} + \frac{P_{\mathrm{bolo}}}{E}\right\}. \tag{2.38}$$

What is *wanted* is the confinement time and what is *measurable* is the recycling time

$$\tau_{\mathrm{E}_{\mathrm{recycle}}} \approx \frac{\langle \frac{3}{2} nT \rangle V}{V_{\mathrm{loop}} I + \langle P_{\mathrm{aux}} V \rangle}. \tag{2.39}$$

Just in *steady state*, one has

$$\frac{1}{\tau_{\mathrm{E}}} = \frac{1}{\tau_{\mathrm{E}_{\mathrm{recycle}}}} - \frac{P_{\mathrm{bolo}}}{E}. \tag{2.40}$$

The search of empirical scaling laws of *this* τ_{E} may make sense. The theoretical models for 'transport theory' that should allow prediction of τ_{E} for the design of new devices have failed so far to account for the experimental evidence.

The empirical *scaling laws* that to-date are recognized to best fit most tokamaks are scaling valid for Ohmic discharges [2.5]

$$\tau_{\mathrm{E}} \propto naR^2\sqrt{q} \tag{2.41}$$

and for auxiliarly heated tokamaks plasmas the so called L-mode Kaye–Goldston scaling [2.7], valid for tokamak plasmas with minor radius (and boundary conditions) defined by a material limiter:

$$\tau_{\mathrm{E}}^{\mathrm{Kaye-Goldston}} = 0.052 A_i^{0.5} k^{0.25} I^{0.85} \bar{n}_{19}^{0.1} a^{0.3} R^{0.85} B^{0.3} P_{\mathrm{aux}}^{-0.5}. \tag{2.42}$$

A remarkably unfavourable aspect of this confinement regime is its degradation for increasing auxiliary power. A possible *formal* explanation of this phenomenon can be found by investigating the similarity properties of the heat transport equations, as outlined in chapter 6, but its real physical origin in terms of microscopic mechanisms of energy transfer across the confining magnetic surfaces is not yet understood.

In 1982, on the ASDEX tokamak of the Max Planck Institut für Plasma Physik in Germany, a new more favourable confinement regime was found in a plasma configuration with the equilibrium defined by a magnetic separatrix not touching the material first wall [2.30]. Later this regime was reproduced in other important tokamaks with divertor configuration [2.28].

Above a certain power threshold, roughly proportional the toroidal magnetic field, a sudden transition [2.16] may occur to a regime of improved confinement with an enhancement factor $H \sim 2$–2.5 of τ_{E} with respect to the L-mode regime.

The most recent scaling obtained from databases of all the relevant tokamaks [2.31] is in current notation:

$$\tau_{\mathrm{E}}^{\mathrm{L-Mode96}} = 0.023 A_i^{0.2} k^{0.64} I^{0.96} \bar{n}_{19}^{0.4} a^{-0.06} R^{1.89} B^{0.03} P_{\mathrm{aux}}^{-0.73}. \tag{2.43}$$

The transition to the new regime, called H-mode, is marked by:

(a) a sudden drop of level of the recombination radiation at the magnetic stagnation point(s);
(b) a sudden increase of plasma density;
(c) suppression of gross MHD activity;
(d) a large increase of the stored thermal energy;
(e) a marked increase of the temperature gradient near the plasma edge, within a layer of the order of the ion banana width, with appearance of a 'thermal barrier' originally called 'temperature pedestal'.

The phenomenon is still not fully explained and new varieties of enhanced regimes have appeared since the first discovery.

The transition to the H-mode has been interpreted also as a relaxation process toward an 'optimal' configuration energetically favoured [2.17–2.21].

In chapter 6, the analysis by the central expansion method has been shown to help in the identification of the basic elements of the confinement scaling and in [2.32] the formation of the temperature pedestal was obtained. The concepts and definitions introduced here will be useful in the applications presented in chapter 6.

In the following, we attempt a presentation of different and sometimes unusual physical phenomena, with indication of the need of rigorous formal treatment without pursuing it obsessively to avoid distracting from the interest in the physical aspects of the problems. The reader is therefore encouraged to consult the appropriate references for in-depth study of the formal aspects, which, for conciseness cannot be dealt with in this context.

2.1 Evolution Equations

In the previous section, the problem of the dynamics of an enormous number of (idealized) charged material points has been recast as a problem for 'field' variables of a mathematical continuum.

It has been shown that a very general form of the evolution equations for a 'fluid' model of a system is that of generalized-coupled rate of change equations for the generic density fields $Y_\alpha(\boldsymbol{x}, t) \equiv \{n_\alpha, \boldsymbol{u}_\alpha, T_\alpha, \ldots\}$:

$$\frac{\partial Y_\alpha(\boldsymbol{x}, t)}{\partial t} = -\nabla \cdot [\boldsymbol{u} Y_\alpha(\boldsymbol{x}, t) - \vec{\vec{D}} \cdot \nabla Y_\alpha(\boldsymbol{x}, t)] + S_\alpha - Q_\alpha. \tag{2.1.1}$$

The source–sink terms S_α and Q_α may represent external input of power, density, electric field and are generally known non-linear functions of local plasma parameters, or they describe non-linear interspecies processes such as ionization, recombination or radiative power losses. The closure of the system of equations requires, in general, a phenomenological relation linking the velocity of the process to the state of the system and the local instantaneous amplitude of the other fields leading to expressions of the type $S_\alpha = \sum_k Y_{\alpha,k} c_{\alpha,k} y_\alpha^{p_k}$ and $Q_\alpha = \sum_k V_{\alpha,k} e_{\alpha,k} y_\alpha^{q_k}$ where $Y_{\alpha,k}(x)$ and $V_{\alpha,k}(x)$ account for explicit space inhomogeneity of the sources and sinks, respectively and $c_{\alpha,k}$ and $e_{\alpha,k}$ are constant weighting coefficients.

In the particular, but significant case $\boldsymbol{u} = 0$ which *decouples* from fluid dynamics and includes binary process involving the densities of two species, equations (2.1.1) take the form of *reaction–diffusion equations* [2.24]:

$$\frac{\partial Y_\alpha(\boldsymbol{x}, t)}{\partial t} = -\nabla \cdot [\vec{\vec{D}} \cdot \nabla Y_\alpha(\boldsymbol{x}, t)] + c_\alpha Y_\alpha^{p_\alpha} \tag{2.1.2}$$

which owe their name to their role in the study of kinetics of chemical reactions, but are of interest here because this form covers also the equations of several problems of heat and particle transport in multispecies plasmas, namely in thermonuclear conditions. These partial differential equations belong to the class of second-order parabolic equations and have attracted considerable attention because of their ubiquitous appearance in science and their interesting mathematical properties. The majority of these studies have been concerned with Cauchy problems and even neglecting non-linear loss effects, no general ana-

lytic solution in terms of known transcendental functions can be found because Painlevè criteria are violated (absence of movable singularities other than simple poles) [2.15]. General approximation methods of treating the problems of this type of non-linear equation must resort to preliminary, physically based ordering of time and space scales to allow the use of a variety of approximate methods. However, many interesting results escape systematic approximation procedures and can be found more conveniently by *ad-hoc* transformations of both the independent and the dependent variables, which lead to directly integrable equations or allow synthetic understanding of the properties of the solution in appropriate representation spaces.

These techniques are well founded, but often not systematic, except for the topological methods of phase space analysis. The most useful approach is therefore the presentation of a collection of instructive examples that may become the paradigms of treatment of many new problems. In the following chapters, we shall attempt an organization of significant examples considering in detail, exact solutions of the typical non-linear reaction–diffusion equations.

References

[2.1] Artsimovich L A 1972 Tokamak devices *Nucl. Fus.* **12** 215

[2.2] Balescu R 1998 *Transport Processes in Plasmas parts 1 and 2* (Amsterdam: North Holland)

[2.3] Bernstein I B 1974 Transport in axisymmetric systems *Phys. Fluids* **17** 547

[2.4] Braginskii S I 1965 Transport processes in a plasma *Reviews of Plasma Physics* ed Leontovich M A (New York: Consultants' Bureau) vol. I p 205

[2.5] Coppi B and Mazzuccato E 1979 Transport of electron thermal energy in high temperature plasmas *Phys. Lett.* **71A** 337

[2.6] Galeev A A and Sagdeev R Z 1963 Transport phenomena in rarefied plasma in troidal magnetic traps *ZhETF* **53** 338 (in Russian)

[2.7] Goldston R J 1984 Energy confinement scaling in tokamaks *Plasma Phys. Contr. Fus.* **26** 1A 87

[2.8] Gorbunov E P and Razumova K A 1963 Effect of strong magnetic field on magnetohydrodynamic stabilty of plasma and confinement of charged particles in the tokamak device *Atomic Energy* **15** 363 (in Russian)

[2.9] Grad H, 1949a Note on n dimensional hermite polynomial *Comm. Pure Appl. Math.* **2** 325

[2.10] Grad H 1949b On the kinetic theory of rarefied gases *Comm. Pure Appl. Math.* **2** 331

[2.11] Grad H 1967 Toroidal containment of a plasma *Phys. Fluids* **10** 137

[2.12] Hazeltine R D and Meiss J D 1992 *Plasma Confinement* (Redwood City, CA: Addison Wesley)

[2.13] Hinton F L and Hazeltine R D 1976 Theory of plasma transport in toroidal confinement systems *Rev. Mod. Phys.* **48** 239

[2.14] Hirschman S P and Sigmar D J 1981 Neoclassical transport of impurities in tokamak plasmas *Nucl. Fus.* **21** 1079
[2.15] Jancel R and Wilhelmsson H 1991 Quasilinear parabolic equation: some properties of physical significance *Phys. Scripta* **43** 393
[2.16] Lackner K 1989 Confinement regime transitions in ASDEX *Plasma Phys. Contr. Fus.* **31** 1629
[2.17] Lazzaro E *et al* 1989 Relaxation model of H-modes in JET *Plasma Phys. Contr. Fus.* **31** 1199
[2.18] Lazzaro E and Minardi E 2000 Privileged negative- or low magnetic shear equilibria in auxiliarly heated tokamaks *J. Plasma Phys.* **63** 1
[2.19] Minardi E 1999 Transition thresholds and transport properties of the H state in the light of the magnetic entropy concept *J. Plasma Phys.* **62** 319
[2.20] Kadomtsev B B 1987 Self-organisation in tokamak plasma *Sov. J. Plasma Phys.* **13** 771
[2.21] Kadomtsev B B 1992 *Tokamak Plasma; a Complex Physical System* (Bristol: IOP)
[2.22] Klimontovich Yu I 1967 *The Statistical Theory of Non-Equilibrium Processes in a Plasma* (New York: Pergamon)
[2.23] Krall N A and Trivelpiece A W 1973 *Principles of Plasma Physics* (New York: McGraw-Hill)
[2.24] Nicolis G and Prigogine I 1977 *Self-Organisation in Nonequilibrium Systems* (New York: Wiley)
[2.25] Sakharov A D 1958 Theory of magnetic thermonuclear fusion reactor (part 2) *Plasma Physics and Problems of Controlled Fusion* Akademia Nauk SSSR vol. I 20–30 (in Russian)
[2.26] Spitzer L 1962 *Physics of Fully Ionized Plasmas* (New York: Interscience)
[2.27] Tamm 1958 Theory of magnetic thermonuclear fusion reactor (part 1) *Plasma Physics and Problems of Controlled Fusion* Akademia Nauk SSSR vol. I 3–19 (in Russian)
[2.28] Tanga A *et al* 1987 Magnetic separatrix experiments in JET *Nucl. Fus.* **27** 1877
[2.29] Van Kampen N G and Felderhof B U 1967 *Theoretical Methods in Plasma Physics* (New York: Wiley)
[2.30] Wagner F and ASDEX Team 1982 Regime of improved confinement and high beta in neutral-beam heated divertor discharges of the ASDEX tokamak *Phys. Rev. Lett.* **19** 1408
[2.31] Wesson J 1987 *Tokamak*s (Cambridge, UK: Oxford University Press)
[2.32] Wilhelmsson H 1993 Pedestal break-point formation of fusion plasma profiles – a possible tool for diagnostics *Phys. Scripta* **47** 278

Chapter 3

Modelling a System with a Finite Number of Variables

In the previous chapter, a procedure has been briefly outlined to reduce the study of the dynamics of all the plasma particles to that of the evolution of a denumerable or, under suitable assumptions, finite number of state variables, in the form of continuum fields. Since the degrees of freedom are now the amplitudes of the field variables at each *observation point* their number is still infinite. Furthermore, the type of the evolution differential equations is still formidable as they are non-linear and partial, PDE. There is scope for further simplifications without destroying essential information. A strong motivation is that in the real world, all the concrete information about the state of a system is always available (even in principle!) only in terms of a finite number of values (amplitudes, phases) of the field variable under study (still an abstract quantity!). In some cases, it is indeed possible to extend to configuration space the procedure used to construct moments in velocity space.

In principle, consider the simplest example of a first-order fluid evolution equation, presently supposed with linear sources

$$\frac{\partial Y_\alpha}{\partial t} = -\nabla \cdot [\boldsymbol{u} Y_\alpha] + S(Y_\alpha). \tag{3.1}$$

Taking some suitable complete basis of orthonormal functions $\{\psi_k(\boldsymbol{x}, t)\}$, one may expand the field variable and the source function

$$\begin{aligned} Y_\alpha(\boldsymbol{x}, t) &= \sum_k c_k^\alpha \psi_k(\boldsymbol{x}, t), \quad \boldsymbol{v}(\boldsymbol{x}, t) \\ &= \sum_k \boldsymbol{b}_k \psi_k(\boldsymbol{x}, t), \quad S(\boldsymbol{x}, t) = \sum_k s_k \psi_k(\boldsymbol{x}, t) \end{aligned} \tag{3.2}$$

where the coefficients are defined in terms of a suitable scalar product in the relevant functional space, $c_k^\alpha = (u_\alpha, \psi_k), \boldsymbol{b}_k = (\boldsymbol{u}, \psi_k), s_k = (S, \psi_k)$ and obtain a set of infinite rate equations for the field amplitudes, necessarily coupled with the momentum balance equation (not written here for brevity).

$$\frac{\mathrm{d}c_k^\alpha}{\mathrm{d}t} = -\sum_{k'} c_{k-k'}^\alpha \boldsymbol{b}_{k'} \cdot [(\nabla\psi_{k'}, \psi_{k-k'}) + (\psi_{k'}, \nabla\psi_{k-k'})] + s_k. \tag{3.3}$$

In most cases, the higher-order amplitudes are of decreasing amplitude and further truncation is possible reducing the system to the description of a *finite* number of amplitudes.

The procedure is applicable also in the general and most important case of non-linear evolution equations [3.3]. However, since the use of a complete basis yields complicated convolution products, it may be possible and convenient to define *ad hoc* synthetic labels of the field variables associated with integral properties, such as energy, or characteristics of the envelope shape of solutions, e.g. a suitable amplitude, width, skewness. The evolution of these concentrated variables will be determined by coupled first-order ODEs in time and their study may take advantage of topological methods of phase space and of the advanced theory of non-linear systems and bifurcation theory. In this way, a synthetic view of the dynamics of the systems is often possible, achieving great insight even with a limited amount of explicit calculations.

The procedure to obtain such a description of a system eventually in a finite dimensional space is, of course, not unique and not systematic and there is always the risk of missing out important physics, when the reduction is too drastic or based on unclear *a priori ordering* of the relevant effects. However, this motivates a rational review and orderly collection of interdisciplinary applications, which on one hand produce new, sometimes unexpected results that guide full-blown numerical simulations, and on the other can help progress in achieving a higher standard of rigour.

We shall consider examples in burning plasma physics transport problems, in non-linear electromagnetic waves and in the description of some non-linear resistive MHD perturbations.

3.1 Non-linearities due to Inelastic Collisions

The collision operator indicated symbolically in the previous chapter takes naturally different forms and plays a different role according with the type of interaction considered and the physical regimes considered. The main broad distinction is, however, between the two classes of elastic and inelastic processes among the interacting species, which have different properties with respect to conservation of number of particles, momentum and energy. For the purposes of

our presentation, it is sufficient to recall the qualitative aspects of some interesting processes.

We summarize first non-linear processes that are important in low-temperature and partially ionized plasmas and therefore are important in the formation stage of most plasma experiments, but are less relevant for the conditions required in fusion experiments.

An important channel of electron energy loss in plasmas is due to inelastic collisions of the electrons with the residual neutral atoms present in the plasma, and their subsequent excitation to higher energy levels. The minimum energy for excitation of electron energy levels is of the order of 10 eV. The information on the excitation cross-section is available from experiments for many atoms. The cross-section is a fast growing function of energy, just below the excitation threshold, with a maximum close to the threshold, followed by a decaying behaviour, due to the decrease of the interaction time of the electron with the atom. The inelastic collisions lead to the formation of atoms in excited states, which last typically 10^{-8} s before relaxation through emission of radiation. The concentration of excited atoms at energy level j is determined by the collision frequency and the state lifetime, so that the ratio of excited to normal atoms is $n_j/n_0 = \nu^{0j}\tau_j$ [3.4, 3.2].

Of course, disexcitation of an excited atom leads to the inverse process $e + a^0 \leftrightarrow a^j + e$ of formation of electrons with energy equal to the difference between impact energy and excited energy level. The rate of ionization in plasma is determined by the total ionization cross-section $\sigma_a^i(v)$

$$\left(\frac{\partial n}{\partial t}\right)_{\mathrm{i}} = \langle \sigma_{\mathrm{a}}^{\mathrm{i}}(v)v\rangle n_{\mathrm{e}} n_{\mathrm{a}} \tag{3.1.1}$$

where the average is performed over the distribution of electrons with energy exceeding the ionization threshold $k_{\mathrm{i}} = \langle \sigma_a^{\mathrm{i}}(v)v\rangle$ is called the constant of the process. Besides the direct ionization process, in some instance two-step ionization events may be important in electron–atom collisions and consist first of an inelastic collision between an electron and an atom, which goes into an excited state, followed by a further collision between the excited atom and another electron, ending up in an ion and two electrons. The rate of secondary ionization is then determined by

$$\left(\frac{\partial n}{\partial t}\right)_{\mathrm{is}} = k_{\mathrm{i}}^{\mathrm{s}} n_{\mathrm{e}}^2 n_{\mathrm{a}} \tag{3.1.2}$$

with a constant of the process $k_{\mathrm{i}}^{\mathrm{s}}$ being a function of electron temperature.

The inverse process of neutralization of an ion by recombination with low-energy plasma electrons, interacting for a sufficiently long time, is another important case of inelastic collisions, which decreases the number of charged

particles at a rate

$$\left(\frac{\partial n}{\partial t}\right)_{\mathrm{r}} = -\alpha_{\mathrm{r}} n^2 \tag{3.1.3}$$

where $n = n_{\mathrm{e}} = n$ and $\alpha_{\mathrm{r}} = \langle \sigma^{\mathrm{r}}_{\mathrm{ei}}(v) v \rangle$ is the recombination coefficient.

The recombination processes are complex, and require a three-body interaction (e.g. two electrons and one ion or two ions and one electron) to satisfy momentum and energy balance. The recombination occurs in two phases, which in a semiclassical mechanics description, may be summarized as a first capture of a free streaming electron into a bounded orbit around a (positively) charged ion, corresponding to a highly excited state and then a transition of the electron to much lower bounded energy level through emission of a radiation quantum or a collision with an electron. Therefore, radiative recombination may occur with emission of a quantum of radiation associated with the formation of a neutral atom and this is the inverse of a process of photoionization. This process becomes more important at lower densities and higher temperatures. Also a form of dissociative recombination exists where neutralization of a molecular ion is accompanied by dissociation of the molecule into two neutral atoms. The recombination coefficients for the various processes are decreasing functions of temperature. An estimate of α_{r} for a recombination involving two electrons with an ion is $\alpha_{\mathrm{r}} \approx 10^{-25} n T_{\mathrm{e}}^{-9/2}$ [cm^3 s^{-1}] and $\alpha_{\mathrm{r}} \approx 10^{-13} T_{\mathrm{e}}^{-1/2}$ [cm^3 s^{-1}] for radiative recombination. Here temperature is in eV and density in cm^{-3}.

These are examples of non-linear source or loss terms that may appear in particle balance equations describing complex processes.

Inelastic collisions of ions with neutral atoms and with other ions are similar but more complex processes producing non-linear rates of accretion of charged species. In the formal discussion of the equations governing the evolution of particles species which follows, the coefficients k_{i}^s and α_{r} will be labelled generically as c or e, taken constant, to be intended of the corresponding order of magnitude, when referring to modelling of ionization–recombination events.

As anticipated, the relevance of these processes depends on the temperature regime of the plasma considered. In the models discussed in the following paragraphs, the magnitude of the various non-linear terms is expressed by symbolic coefficients (for instance a, c, s; see list of symbols) that must be appropriately evaluated in terms of realistic plasma parameters in each case. The interest here is primarily that of studying the formal properties of these solutions.

In the context of fusion research, the most important collision processes are, of course, those occurring at high temperature between light ions (typically deuterium and tritium) resulting in thermonuclear reaction with production of particles with high kinetic energy (typically 14 MeV neutrons) and helium nuclei (alpha particles):

$$\mathrm{D} + \mathrm{T} \rightarrow \mathrm{He}^4(3.5\ \mathrm{MeV}) + n(14\ \mathrm{MeV}). \tag{3.1.4}$$

The fusion power density released by a D–T reaction is

$$P_\alpha = P_{\mathrm{DT}} = 5.6 \times 10^{-13} n_{\mathrm{D}} n_{\mathrm{T}} \langle \sigma v \rangle_{\mathrm{DT}} \,[\mathrm{erg\ s^{-1}}] \tag{3.1.5}$$

with $\langle \sigma v \rangle_{\mathrm{DT}} = 3.68 \times 10^{-12} \mathrm{T}^{-2/3}\, \mathrm{e}^{-19.94 T^{-1/3}}$ [$\mathrm{cm^3\ s^{-1}}$].

It is worth recalling that for a reactor-grade device confining plasma with equal ion and electron temperatures the most common criteria to define fusion power production performances are [3.6]:

(a) *breakeven conditions*, reached when the total fusion power produced balances the (total) input power. Fusion conditions are then self-sustained as long as D and T fuel is supplied;
(b) *ignition*, attained when the power absorbed by particles during the fusion is equal to the power lost by radiation, conduction, and convection;
(c) *Lawson criterion*, expressed in terms of a minimum value of the triple product $nT\tau_{\mathrm{E}}$ (τ_{E} is the energy replacement time); it is fulfilled when the energy recovered by fusion reactions is equal to all the energy required to sustain the fusion conditions (assuming 30% efficiency in the conversion of the heat produced by slowing down the neutrons to electrical energy).

In hot plasma oriented to fusion, the other non-linear processes that are relevant in determining a power balance are radiative losses and auxiliary heating input. We mention here the electron–ion bremsstrahlung power density loss, important for frequencies away from the cyclotron frequencies and their harmonics:

$$P_{\mathrm{brems}} = \left(\frac{8\pi Z^2 e^6}{3 m_{\mathrm{e}} c^3 \hbar} \right) n_{\mathrm{e}} n_{\mathrm{i}} v_{\mathrm{th_e}}. \tag{3.1.6}$$

Furthermore, one has to consider the cyclotron (synchrotron) radiation yielding a power loss

$$P_{\mathrm{synch}} = 5 \times 10^{-24} B^2 n^2 T^2 \quad [\mathrm{erg\ s^{-1}}]. \tag{3.1.7}$$

These source and loss terms are embodied in one-dimensional transport equations (2.26) and (2.30) that then take the specific reaction–diffusion form of interest.

3.2 Exact Solutions of Reaction–Diffusion Equations in the Presence of Losses

A realistic problem in the field of hot plasmas confined in a magnetic configuration is characterized by time and space scales dictated both by the

macroscopic magnetostatic force balance condition and by the microscopic particles motion, and the relevance of effects related to strong non-linear sources and sink effects has to be assessed in each case with specification of the order of magnitude of the non-linear terms. In order to frame a problem correctly, it is useful to have a rather detailed knowledge of the properties of formal solutions of this type of equations, and this is the scope of this chapter. The essential physical processes of diffusion and reaction occurring simultaneously lead to special solutions, which do not exist if only one kind of process contributes to the dynamics of the system [3.1, 3.11, 3.12]. Exact solutions are rare in these conditions and systematic analytic methods of approximation are also cumbersome. Although modern computing techniques *may* overcome the practical difficulty of solving even huge systems of non-linear PDEs, it is of great importance to be able to provide insight and guidance through analytic calculations, through the construction of particular solutions, which may become the paradigm of more complex situations.

Before considering applications to realistic problems of a magnetically confined plasma where the configuration size is determined by the designed MHD equilibrium condition, we examine in some detail the striking properties of paradigmatic cases of solutions of reaction–diffusion equations, where the size of profiles is governed by the competition of source and loss terms.

Consider the one-dimensional equation, with non-linear source and sink terms

$$\frac{\partial n}{\partial t} = \frac{\partial}{\partial x}\left[D\frac{\partial n}{\partial x}\right] + cn^p - en^q. \tag{3.2.1}$$

Here $n(x, t)$ describes the particle density, c and $e > 0$ are constant coefficients representing sources and losses, respectively, D is a non-linear diffusion coefficient of the form $D = an^\delta$ and a, $p > 1$ and $\delta > 0$ are constants.

Interesting results concern exact particular solutions of equation (3.2.1), which for particular choice of parameters were obtained for the Ginzburg–Landau equation in the case of a subcritical bifurcation [3.7, 3.9]. Here, we present the results for a wider range of combination of parameters and make comparisons with other exact particular solutions.

Assume a particular solution of the form

$$n = A \text{ sec } h^\lambda(x/L) \tag{3.2.2}$$

with $\lambda \neq 0$.

Equation (3.2.1) is satisfied by expression (3.2.2) if

$$\begin{aligned} \lambda(p-\delta-1) &= 2 \\ \lambda(q-\delta-1) &= 0 \end{aligned} \tag{3.2.3}$$

and

$$A = \left[\frac{e(p+q)}{2cq}\right]^{1/(p-q)} \tag{3.2.4}$$

$$L = \frac{2}{p-1}\left(\frac{qa}{e}\right)^{1/2}.$$

For the special choice, $\delta = 0, p = 3, q = 1$ and $\lambda = 1$, one recovers the previous results of Turytsin.

We point out that equation (3.2.1) is satisfied exactly with the combinations of parameters shown in the following table.

δ	p	q	λ
0	3	1	1
0	2	1	2
$-1/2$	5/2	1/2	1
$-1/2$	3/2	1/2	2

Using the expansion $\sec h(x/L) = 2\sum_{k=0}^{\infty}(-1)^k \exp[-(2k+1)(x/L)]$ and

$$(1+x/L)^n = \sum_{k=0}^{n}\binom{n}{k}(x/L)^k$$

one obtains the expansion for $\sec h^{\lambda}(x/L)$, for $x < L$:

$$\begin{aligned} \sec h^{\lambda}(x/L) = 1 &- \frac{\lambda}{2}(x/L)^2 + \frac{\lambda}{24}(3\lambda+2)(x/L)^4 \\ &- \frac{\lambda}{720}(75\lambda-14)(x/L)^6 + \cdots \end{aligned}$$

For the sake of comparison, it is interesting to note that exact particular solutions to equation (3.2.1) with $\partial n/\partial t \neq 0$ exist in cases where: (a) the source term is missing ($c = 0$), $\delta = -1/2$ and $q = 1/2$ and when (b) the loss term is absent ($e = 0$) and $p = \delta + 1$.

Introducing conveniently renormalized variables $x \to x\sqrt{ea}$, and $t \to et$, one gets for case (a), absence of source:

$$n = \frac{9}{16}(t_0 - t)^2 \ \text{sec}\ h^4(x\sqrt{2}/4) \tag{3.2.5}$$

where t_0 denotes the finite time, from time $t = 0$ during which the solution relaxes to zero from a given initial value. Analogously for case (b), absence of losses, one has:

$$n = \left(\frac{2p}{p^2 - 1}\right)^{1/(p-1)} (t_0 - t)^{-1/(p-1)} \ \cos^{2/(p-1)}[x(p-1)/2\sqrt{p}\ ] \tag{3.2.6}$$

with $p = \delta + 1,\ \delta \neq 0$ and the time t_0 is now the time of blow-up of the solution from the initial value.

It is noteworthy that for $p = 1/2$, and $\delta = -1/2$, solution (3.2.6) can be obtained from solution (3.2.5) through the complex transformation of variables $t \to -t$ and $x \to \mathrm{i}x$. The exact solutions presented correspond to cases without spatial boundary conditions but can be extended to consider the effects of boundaries.

As shall be discussed further, the solutions of the type (3.2.5) and (3.2.6) have attractor-like properties, in the sense that 'nearby' states tend to be attracted to the particular shapes defined by the exact solutions.

This property can be thought to be related to the problem of stiffness and profile consistency often assumed to characterize the temperature profiles of hot plasmas confined in tokamak magnetic configuration.

The temperature profiles of fusion plasmas often exhibit two equilibria, one corresponding to high temperatures and another to low temperatures. In the model described by equation (3.2.1) in the absence of a loss term $(e = 0)$ only the 'high-temperature' formal solution exists, and it is stable and could be said to have attractor-like properties. In the presence of losses $(e \neq 0)$, the 'low-temperature' solution appears, but it is unstable. The exact solution defined by expression (3.2.2) with (3.2.3) and (3.2.4) corresponds to the 'low-temperature' unstable equilibrium that vanishes in the absence of losses.

The results obtained for the special case $\delta = 0$, and $p = 3$, and $q = 1$ as well as the generalized solutions just presented could be a model for understanding fusion plasma equilibria. Similar questions are also encountered in laser physics in connection with the generation of femtosecond pulses.

3.3 Explosive Instabilities of Reaction–Diffusion Equations

In the basic fluid model of plasma physics, the energy transport and continuity equations, with non-linear source and loss terms, have the form of generalized

reaction–diffusion equations similar to those occurring in many fields of science, in physics as well as in chemistry or biology. The essential physical processes of diffusion and reaction occurring simultaneously lead to special solutions, which do not exist if only one kind of process contributes to the dynamics of the system [3.11, 3.12]. Particularly interesting phenomena occur when the non-linear reaction term drives solutions of large amplitude.

As a result of balance between the diffusion and reaction terms amplitudes grow to infinity in a finite time interval. This type of instability is classified as explosive. In spite of the fact that there are no general solutions in the presence of diffusion, it is possible and instructive to demonstrate in detail the existence of astonishingly simple particular ones [3.10] with exact analytical methods.

Let us consider the one-dimensional continuity equation, with a source term representing, for instance, a one-dimensional model of an electron–ion recombination process:

$$\frac{\partial n}{\partial t} = \frac{\partial}{\partial x}\left[D\frac{\partial n}{\partial x}\right] - bn + cn^p \tag{3.3.1}$$

Here $n(x,t)$, describes the particle density, b and $c > 0$ are constant coefficients, D is a non-linear diffusion coefficient of the form $D = an^\delta$ and a, $p > 1$, and $\delta > 0$ are constants.

Interesting cases are $\delta = 1$ (fully ionized gas), and $p = \delta + 1$ because the equation is separable in time and space. This property is essential for analysis and has important consequences for the results. Through the transformation

$$n = N\mathrm{e}^{-bt}, \quad \tau = [(p-1)b]^{-1}[1 - \mathrm{e}^{-(p-1)bt}]. \tag{3.3.2}$$

The linear dissipative term is removed and the equation obtained has the same aspect of equation (3.3.1) with $b = 0$ and the space and time renormalizations $(c/a)^{1/2}x \to x$ and $ct \to t$.

It is convenient therefore to consider the preliminary case with $b = 0$. Then equation (3.3.1) is transformed into

$$\frac{\partial n}{\partial t} = \frac{\partial}{\partial x}\left[n^\delta\frac{\partial n}{\partial x}\right] + n^p. \tag{3.3.1$'$}$$

The class of explosive solutions can be investigated considering a *similarity transformation* of the dependent and independent variables

$$n(x,t) = \phi(\xi)(t_0 - t)^\mu \tag{3.3.3}$$

$$\xi = x/(t_0 - t)^\nu. \tag{3.3.4}$$

The exponents μ and v are determined inserting relations (3.3.3) and (3.3.4), the space and time renormalization of equation (3.3.1) and matching powers of $(t_0 - t)$

$$\mu = -1/(1-p), \quad v = \tfrac{1}{2}(1 + \mu\delta) \tag{3.3.5}$$

and the following non-linear ODE is obtained for $\phi(\xi)$

$$\frac{\partial}{\partial\xi}\left[\phi^{\delta}\frac{\partial\phi}{\partial\xi}\right] = \frac{1}{p-1}\phi - \phi^{p} + \frac{1}{2}\left[1 - \frac{\delta}{p-1}\right]\xi\frac{\partial\phi}{\partial\xi}. \tag{3.3.6}$$

Explicit integration is possible in the cases where $\delta = p - 1$, e.g. (a) $p = 2$, $\delta = 1$ or (b) $p = 3$, $\delta = 2$. In this case, the last term on the r.h.s. of (3.3.6) vanishes and $\xi = x$.

In case (a), the equation is

$$\frac{\partial}{\partial\xi}\left[\phi\frac{\partial\phi}{\partial\xi}\right] = \phi - \phi^{2} \tag{3.3.7}$$

and in case (b),

$$\frac{\partial}{\partial\xi}\left[\phi^{2}\frac{\partial\phi}{\partial\xi}\right] = \frac{1}{2}\phi - \phi^{3}. \tag{3.3.8}$$

Equations (3.3.7) and (3.3.8) can be integrated by multiplying both sides by $\phi\,(\partial\phi/\partial\xi)$ and $\phi^{2}\,(\partial\phi/\partial\xi)$, respectively. The result of equation (3.3.7) is expressed implicitly as:

$$x - x_0 = \pm\frac{\sqrt{6}}{2}\int_{\phi_0}^{\phi}\frac{\phi\,\mathrm{d}\phi}{\sqrt{\phi^{3} - \phi_{\mathrm{c}}^{3} - \frac{3}{4}(\phi^{4} - \phi_{\mathrm{c}}^{4})}} \tag{3.3.9}$$

where ϕ_{c} is a constant of integration. Choosing $\phi_{\mathrm{c}} = 0$ or $\phi_{\mathrm{c}} = 4/3$, the result is identical. In the particular case $x_0 = 0$, $\phi_{\mathrm{c}} = 4/3$, equation (3.2.9) can be integrated and inverted yielding

$$\phi = \tfrac{2}{3}[1 + \cos(x/\sqrt{2})] \tag{3.3.10}$$

and consequently from the space and time renormalization of equation (3.3.1)

$$n(x,t) = \frac{1}{2}\frac{n_0}{1 - \frac{3}{4}cn_0t}\left[1 + \cos\left(x\sqrt{\frac{c}{2a}}\right)\right] \tag{3.3.11}$$

showing that for $p = 2$, $\delta = 1$ and $\mu = -1$, the density evolves explosively from an initial value n_0 over a time scale $(\frac{3}{4}cn_0)^{-1}$.

From equation (3.3.8), the corresponding calculation yields:

$$x - x_0 = \pm\frac{1}{2}\int_{\phi_0}^{\phi} \frac{\phi^2 \mathrm{d}\phi}{\sqrt{\phi^4 - \phi_c^4 - \frac{4}{3}(\phi^6 - \phi_c^6)}} \tag{3.3.12}$$

which can be explicitly integrated choosing indifferently $\phi_c = 0$ or $\phi_c = \sqrt{3}/2$ leading to $\phi = \sqrt{3}/2[1 + \cos(x/\sqrt{3})]$ and again an explosive behaviour for $p = 3$, $\delta = 2$, and $\mu = -(1/2)$:

$$n(x,t) = \frac{n_0}{[1 - \frac{4}{3}cn_0^2 t]^{1/2}} \cos^2\left(x\sqrt{\frac{c}{3a}}\right). \tag{3.3.13}$$

This is an exact explosive localized solution (ELS) of the reaction–diffusion problem considered. In figure 3.1, the time development is plotted for a shape preserving solution (3.3.11) of equation (3.3.6), corresponding to $p = 2$ and $\delta = 1$, that has an explosive type of evolution, while remaining localized in space. Therefore the notation ELS, for explosive localized solution, is used here and in the following. To distinguish it from 'soliton', the name 'singleton', is also sometimes used for ELS. The principal difference is that whereas a soliton is produced by the balance between the physical processes of dispersion and non-linear creation, a singleton refers to the balance between diffusion and non-linear creation. The theory of reaction–diffusion type should not, however, be confused with a trivial extension of, or parallel to, soliton theory.

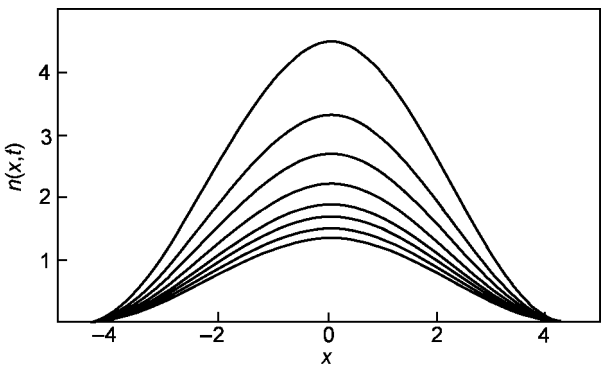

Figure 3.1. Explosive localized solution (ELS) for $p = 1 + \delta$, $\delta = 1$ and $\gamma = 0$, exhibiting the non-linear growth given by expression (3.3.13).

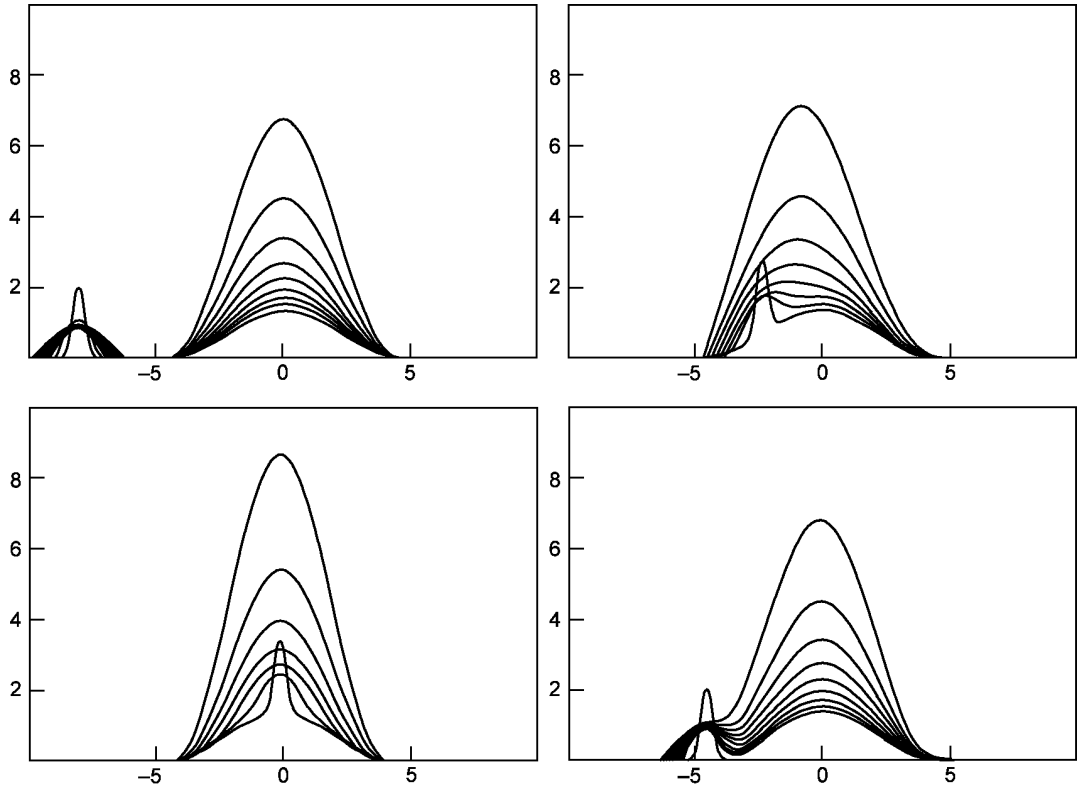

Figure 3.2. Evolution and interaction of a narrow profile and an ELS for various mutual positions in the initial state, and for $p = 1 + \delta$, $\delta = 1$ and $\gamma = 0$ given by expression (3.3.11).

The reaction–diffusion equations do not admit, as the soliton equations do, expansions in terms of non-linear elements (e.g. singletons) and the treatment of reaction–diffusion problems may therefore be considered, in principle, more difficult and in practice, more elaborate than the soliton problems.

The half-width for the ELS for the case $p = 2$ and $\delta = 1$ of this example follows from the expression (3.3.11) to be determined by $x\sqrt{c/2a} = \pi/2$. It can, therefore, be large or small according to the ratio of the diffusion and source term coefficients.

In figure 3.2, the evolution and interaction of a narrow profile and an ELS ($p = 2$ and $\delta = 1$) is plotted for various mutual positions of the particles. From the figure, one concludes that the narrow profile vanishes with time, since the steep profile wings give rise to strong diffusion, spreading the profile, whereas the ELS grows explosively with preserved shape.

In figure 3.3, two narrow profiles interact to form finally one ELS. The originally steep profiles widen and diminish in amplitude before their mutual interaction transforms them to one structure that approaches asymptotically an exploding ELS.

At this stage, one can easily extend the solutions (3.3.11) and (3.3.13) to include the linear dissipation (or growth) represented by the term $-bn$ in equation (3.3.1). For $b \neq 0$, we therefore apply the ttransformation (3.3.2). The time of explosion becomes $t_\infty = -b^{-1}\ln[1 - b\tau_\infty]$ where τ_∞ is the corresponding explosion time in absence of damping, e.g. $\tau_\infty = \frac{4}{3}(n_0 c)^{-1}$ and $\tau_\infty = \frac{4}{3}(n_0 c)^{-1}$ for the two cases, respectively. For $b\tau_\infty > 1$, the growth will be

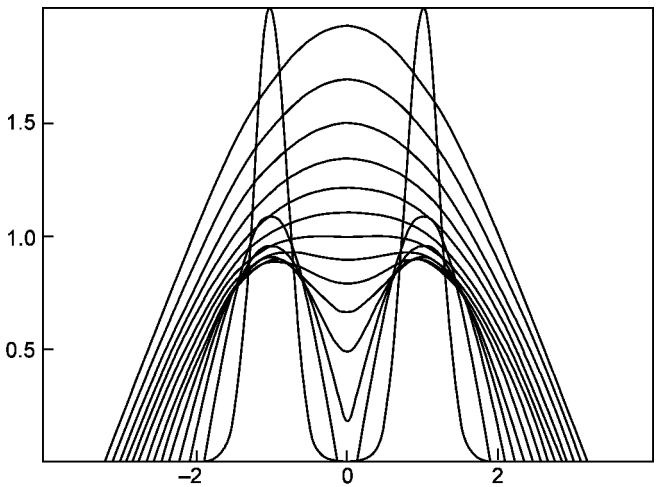

Figure 3.3. Evolution and interaction of a two profiles of initial widths smaller than that of an ELS. Each profile widens due to the steep gradients, mutual interaction carries asymptotically the total structure in the shape of a single ELS.

limited to such an extent that explosion will not occur in a *finite* time but only asymptotically for t approaching infinity.

A further interesting extension, which has a likeness with the dynamics of coupled wavepackets discussed in chapter 9, describes the coupled interaction of two populations

$$\begin{aligned}\frac{\partial n_1}{\partial t} &= \frac{\partial}{\partial x}\left[D_1 \frac{\partial n_1}{\partial x}\right] + c_1 n_1^2 + g_1 n_1 n_2 \\ \frac{\partial n_2}{\partial t} &= \frac{\partial}{\partial x}\left[D_2 \frac{\partial n_2}{\partial x}\right] + c_2 n_1^2 + g_2 n_1 n_2.\end{aligned} \tag{3.3.14}$$

Here, we propose the example $D_1 = D_2 = A(n_1 + n_2)$, $n_j = a_j n$ $(j = 1, 2)$ where n is solution of

$$\frac{\partial n}{\partial t} = a \frac{\partial}{\partial x}\left[n \frac{\partial n}{\partial x}\right] + cn^2$$

given by expression (3.3.11).

In this case, the individual solutions are obtained with:

$$a_1 = \frac{c_2 - g_1}{c_2 c_2 - g_1 g_2}, \quad a_2 = \frac{c_1 - g_2}{c_2 c_2 - g_1 g_2}$$

where $a = A(a_1 + a_2)$ in the expression (3.3.11). Similar solutions and considerations for coupled equations apply also in the case $\delta = 2$ and $p = 3$.

3.4 Self-formation and Evolution of Singletons

The examples of explosive solutions of non-linear reaction–diffusion equations described in the previous section can be generalized to higher dimensions—one, two and three—and new explicit solutions can be found with several striking properties. The non-linear explosive time evolution may preserve certain particular localized space profiles. Thus, depending on the initial conditions, the solutions may have the form of isolated, compact support structures that have been called 'singletons' or periodic structures called 'polytons'. They can exist in one, two or three dimensions.

Saturation effects typically lead to the formation of a density maximum in time for a singleton followed by a non-linear decay, which mirrors the explosive growth phase. Repetitive 'explosions' in time of singletons or polytons may also occur as a result of non-linear saturation effects.

It is of fundamental importance that nearby 'states' are attracted to the singletons. Consequently, the singletons have the property of *self-formation* and

a variety of initial space profiles tends to approach a singleton form when the time approaches the explosion time. Singletons are stable against perturbations with scale length smaller than one-fourth of the singleton's width. At explosion time, the amplitude may remain finite when non-linear saturation effects are included. In the decay phase, the perturbation returns to the initial profile.

A generalization of the equation (3.2.1) to one, two and three dimensions is:

$$\frac{\partial n}{\partial t} = x^{-\gamma}\frac{\partial}{\partial x}x^{\gamma}\left[D\frac{\partial}{\partial x}\right] - bn + cn^{p} \tag{3.4.1}$$

where $\gamma = d - 1$ is related to the dimensions d, $p > 1$ and the diffusion coefficient scales as $D = an^{\delta}$.

Proceeding as in section 3.2, the linear dissipative term can be eliminated by suitable transformations of the independent and dependent variables and the resulting equation

$$\frac{\partial n}{\partial t} = x^{-\gamma}\frac{\partial}{\partial x}x^{\gamma}\left[n^{\delta}\frac{\partial}{\partial x}\right] + cn^{p} \tag{3.4.2}$$

for $p = \delta + 1$ has a solution of a form that generalizes (3.3.11) and (3.3.13)

$$n(x,t) = \Phi_0(t_0 - t)^{(p-1)^{-1}}\cos^{\lambda}[x/L - \varepsilon(x/L)^3] \tag{3.4.3}$$

where $\lambda = 2/(p-1)$, $\varepsilon = \gamma/12(3+\gamma)$ and the typical amplitude and fundamental pulse width are

$$\Phi_0 = \left[\frac{2p + \gamma(p-1)}{p^2 - 1}\right]^{(p-1)^{-1}} \tag{3.4.4}$$

$$L^2 = \frac{2}{(p-1)^2}[2p + \gamma(p-1)]. \tag{3.4.5}$$

Expression (3.4.3), which is symmetrical in x and has a bell-shaped profile, is an exact solution of equation (3.4.2) for $\gamma = 0$ as we have seen in the preceding section, and for $\gamma = 1, 2$ it satisfies equation (3.4.2) up to $O(x^2)$ if $\Phi(x)$ is expanded up to $O(x^4)$.

Indeed since $1 + \cos[x/\sqrt{2}] = 2\cos^2[x/2\sqrt{2}]$ equations (3.3.10) and (3.4.3) coincide for $\gamma = 0$, $p = 2$ $(\delta = 1)$. If initially at $t = 0$, the spatial profile of $n(x,0)$ has the shape

$$\Phi(x,0) = \tfrac{4}{3}\cos^2[x/2\sqrt{2}] \tag{3.4.6}$$

Table 3.1. Shapes of singleton and polyton.

State	Initial condition	Region
Singleton	$\Phi = \Phi(x)$	$0 < x < x_c$
	$\Phi = 0$	$\lvert x\rvert > x_c$
Polyton	$\Phi = \Phi(x)$	All x ($\gamma = 0$)

the time evolution of $n(x,t)$ will be explosive maintaining its shape. The initial shape (3.4.6) could be restricted within the interval $|x| \leq x_c \equiv \pi/\sqrt{2}$ with $\Phi(x,0) = 0$ outside: it would then be a 'singleton' of fixed form localized in space at all times up to the explosion time. Alternatively, the initial condition could be periodic in space giving rise to an explosive 'polyton', as summarised in table 3.1.

3.5 Non-linear Saturation Effects

The explosive time behaviour may be limited by mechanisms of non-linear saturation, which in the case of equation (3.3.2) with $\delta = 1$ and $p = 2$, lead to a modification of the type

$$\frac{\partial n}{\partial t} = \pm\Lambda(n)\left[\frac{1}{2}\frac{\partial^2 n^2}{\partial x^2} + n^2\right] \tag{3.5.1}$$

with a saturation factor containing two control parameters (a_1, a_2)

$$\Lambda(n) = \left\{1 - n^2\left(a_1 - \frac{a_2}{n^4}\right)^2\right\}^{1/2}. \tag{3.5.2}$$

The solution of equation (3.5.1) with $a_2 = 0$ can be written

$$n(x,t) = [(t_1 - t)^2 + a_1^2]^{-1/2}\Phi(x). \tag{3.5.3}$$

The meaning of expression (3.5.3) is that the solution evolves in time after the time in which it reaches its peak and being even in $t - t_1$ takes up the same values at times $t = t_1 \pm |\Delta t|$.

3.6 Stability of Explosive Localized Solutions, ELS

The simplicity of expression (3.3.11)

$$n(x,t) = \frac{1}{2}\frac{n_0}{1 - \frac{3}{4}cn_0 t}\left[1 + \cos\left(x\sqrt{\frac{c}{2a}}\right)\right]$$

allows an easy investigation of the stability properties of the ELS [3.14].

Let us assume that a small perturbation $\Delta n(x,0)$ is superimposed to the initial state:

$$\Delta n(x,0) = \varepsilon n_0 \cos[(x - x_1)/L_1]. \tag{3.6.1}$$

Substituting this expression in equation (3.3.1), one obtains

$$\frac{\partial \Delta n(x,\tau)}{\partial \tau} = \frac{\partial}{\partial x}\left[n\frac{\partial \Delta n}{\partial x}\right] + \frac{\partial}{\partial x}\left[\Delta n \frac{\partial n}{\partial x}\right] + 2n\,\Delta n = -[L_1^2 - 2]n\,\Delta n \tag{3.6.2}$$

having used $\left.\dfrac{\partial \Delta n}{\partial x}\right|_{x_1} = 0$. From the r.h.s. of equation (3.6.2) near $x \approx x_1$ one obtains

$$\frac{\Delta n(x,\tau)}{\Delta n(x,0)} = [1 - \tfrac{3}{4}n_0\tau]^{\beta} \tag{3.6.3}$$

with the exponent $\beta = \frac{2}{3}[L_1^{-2} - 2][1 + \cos(x/\sqrt{2})]$, which is positive for $L_1^2 \leq 1/2$. Therefore, in these conditions, the perturbation is quenched when $\frac{3}{4}n_0\tau \to 1$. Otherwise, for perturbation with width comparable to the zero-order solution, the exponent would be negative and the perturbation would be explosive on the same time scale of the ELS.

3.7 Attraction to the Form of a Singleton for States of Various Initial Widths and Amplitudes

The discussion of the properties of the singleton solutions leads naturally to the question of the dynamic evolution toward this type of solution of arbitrary initial perturbations. The form of the solution (3.4.3) can be extended from

$$\Phi(x,t) = \Phi_0(t_0 - t)^{-(p-1)^{-1}} \cos^{\lambda}[(x/L) - \varepsilon(x/L)^3] \tag{3.7.1}$$

to

$$\Phi(x,t) = \Phi_0(t_0 - t)^{-(p-1)^{-1}} \cos^{\lambda}[\varepsilon^{-1/2}\sin(\varepsilon^{1/2}x/L)] \tag{3.7.2}$$

showing that the notion of localized solution requires further explanations. The latter expression may or may not correspond to a localized solution depending on the choice of initial conditions.

It is then appropriate to introduce a specific technique of analysis of localized solutions, which has proven useful in a variety of non-linear problems [3.11, 3.12] and that will be generalized and applied extensively in our examples. The 'polyton' solution (3.4.3) may be considered a particular case of a class of solutions of (3.2.1) of the general form

$$n(x,t) = A(t)F(x/L(t)) \tag{3.7.3}$$

where both the amplitude $A(t)$ and the width $L(t)$ are considered as functions of time, to be determined by the constraints of matching arbitrary initial conditions and dynamic ODEs obtained from the original PDE for $n(x,t)$ by direct substitution and appropriate ordering in some small parameter, without suppression of the non-linear character of the problem. The advantages of this seemingly cumbersome procedure will be pointed out and discussed in the following chapters.

When an initial profile has a width not coinciding with that of expression (3.4.3), we must consider the evolution of $A(t)$ and $L(t)$. In our example, with $\delta = p - 1$,

$$F(x/L) = \cos^{\lambda}[(x/L) - \varepsilon(x/L)^3]. \tag{3.7.4}$$

For clarity, the dynamic equations are obtained here explicitly as introduction to a more general procedure described in chapter 4:

$$\frac{\partial A}{\partial t}F - A\frac{x}{L^2}F'\frac{\partial L}{\partial t} = \frac{A^p}{L^2}\left[F^{p-1}F'' + (p-1)F^{p-2}(F')^2 + \frac{\gamma}{x/L}F'F^{p-1}\right] + A^pF^p \tag{3.7.5}$$

where the prime on F indicates derivation with respect to x/L. Expanding equation (3.7.5) with $\lambda = 2/(p-1)$ and $\varepsilon = \gamma/12(3+\gamma)$ from expression (3.4.3), to second order in x/L and matching terms up to $(x/L)^2$ included, one obtains for $p = \delta + 1$, two coupled equations which govern the non-linear evolution of $A(t)$ and $L(t)$:

$$\frac{1}{A}\frac{\partial A}{\partial t} = -A^{p-1}\left[\frac{2(1+\gamma)}{(p-1)L^2} - 1\right] \tag{3.7.6}$$

$$\frac{1}{L^2}\frac{\partial L^2}{\partial t} = -A^{p-1}\left[\frac{2[2p+\gamma(p-1)]}{(p-1)L^2} - (p-1)\right] \tag{3.7.7}$$

Substituting A from equation (3.7.7) into equation (3.7.6) and integrating one obtains:

$$\frac{A}{A_0} = \left|\frac{L_0^2}{L^2}\right|^{(1+\gamma)/[2p+\gamma(p-1)]} \times \left|\frac{L_\infty^2 - L_0^2}{L_\infty^2 - L^2}\right|^{[(p+1)/(p-1)]/|2p+\gamma(p-1)|} \tag{3.7.8}$$

where, for $p > 1$,

$$L^2 \leq L_\infty^2 \equiv \frac{2[2p + \gamma(p-1)]}{(p-1)^2} \tag{3.7.9}$$

and A_0, L_0 are the initial values of $A(t = 0)$ and $L(t = 0)$, respectively, while L_∞^2 indicates clearly the width at the explosion time.

The interesting point is that in its evolution from an arbitrary initial width L_0, the perturbation reaches an asymptotic state with a width L_∞^2 coinciding with the expression (3.4.5) of the ELS. In early stages of its evolution, the amplitude collapses to a minimum value reached when

$$L^2 = L_{A_{\min}}^2 \equiv \frac{2(1+\gamma)}{p-1}$$

as seen from equation (3.7.6).

Introducing the expression (3.7.8) for $A(t)$ in the equation (3.7.7) one can express the time t as a function of L^2:

$$t = \Lambda \int_{L_0^2}^{L^2} \left(\frac{y}{L_\infty^2 - y}\right)^{[(1+\gamma)(p-1)]/[2p+\gamma(p-1)]} \mathrm{d}y \tag{3.7.10}$$

where

$$\Lambda^{-1} = Af^{-1}(p-1)[L_0]^{(1+\gamma)(p-1)/[2p+\gamma(p-1)]}[L_\infty - L_0]^{(p+)/[2p+\gamma(p-1)]}.$$

The explosion time t_∞ can be obtained setting $L^2 = L_\infty^2$ in equation (3.7.10). Similarly, the time $t_{A_{\min}}$ for which the amplitude reaches its minimum is obtained setting $L^2 = L_{A_{\min}}^2$. The integral (3.7.10), depending on the exponents, leads to different forms of logarithmic or trigonometric functions.

As an example in the double entry table 3.2, the ratio $t_{A_{\min}}/t_\infty$ is reported for particular cases of $p = 1 + \delta$ and $d = 1 + \gamma$, illustrating that the approach to explosion, dominated by the diffusion mechanism, is preceded by an early contraction of the amplitude.

It is important to consider the general cases with $p \neq 1 + \delta$. For this purpose, it is convenient to assume an expansion of the type:

Table 3.2. Ratio of the time required for the amplitude to reach minimum and infinite values $t_{A_{\min}}/t_\infty$ for $L_0^2 \ll L_\infty^2$ from expression (3.7.10).

p	1	2	3
2	0.132	0.168	0.182
3	0.158	0.182	0.193

$$\Phi \cong \Phi_0 \left[1 - \frac{\xi^2}{\Lambda^2} + \eta \frac{\xi^4}{\Lambda^4} \right] \tag{3.7.11}$$

where the independent variable embodies the transformation (3.3.4) $\xi = x/(t_0 - t)^v$, with (3.3.5) $v = \frac{1}{2}[1 + \delta/(1-p)]$ and η and Λ are constants to be determined consistently. Proceeding as before expressions corresponding to equations (3.4.4) and (3.4.5) are obtained for the amplitude and fundamental width

$$\Phi_0 = [(p-1)K]^{-1/(p-1)} \tag{3.7.12}$$

$$\Lambda^2 = \frac{2(1+\gamma)[(p-1)K]^{1-\delta/(p-1)}}{1-K} \tag{3.7.13}$$

with the shape parameters determined so that expressions (3.7.12) and (3.7.13) coincide with equations (3.4.4) and (3.4.5) when $p = 1 + \delta$:

$$K = 1 - \frac{\delta}{p-\delta} \frac{(1+\gamma)}{(2\eta+\delta)\dfrac{3+\gamma}{p-\delta} - (1+\gamma)} \tag{3.7.14}$$

$$\eta = \frac{p-1}{2} \left[\frac{2+\gamma}{3+\gamma} - \frac{p-2}{p-1} \right]. \tag{3.7.15}$$

In the case $p = 1 + \delta$, Λ^2 corresponds to $(p-1)L^2$.

The dynamic evolution from arbitrary initial width and amplitude is obtained along the lines of the previous example setting $n(x,t) = A(t)G(\xi/\Lambda(t))$ with the ansatz expansion in ξ/Λ:

$$G \cong 1 - \left(\frac{\xi}{\Lambda} \right)^2 + \eta \left(\frac{\xi}{\Lambda} \right)^4. \tag{3.7.16}$$

For $O((\xi/\Lambda)^2)$, introducing the convenient transformation $\mathscr{L}^2(t) = \Lambda^2(t)(t_0 - t)^{1-\delta/(p-1)}$, which preserves the ratio $\xi/\Lambda = x/\mathscr{L}$, the rate equations

analogous to equations (4.2.14) and (4.2.15), but valid for $p \neq 1 + \delta$ are obtained:

$$\frac{1}{A}\frac{\mathrm{d}A}{\mathrm{d}t} = -2(1+\gamma)\frac{A^{\delta}}{\mathscr{L}^2} + A^{p-1} \tag{3.7.17}$$

$$\frac{1}{\mathscr{L}^2}\frac{\mathrm{d}\mathscr{L}^2}{\mathrm{d}t} = 2[\delta(3+\gamma)+3-p]\frac{A^{\delta}}{\mathscr{L}^2} - (p-1)A^{p-1}. \tag{3.7.18}$$

These equations admit solutions of the type

$$\frac{A}{A_0} = \left(\frac{t_\infty - t_i}{t_\infty - t}\right)^{1/(p-1)} \tag{3.7.19}$$

$$\frac{\mathscr{L}^2}{\mathscr{L}_0^2} = \left(\frac{t_\infty - t}{t_\infty - t_i}\right)^{(1-\delta)/(p-1)} \tag{3.7.20}$$

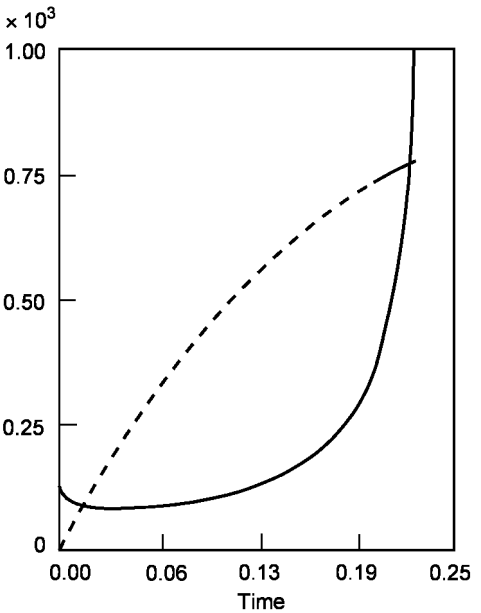

Figure 3.4. Evolution of A and L^2 for $p = 1 + \delta$, $\delta = 1$ and $\gamma = 0$, $A_0 = 25$, $\mathscr{L}_0^2 = 0.1$.

which means that there is a 'constant of motion' $(A/A_0)^{-(p-1-\delta)}(\mathscr{L}^2/\mathscr{L}_0^2) = 1$ and also for $p = \delta + 1$, $(\mathscr{L}^2/\mathscr{L}_0^2) = \text{const}$ and that for $p > 1 + \delta$ the solution for A is 'explosive' with the width collapsing in a finite time, while for $p < 1 + \delta$ it is explosive, with $\mathscr{L}^2$ diverging in finite time.

For these cases of *collapse* and *anti-collapse*, there is no transition through a minimum value of the amplitude. The previous case with exactly $p = 1 + \delta$ marks, therefore, the border between these two behaviours. The typical time evolution of the amplitude A and the squared width $\mathscr{L}^2$ is shown in figure 3.4 for the parameter choice $p = 2$, $\delta = 1$ and $\gamma = 0$ with the initial values $A_0 = 25$ and $\mathscr{L}_0^2 = 0.1$. The amplitude (full line) grows to infinity in a finite time whereas $\mathscr{L}^2$ (dashed line) reaches a limiting finite value at the same time. In figure 3.5, a case of *collapse* is described, occurring for $p = 3$, $\delta = 2$, and $\gamma = 0$ and initial value $A_0 = 1$, $\mathscr{L}_0^2 = 0.1$. The amplitude A explodes (full curve) and $\mathscr{L}^2$ (dashed line) goes to zero in a finite time. An example of *anti-collapse* is illustrated in figure 3.6, with the parameter choice $p = 3$, $\delta = 2$ and $\gamma = 0$ and $A_0 = 1$, $\mathscr{L}_0^2 = 8$. The *anti-collapse* is characterized by the explosion of both A and $\mathscr{L}^2$.

An asymptotic equilibrium with finite A and L^2 can, on the contrary, be approached with parameters $p = 3$, $\delta = 1$, $\gamma = 0$, $A_0 = 4$, and $\mathscr{L}^2 = 4$, as shown in figure 3.7.

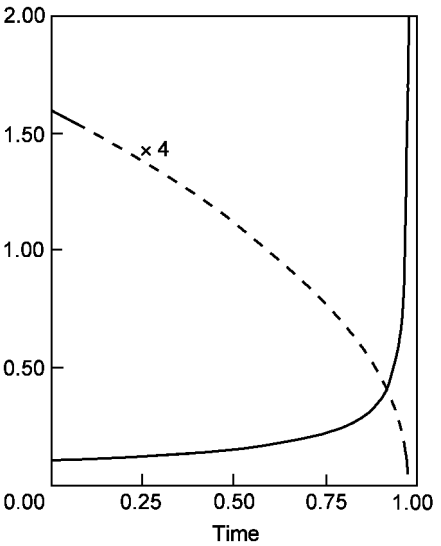

Figure 3.5. Collapse of A for $p = 2 + \delta$, $\delta = 1$ and $\gamma = 0$, $A_0 = 1$, $\mathscr{L}_0^2 = 4$.

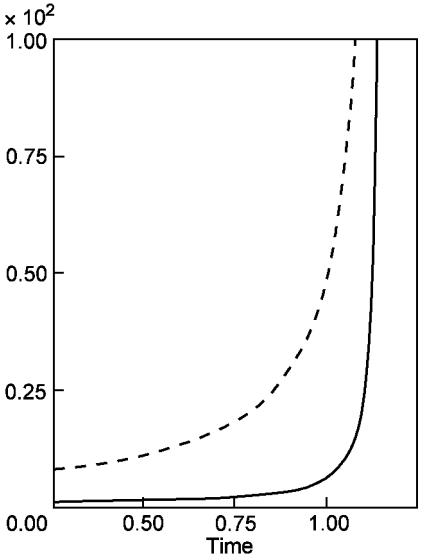

Figure 3.6. Anti-collapse of A for $p = 1 + \delta$, $\delta = 2$ and $\gamma = 0$, $A_0 = 1$, $\mathscr{L}_0^2 = 8$.

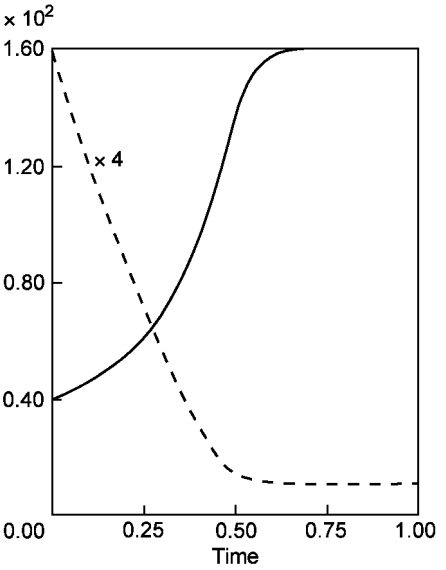

Figure 3.7. Asymptotic approach to equilibrium of A for $p = 2 + \delta$, $\delta = 1$ and $\gamma = 0$, $A_0 = 4$, $\mathscr{L}_0^2 = 4$.

3.8 Interaction of Explosive Localized Structures

The interaction of several ELS governed by coupled reaction–diffusion equations is the next subject to be discussed. The present analysis may serve as a guidance for detailed numerical studies.

Let us consider the interaction of two identical one-dimensional ELS structures that are centered at two separate points x_1 and x_2. Taking into account the effect of non-linear interaction of the two structures by introducing a modified time scale such that $\tau \to f\tau$ with $f = f(x_2 - x_1, x)$, the solution of equation (3.2.1),

$$\frac{\partial n}{\partial t} = \frac{\partial}{\partial x}\left[D\frac{\partial n}{\partial x}\right] - bn + cn^p$$

where $D = an$ and a, b, c are coefficients of terms representing diffusion linear damping $(b > 0)$ and reaction. With $p = 2$, it can be written as

$$n_\tau = (N_1 + N_2)\,\mathrm{e}^{-bt}$$

where

$$N_i = \tfrac{1}{2}\frac{N_0}{1 - \frac{1}{4}f\tau N_0}[1 + \cos((x - x_i)/\sqrt{2})] \quad (i = 1, 2).$$

When $x_2 = x_1$, i.e. there is full overlapping of the two solutions, $f = 2$. For this case, we may regard $N_\tau = N_1 + N_2$ as a superposition of two structures each evolving twice as fast as it would in the absence of the other one. When the two structures N_1 and N_2 are separated so that there is no overlap (for $x_2 - x_1 > 2\sqrt{2}\pi$), we have $f = 1$.

We analyse now the evolution in the intermediate cases. In the particular case, $x_2 - x_1 = 2\sqrt{2}\pi$, the overlap interval extends over half the width of each pulse, $N_\tau(x, 0) = N_{\tau 0}$ corresponds to the flat top in the interaction domain, and it evolves with $f = 4/3$, e.g. as

$$N_\tau(x, \tau) = \frac{N_0}{1 - N_0\tau} \quad \text{for } x_1 < x < x_2$$

whereas for $x < x_1$, $x > x_2$ the growth is determined by $f = 1$ typical of the two separate structures.

It is convenient to introduce as a measure of the change in time scale the difference $\Delta f = f - 1$. In the early stage of evolution, the diffusion term in the equation for N_i deduced from (3.2.1) can be neglected and one obtains

$$\Delta f = \frac{R}{N}$$

where

$$R = \tfrac{1}{3}\{2 + \cos((x_2 - x_1)/2\sqrt{2})\} + \cos((x_2 - x_1)/2\sqrt{2})\}$$

$$N = 1 + \cos((x_2 - x_1)/2\sqrt{2})\cos((2x - x_2 - x_1)/2\sqrt{2}).$$

For the special case, $x_2 - x_1 = \pi\sqrt{2}$, we may see that $\Delta f = 1/3$, e.g. $f = 4/3$, that is in agreement with the previous conclusion leading to relation $N_\tau(x, \tau) = (N_0/1 - N_0\tau)$.

For the case of a slight overlap with $x_2 - x_1 = \frac{3}{2}\pi$, we obtain $\Delta f = -0.15$ for $x = (x_2 + x_1)/2$, indicating that in the small interaction domain $f < 1$, the growth of the combined system is slower than for the independent components.

We may interpret this as a result of the fact that each of the separate structures experiences the influence of the other as a narrow localized perturbation that it tries to get rid of. Therefore the total effect is a reduction of the growth in the interaction domain. In the case close to complete overlap, $x = (x_2 + x_1)/2$ and $x_2 - x_1 = \pi\sqrt{2}/2$, we obtain $\Delta f = 0.80$, whereas for $x = x_1$ or $x = x_2$, $\Delta f = 7/9$.

These arguments can be extended to the interaction of three ELSs, as indicated in [3.14].

The examples discussed are meant to introduce to some of the most striking and significant properties of ELSs. The case of two interacting structures having different initial amplitudes can also be treated and leads to interesting results. It is sufficient to quote the results here.

The interaction of 'bell-shaped' structures, solutions of reaction–diffusion equations, depends on the parameter p, on their peak amplitudes, $A_1 \neq A_2$, widths L_1, L_2 and separation. In the paper by Wilhelmsson [3.17], it is shown that several regimes of interaction exist depending on the values of the mentioned parameters. Namely one may have mutual attraction of the two structures with a common explosive growth or 'run-away' of the structures from each other.

In the following chapters, it will be shown that there is a strict relation between the technique applied and the theory of similarity transformations, wherein $A(t)$ and $L(t)$ appear as *time varying* scale factors of the similarity transformation. It is shown that the procedure can be extended and used to deal with a variety of problems involving coupled equations of the reaction–diffusion type, providing insight in the nature of the solutions that normally can be obtained only by heavy numerical calculations.

The survey of the basic properties of the non-linear solutions of reaction–diffusion equations can now be considered a tool to be used to identify robust patterns of strong non-linear behaviour in more realistic problems. Of course, the goal of controlled fusion theory and experiment are not explosive solutions! Furthermore, one must be aware that the configuration equilibrium required by

fusion theory and experiment entails many open problems of stability of dissipative modes that become more and more important in supposedly long-lasting (eventually steady-state) operating conditions of a reactor.

References

[3.1] Anderson D, Jancel R and Wilhelmsson H 1984 Similarity solutions of the evolution equation describing the combined effects of diffusion and recombination in plasmas *Phys. Rev.* A30 2113

[3.2] Anders A 1990 *A Formulary for Plasma Physics* (Berlin: Akademie-Verlag)

[3.3] Dimova S and Vasileva D P 1995 Lumped-mass finite element method with interpolation of the nonlinear coefficients for a quasilinear heat transfer equation *Num. Heat Transf.* **28 B** 199

[3.4] Hasted J B 1964 *Physics of Atomic Collisions* (London: Butterworths)

[3.5] Jancel R and Wilhelmsson H 1991 Quasilinear parabolic equations: some properties of physical significance *Phys. Scripta* **43** 393

[3.6] Miyamoto K 1980 *Plasma Physics for Nuclear Fusion (*Cambridge, MA: The MIT Press)

[3.7] Pereira N R and Stenflo L 1977 Nonlinear Schrödinger equation including growth and damping *Phys. Fluids* **20** 1733

[3.8] Trubnikov B A 1965 Particles collisions in fully ionized plasma *Reviews of Plasma Physics* ed M A Leonovich (New York: Consultants Bureau) vol. 1

[3.9] Turytsin S K 1993 Nonstable solitons and sharp criteria for wave collapse *Phys. Rev.* **E47** R13

[3.10] Wilhelmsson H 1987 Explosive instabilities of reaction–diffusion equations *Phys. Rev. A* **36** 965

[3.11] Wilhelmsson H 1988 Solution of reaction–diffusion equations describing dynamic evolution towards explosive localised states *Phys. Rev. A* **38** 2667

[3.12] Wilhelmsson H 1988 Simultaneous diffusion and reaction processes in plasma dynamics *Phys. Rev. A* **38** 1482

[3.13] Wilhelmsson H, Benda M, Etlicher B, Jancel R and Lehner 1988 Nonlinear evolution of densities in the presence of simultaneous diffusion and reaction processes *Phys. Scripta* **38** 863

[3.14] Wilhelmsson H 1989 Evolution and interaction of explosive localised structures *Phys. Scripta* **39** 606

[3.15] Wilhelmsson H 1990a Explosive growth of interacting structures governed by reaction–diffusion processes with special regard to effects of asymmetry *Phys. Scripta* **42** 714

[3.16] Wilhelmsson H Jancel R 1990c Self generation and nonlinear diffusion – an analytic approach *Phys. Scripta* **41** 269

[3.17] Wilhelmsson H 1990b Diffusion, creation and decay processes in plasma dynamics: evolution towards equilibria and the role of bifurcated states *Nuc. Phys.* **A518** 84

Chapter 4

General Procedure of Central Expansion for Reaction–Diffusion Equations

After the introductory analysis of particular examples, here we consider more formally general aspects of the second-order parabolic equations with non-linear source terms. Assuming power non-linearities, the typical equation has the form, already presented:

$$x^{-\gamma}\frac{\partial}{\partial x}\left[x^{\gamma}Y^{\delta}\frac{\partial Y}{\partial x}\right]+kY^{p}-\frac{\partial Y}{\partial t}=0. \tag{4.1}$$

Such equations exhibit, as already shown, new properties linked with the existence of spatially localized solutions unbounded in the time domain (explosive type). The localization of the solutions of (4.1) is due to the non-linear competition between the dissipative and source terms; when these terms balance non-stationary dissipative structures may be formed which generalize the stationary ones well studied in the specialized literature [4.4, 4.10].

The study of such non-stationary solutions leads to new concepts, so far introduced semiempirically, such as that of a fundamental width of the solution and the relation of the characteristics of the solution to those of the non-linear medium, condensed in the exponents p and δ in the case of equation (4.1).

The structure of solutions in explosive regimes is essentially linked with properties of invariance, or self-similarity. A group theoretical analysis of the invariance properties has been performed by Jancel and Wilhelmsson [4.6] and it leads to the conclusion that for power non-linearities the evolution of the self-similar solutions is characterized by three asymptotic regimes: (a) the S regime with $p = d + 1$, in which the diffusive and source term are of the same order and lead to *localized* structures with a *fundamental width*; (b) the HS regime with $1 < p < \delta + 1$, in which the diffusive effects are dominant and the resulting unbounded self-similar states are non-localized; (c) the LS regime with

$1 < \delta + 1 < p$ in which the source terms are dominant and several self-similar localized states may exist whose number is related to the solution of an associated linear problem.

In general, the approach to the study of the properties of the solutions of the prototype problem (4.1) can be organized in the following three steps: (a) a group theoretical analysis, which allows the determination of the invariant solutions of self-similar type, which have to satisfy certain non-linear ODEs; (b) the study of this non-linear equation, which is generally non-integrable and whose solution can only be investigated qualitatively; (c) the elaboration of *ad hoc* new methods combining phase space analysis and numerical experiments to explore the behaviour of the solution over a wide range of the significant parameters p and δ in particular with the objective of assessing the structural stability of the solutions obtained. Here we give just some guidance to more general theoretical methods developed in detail in [4.6] and references therein. The outline of the fundamental procedure of determining the invariance properties of equation (4.1) is illustrated below.

The method consists in considering infinitesimal transformations of both the independent (t, x) and dependent $Y(x, t)$ variables, according to the definitions:

$$\widehat{x} = x + \varepsilon\xi(x, t, Y), \quad \widehat{t} = t + \varepsilon\tau(x, t, Y), \quad \widehat{Y} = Y + \varepsilon\eta(x, t, Y) \tag{4.2}$$

where ε is a small parameter and higher-order terms can be neglected.

The deviations (ξ, τ, η) that are functions both of the independent and the dependent variables (x, t, Y), are the components of a vector field function $\vec{\rho} \equiv \{\xi, \tau, \eta\}$ in (ξ, τ, η) space. If this transformation of variables is such as to leave some scalar function $F(x, t, Y)$ (surface in the (x, t, Y) space) invariant, this means that

$$F(\widehat{x}, \widehat{t}, \widehat{Y}) - F(x, t, Y) \cong \varepsilon\left[\xi\frac{\partial F}{\partial x} + \tau\frac{\partial F}{\partial x} + \eta\frac{\partial F}{\partial Y}\right] \equiv 0. \tag{4.3}$$

The latter form is compactly expressed in an invariance condition

$$\vec{\rho} \cdot \nabla F = 0 \tag{4.4}$$

and is in fact a quasilinear first-order PDE, which is equivalent to the characteristic system

$$\frac{\mathrm{d}x}{\xi} = \frac{\mathrm{d}t}{\tau} = \frac{\mathrm{d}Y}{\eta}. \tag{4.5}$$

The general solution depends on two parameters, one of which is taken as a new independent variable $\xi(x, t, Y)$, called the similarity variable and the other is used as a new dependent (state) variable $\widehat{Y} = \Phi(\zeta)$.

By putting such a transformation in the original PDE, an ODE for $\widehat{Y} = \Phi(\zeta)$ is obtained. This procedure is well known for the heat diffusion equation, for instance. In the following, we apply this method of looking for invariance under infinitesimal transformations, as an example, to the equation (4.1) rewritten as

$$F(x,t,Y,Y_t,Y_x,Y_{xx}) \equiv x^{-\gamma}\frac{\partial}{\partial x}\left[x^{\gamma}Y^{\gamma}\frac{\partial Y}{\partial x}\right] + kY^{p} - \frac{\partial Y}{\partial t} = 0. \tag{4.6}$$

It is convenient to consider the particular case $p \neq \delta + 1,\ \gamma = 0$ from which all the interesting cases can be deduced.

It is shown in [4.6], after a large amount of unavoidable but tedious algebra which we do not report here, that the transformation of variables that gives invariance is

$$\xi = \alpha x\left(\frac{\delta - p + 1}{2(p-1)}\right), \quad \tau = \alpha t + \beta, \quad \eta = \frac{\alpha Y}{p-1}. \tag{4.7}$$

By substitution in the equations for the characteristics and putting

$$v = -\left(\frac{\delta - p + 1}{2(p-1)}\right)$$

and $t_0 = \beta/\alpha$, one obtains the two equations:

$$\frac{\mathrm{d}v}{\mathrm{d}x} = \frac{\mathrm{d}t}{t - t_0}, \quad \frac{\mathrm{d}t}{t - t_0} = (1-p)\frac{\mathrm{d}Y}{Y}. \tag{4.8}$$

The solution of the the first part of (4.8) is clearly

$$\ln[x] = \ln|t - t_0|^{v} + C \tag{4.9}$$

where C is an integration constant and the solution can be rewritten as $x|t - t_0|^{-v} = \text{const.}$ and the new independent similarity variable can be then defined as $\zeta = x|t - t_0|^{-v}$. Integration of the second characteristic equation gives $Y = Y_0[t_0 - t]^{-1/(p-1)}$ from which the new dependent variable can be defined:

$$Y_0 = \widehat{Y} = \Phi(\zeta) = Y[t_0 - t]^{1/(p-1)}. \tag{4.10}$$

By substituting these new variables into the original PDE (4.1), one gets an ODE for $\Phi(\zeta)$:

$$\zeta^{-\gamma}\frac{\partial}{\partial\zeta}\left[\zeta^{\gamma}\Phi^{\delta-1}\frac{\partial\Phi}{\partial\zeta}\right] + k\Phi^{p} - \frac{\Phi}{p-1} - v\zeta\frac{\partial\Phi}{\partial\zeta} = 0 \tag{4.11}$$

which can be greatly simplified in the case $\nu = 0$ for which separation of variables is possible.

The class of transformations satisfying the invariance constraint expressed by (4.10) belongs to the Lie point symmetry group [4.5–4.7]. This group analysis has led to the finding that the PDE (4.1) admits quite generally (for $p \neq \delta + 1,\ \gamma \neq 0$) self-similar solutions of the type

$$Y = \Phi(\zeta)[t_0 - t]^{-1/(p-1)} \tag{4.12}$$

where $\Phi(\zeta)$ has to satisfy the ODE (4.11). In this way the self-similar transformations introduced *ad hoc* in the previous chapters appear in the frame of a general theory. The behaviour of the self-similar solutions depends therefore on the properties of the equation (4.11), which can be tackled by approximate analytic methods or numerically.

It is instructive to consider the only particular case in which equation (4.11) can be completely integrated analytically, which is the case with $\nu = 0$ and $\gamma = 0$.

In this (one-dimensional) case $\zeta = x$ and the solution of (4.11) can be found through the substitution $\Phi = u^{2/(p-1)}$ which gives:

$$uu'' + \frac{p+1}{p-1}(u')^2 + \frac{k}{2}(p-1)u^2 - \frac{1}{2} = 0 \tag{4.13}$$

which can be integrated a first time to obtain

$$\frac{\mathrm{d}u}{\mathrm{d}x} = \left\{ \frac{p-1}{2(p+1)} \left[1 - \frac{k}{2p}(p^2-1)u^2 \right] + Ku^{-2(p+1)/(p-1)} \right\} \tag{4.14}$$

where K is an integration constant. The case $K = 0$ leads to an elementary exact solution, which appears to be very important for the physical interpretation. It is indeed easily seen that for $K = 0$ the solution, up to a phase shift, is of the form:

$$u = \left[\frac{2p}{k(p^2-1)} \right]^{1/2} \cos[k(p-1)x/2\sqrt{p}]. \tag{4.15}$$

Therefore, one has for Φ the expression

$$\Phi(x) = \left[\frac{2p}{k(p^2-1)} \right]^{1/(p-1)} \cos^{2/(p-1)}\left(\frac{x}{L}\right) \tag{4.16}$$

where

$$L^2 = \frac{4p}{k^2(p-1)^2} \tag{4.17}$$

is a *fundamental length* related to the characteristic width $x_c = \pi L/2$ of the bell-shaped spatial structure $\Phi(x)$. According to the result (4.16) obtained previously, such a structure is preserved during the evolution and it corresponds to an ELS realized for *special* initial conditions.

A generalization for $K \neq 0$ is possible, leading to an exact solution given in inverse form [4.6] reported here for completeness:

$$x - x_0 = \pm\left[\frac{(p^2-1)}{2}\right]^{1/2} \times \int_{\Phi_0}^{\Phi} \left\{\chi^{p+1} - \frac{k(p^2-1)}{2p}\chi^{2p} + \frac{2K(p^2-1)}{(p-1)^2}\right\}^{-1} \chi^{p-1}\mathrm{d}\chi. \tag{4.18}$$

This expression cannot be evaluated in general in terms of known trascendental form, except for $p = 2$ when it can be reduced to elliptic integrals.

For $\delta = p - 1$ and $\gamma = 0$ this integrable case is reduced to separable variables:

$$\frac{\partial}{\partial x}\left[Y^{(p-1)}\frac{\partial Y}{\partial x}\right] + kY^p - \frac{\partial Y}{\partial t} = 0 \tag{4.19}$$

whose particular solutions can be obtained by setting $Y = A(t)\Phi(x)$. It is easily checked that the separation of variables (x, t) then leads to solutions of the form $Y = \Phi(x)(t_0 - t)^{-1/(p-1)}$ where $\Phi(x)$ obeys an equation of type (4.11)

$$\frac{\partial^2}{\partial x^2}[\Phi^p] + kp\Phi^p - \frac{p\Phi}{p-1} = 0 \tag{4.11$'$}$$

which reduces to (4.13) through the change of variable $\Phi = u^{2/(p-1)}$.

The form and properties of these exact solutions obtained for special values of the parameters p, γ and δ are essential in progressing toward methods for the general case, which are as a rule not solvable in closed form, but can be analysed by means of a generalization of the structure of the exact limiting cases.

4.1 Singular Point Analysis

The previous results have shown that the problem of solving the non-linear ODE associated with the original reaction–diffusion PDE is far from trivial and that it cannot be expected, except in special cases, that the solution can be expressed in terms of known trascendental functions. A step forward in the understanding of the properties of the ODE of type (4.11) is provided by an application of the

'Painlevé test' that, for the set of values of the parameters p and δ for which it can be conclusive, allows classification of the solutions expressible in closed form in terms of trascendentals.

The Painlevé property of an equation is the absence of 'movable' critical points of the solution of the given equation. The term 'movable' is associated to the initial conditions, that is to the integration constants. The necessary conditions are determined by the 'Painlevé test', applied to an equation of type (4.11′) written as

$$F(\Phi, \Phi', \ldots \Phi^{(n-1)}, \zeta) = 0 \tag{4.1.1}$$

where F is supposed to be a rational function of $\Phi, \Phi', \ldots \Phi^{(n-1)}$, analytic in ζ.

The procedure consists in considering an expansion of the solution in the neighbourhood of a singular point ζ_0:

$$\Phi(\zeta) = \sum_{k=0}^{\infty} \varphi_k (\zeta - \zeta_0)^{k+\alpha} \tag{4.1.2}$$

and inserting this expression in the equation, obtaining recursive relations for the coefficients, in the form of a polynomial of nth degree

$$P(k)\varphi_k = R_k(\varphi_0, \varphi_1, \ldots, \varphi_{k-1}, \zeta_0). \tag{4.1.3}$$

To have the 'Painlevé property', three conditions must be met: (a) α must be a negative *integer*; (b) the polynomial $P(k)$ has $(n-1)$ positive *integer* roots; (c) at each root ('resonance') the r.h.s. $R_k(\varphi_0, \varphi_1, \ldots \varphi_{k-1}, \zeta_0) \equiv 0$ for any value of ζ_0 and any value of φ_k.

Then the expansion (4.1.2) is a Laurent series with n arbitrary constants $(\varphi_0, \varphi_1, \ldots, \varphi_{n-1}, \zeta_0)$ representing the solution in the neighbourhood of the 'movable' singularity ζ_0. The reader should see the work by Jancel and Wilhelmsson [4.6] for detailed discussion of the examples of application of the test. Here it is sufficient to summarize that for arbitrary values of p and δ meeting the above criterion is impossible and that therefore the self-similar states of equation (4.11) corresponding to the dissipative structures cannot be described either by known higher trascendental functions or by one of the six Painlevé transcendents.

4.2 Similarity Solutions and Basis for the Central Expansion Method

The variable separation technique applicable in the case of equation (4.1.1) to obtain an exact solution has a meaning that goes beyond the technical level and

is related to the nature of similarity solutions. Indeed the amplitude $A(t)$ can be interpreted as a time-varying scaling factor of spacially similar solutions. This suggests that more general cases with arbitrary values of $\delta \neq 0$, γ and $p \neq 1$ could be handled to some order of approximation in a suitable expansion parameter, generalizing the concept of time-varying scaling factor $A(t)$ and fundamental length $L(t)$ introduced above.

It is therefore rather natural to allow some freedom in the form of the solution of an equation such as (4.1), for any value of $\delta \neq 0$, γ and $p \neq 1$, taking a suggestion from the form of one of the exactly solvable cases.

In a neighbourhood of $x = 0$ the assumed form of the solution of the equation

$$x^{-\gamma} \frac{\partial}{\partial x} \left[x^{\gamma} Y^{\delta} \frac{\partial Y}{\partial x} \right] + kY^{p} - \frac{\partial Y}{\partial t} = 0 \tag{4.2.1}$$

may therefore be of the 'central expansion' type, already introduced empirically:

$$Y(x,t) = \mathscr{A}(t) G(x/\mathscr{L}(t)) \tag{4.2.2}$$

where the scaling factors $\mathscr{A}(t)$ and $\mathscr{L}(t)$ are both functions of t only and the profile

$$G\left(\frac{x}{\mathscr{L}(t)}\right) = 1 - \frac{x^2}{\mathscr{L}(t)^2} + \eta(t) \frac{x^4}{\mathscr{L}(t)^4} - \xi \frac{x^6}{\mathscr{L}(t)^6} \tag{4.2.3}$$

may contain one more free function of time $\eta(t)$ and a free constant parameter ξ. For the case, $\eta = \text{const}$, to order $O(x^4/\mathscr{L}(t)^4)$ the equations for the determination of $\mathscr{A}(t)$ and $\mathscr{L}(t)$ are:

$$\begin{aligned} \frac{\mathrm{d} \ln \mathscr{A}(t)}{\mathrm{d}t} &= -2(1+\gamma) \frac{\mathscr{A}(t)^{\delta}}{\mathscr{L}(t)^2} + \mathscr{A}(t)^{p-1} \\ \frac{\mathrm{d} \ln \mathscr{L}(t)^2(t)}{\mathrm{d}t} &= 2\Gamma \frac{\mathscr{A}(t)^{\delta}}{\mathscr{L}(t)^2} - (p-1) \mathscr{A}(t)^{p-1} \end{aligned} \tag{4.2.4}$$

with $\Gamma = (\delta + 2)(\gamma + 3) - (\gamma - 1)$. The constant η is determined from the initial assignment $\mathscr{L}(0) = \mathscr{L}_0$.

The application of the reduced models obtained through central expansion appears to be specially suitable for the investigation of the so called physical 'scaling laws' of a complex process. Indeed the rational concept behind the search of scaling laws is the conjecture that the equations describing fundamental phenomena, if correct, should be endowed by a variety of invariance properties related to a set of similarity transformations of the physical parameters and that these properties should be reflected in the solutions. The

concept of similarity solutions is strictly linked to a rational foundation of dimensional analysis, which plays an important role in mechanics and hydrodynamics. An important contribution in this field was provided by Buckingham [4.1] with his 'π theorem'. The physical content of this theorem is that any physical law can be expressed as a relation among dimensionless variables, and consequently any fundamental theory must contain a minimum number of basic constants.

If a physical law is expressed as a relation

$$y = f(x_1, x_2, \ldots, x_N) \tag{4.2.5}$$

among N quantities, each having certain dimension $[x_i] = M^{\alpha_i} L^{\beta_i} T^{\gamma_i}$ in terms of a basic system of K physical units U_k $(k = 1, 2 \ldots, K)$ (e.g. mass M, length L, time T), global dimensional homogeneity must hold, so that

$$[y] = \prod_i M^{\alpha_i} L^{\beta_i} T^{\gamma_i} = M^{\alpha} L^{\beta} T^{\gamma}. \tag{4.2.6}$$

The set of exponents α_i^k; $i = 0, \ldots, N$; $k = 1, \ldots, K$ is a matrix of rank $r \leq \min(N, K)$.

The surprising and useful statement of the 'π theorem' is that if $y = f(x_1, x_2, \ldots, x_N)$ is dimensionally homogeneous there *exists* a monomial $p = x_1^{\mu_1} x_2^{\mu_2}, \ldots, x_N^{\mu_N}$ having the same dimensions of y, $[y] = [x_1^{\mu_1} x_2^{\mu_2}, \ldots, x_N^{\mu_N}]$, which therefore identifies the 'scaling' of y with the basic physical quantities. Furthermore $y = f(x_1, x_2, \ldots, x_N)$ can be expressed as a function $\pi = F(\pi_1, \pi_2, \ldots, \pi_{N-r})$ of $N - r$ *independent*, dimensionless variables π_i (e.g. ratios of dimensional variables) and $\pi = y/p$. If in the physical law, y the number of independent variables can be reduced by s, the solution of the problem can be called s-fold similar. If the number of independent variables is just one, then it is called self-similar.

If the units U_k are transformed by suitable scaling factors λ_k so that $\bar{U}_k = \lambda_k U_k$ then y is transformed according to

$$\bar{y} = \left(\prod_k^K \lambda_k^{\alpha_k} \right) y = \Lambda y \quad \text{and} \quad \bar{x}_i = \left(\prod_k^K \lambda_k^{\alpha_{k,i}} \right) x_i = \Lambda_i x_i. \tag{4.2.7}$$

A principle of conservation of the physical meaning of y requires that the transformed y be function of the transformed variables, $\bar{y} = f(\bar{x}_1, \bar{x}_2, \ldots, \bar{x}_N)$ which implies that

$$\bar{y} \equiv \Lambda f(x_1, x_2, \ldots, x_N) = f(\Lambda_1 x_1, \Lambda_2 x_2, \ldots, \Lambda_N x_N). \tag{4.2.8}$$

With the support of Buckingham theorem and of the techniques related to group invariant analysis of the goverrning equations, it is meaningful to investigate the scaling laws of dissipative–diffusive systems.

4.3 Non-radially Symmetric Structures Appearing in Non-linear Reaction–Diffusion Processes

Recent research on the possible solutions of non-linear reaction–diffusion equations has shed light on a striking new class of dissipative non-symmetric structures, which are solutions of equations of the type:

$$\frac{\partial u}{\partial t} = \frac{1}{x}\frac{\partial}{\partial x}\left(xu^{\delta}\frac{\partial u}{\partial x}\right) + \frac{1}{x^2}\frac{\partial}{\partial \phi}\left(u^{\delta}\frac{\partial u}{\partial \phi}\right) + u^{p} \tag{4.3.1}$$

in the space–time domain $t > 0,\ 0 < x < \infty,\ 0 < \phi < 2\pi$ and with parameters $p > 1$ and $\delta > 0$. It has been shown [4.2, 4.5–4.8] by using methods of invariant-group analysis, that equation (4.3.1) admits similarity solutions of the type:

$$u(t, x, \phi) = A(t)\Phi(\zeta, \varphi) \tag{4.3.2}$$

with the time-dependent scaling factor $A(t)$ and the independent transformed variables ζ, ϕ:

$$\begin{aligned} A(t) &= (1 - t/t_0)^{-1/(p-1)} \\ \zeta &= x(1 - t/t_0)^{-m}, \qquad m = \frac{p - \delta - 1}{2(p-1)} \end{aligned} \tag{4.3.3}$$

$$\varphi = \phi + \frac{c_0}{p-1}\ln[1 - t/t_0] \tag{4.3.4}$$

with and the ODE for the profile function $\Phi(\zeta, \varphi)$, in the intervals $10 < \zeta < \infty$, $0 < \varphi < 2\pi$:

$$\begin{aligned} &\zeta^{-1}\frac{\partial}{\partial \zeta}\left[\zeta\Phi^{\delta}\frac{\partial \Phi}{\partial \zeta}\right] + \zeta^{-2}\frac{\partial}{\partial \varphi}\left[\Phi^{\delta}\frac{\partial \Phi}{\partial \varphi}\right] \\ &\quad - \frac{p - \delta - 1}{2(p-1)}\frac{1}{t_0}\zeta\frac{\partial \Phi}{\partial \zeta} + \frac{c_0}{(p-1)t_0}\frac{\partial \Phi}{\partial \varphi} - \frac{\Phi}{(p-1)t_0} + \Phi^{p} = 0. \end{aligned} \tag{4.3.5}$$

This equation generalizes to non-radially symmetric problems the equation (3.3.6). Putting, without loss of generality, the position $t_0 = (p-1)^{-1}$, the

homogeneous solution of (4.3.5) is $\Phi_H = 1$. The problem associated to equation (4.3.1) has been studied numerically [4.3] and it has been shown that the solutions have the structure of 'explosive spirals'.

To gain an insight into the nature of these solutions, which generalize the axially symmetric explosive types presented earlier, it is instructive to report the analysis of Dimova and Vasileva [4.3] of the problem linearized around the homogeneous solution by putting

$$\Phi(\zeta, \varphi) = 1 + \alpha y(\zeta, \varphi) \quad \text{with} \quad |\alpha y(\zeta, \varphi| \ll 1. \tag{4.3.6}$$

Substituting into equation (4.3.2) and keeping the linear terms in αy, the equation for the perturbation is

$$\zeta^{-1} \frac{\partial}{\partial \zeta} \left[\zeta \frac{\partial y}{\partial \zeta} \right] + \zeta^{-2} \frac{\partial^2 y}{\partial \varphi^2} - \frac{p - \delta - 1}{2} \zeta \frac{\partial y}{\partial \zeta} + c_0 \frac{\partial y}{\partial \varphi} + (p - 1) y = 0. \tag{4.3.7}$$

It is interesting to consider particular solutions which are periodic in φ, in complex form:

$$Y_k(\zeta, \varphi) = R_k(\zeta) \mathrm{e}^{\mathrm{i}k\varphi} \tag{4.3.8}$$

with integer $k \neq 0$. The equation is linear and therefore the real and imaginary parts of the complex solution are also solutions.

The equation for the radial part $R_k(\zeta)$ is

$$\frac{\mathrm{d}^2 R_k}{\mathrm{d}\zeta^2} + \left(\frac{1}{\zeta} - \frac{p - \delta - 1}{2} \right) \frac{\mathrm{d}R_k}{\mathrm{d}\zeta} + \left(-\frac{k^2}{\zeta^2} + \mathrm{i}kc_0 + p - 1 \right) R_k = 0 \tag{4.3.9}$$

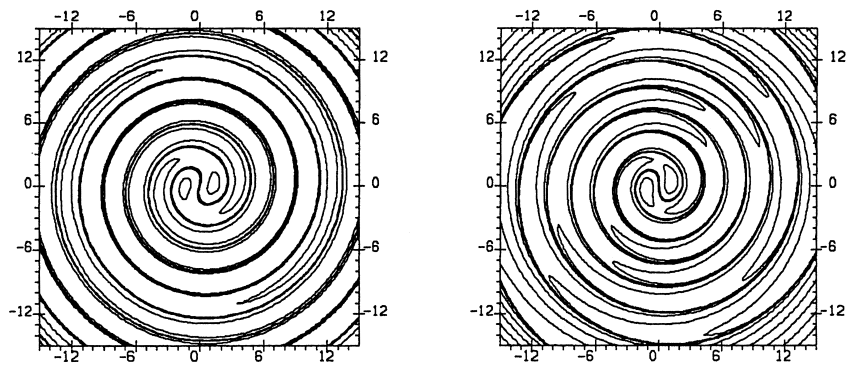

Figure 4.1. Contours of some of the linearised approximations (from *Int. J. Num Meth. Heat Fluid Flow*, **4** 497 (1994) with kind permission of the authors, S N Dimova and D P Vasileva).

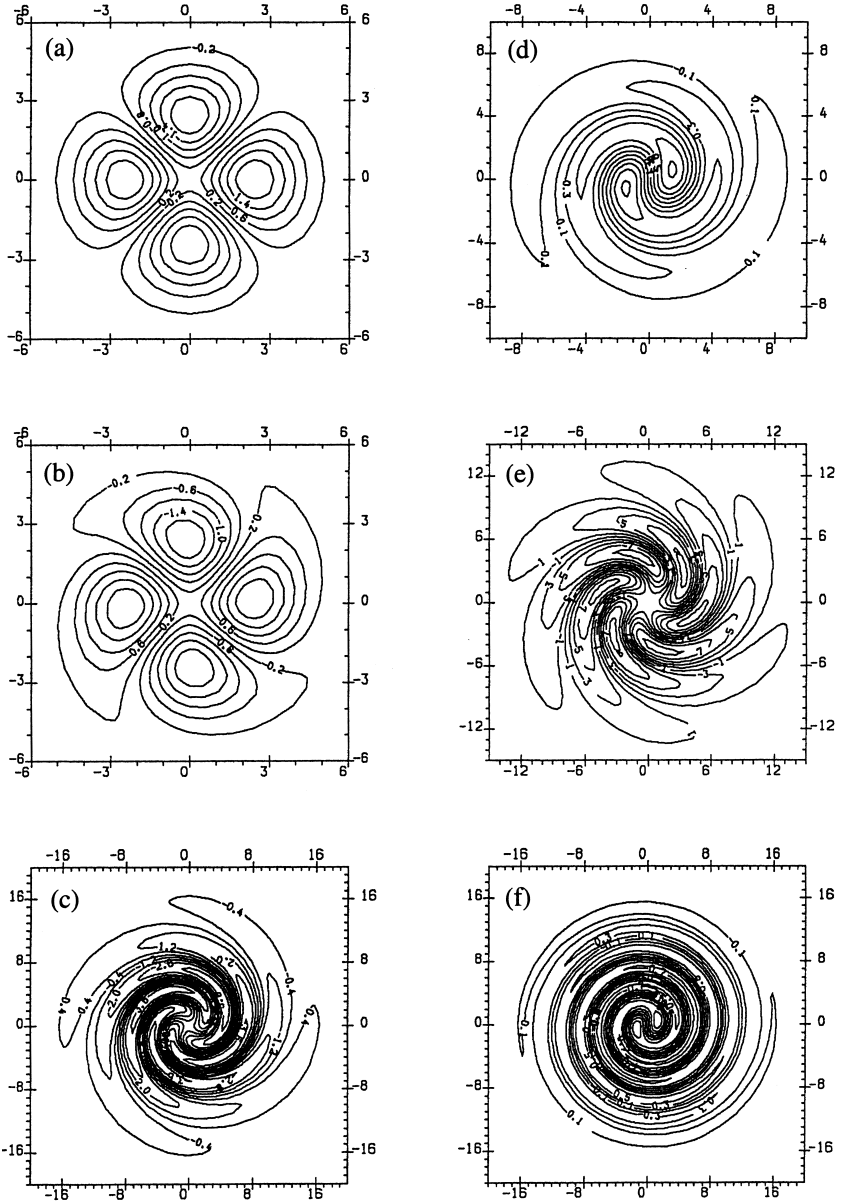

Figure 4.2. (a)–(c) Evolution of the shape of $y(x, \phi)$ depending on the parameter $c_0 (c_0 = 0, 0.1, 1)$. The other parameters are $\delta = 2$, $p = 2.4 < \delta + 1$, $k = 2$ (two-armed spiral). (d) One-armed spiral with the same δ, p and $c_0 = 1$. (e) Three-armed spiral with the same δ, p and $c_0 = 0.5$. (f) One-armed spiral with $\delta = 2$, $p = 2.8$ and $c_0 = 1$.

with the evident property

$$R_k(\zeta, c_0) = R_{-k}(\zeta, -c_0) \tag{4.3.10}$$

which allows considering $k > 0$.

For $p = 1 + \delta$, the radial function is a Bessel function of order k and complex argument

$$R_k(\zeta, c_0) = J_k(z) \quad \text{with} \quad z = \zeta\sqrt{\delta + \mathrm{i}kc_0} \tag{4.3.11}$$

and for $p \neq 1 + \delta$, the radial solution is a confluent hypergeometric function of real argument and complex parameters

$$R_k(\zeta, c_0) = \zeta^k {}_1F_1(a, b, z) \tag{4.3.12}$$

$$\alpha = \frac{p - 1 + \mathrm{i}kc_0}{p - \delta - 1} + \frac{k}{2}, \quad b = 1 + k, \quad z = \frac{p - \delta - 1}{4}\zeta^2. \tag{4.3.13}$$

To study the properties of the solutions of equation (4.3.5) in different ranges of the parameters p, δ and c_0 one may consider

$$y_k(\zeta, \varphi, c_0) = \mathscr{R}e[R_k(\zeta)\mathrm{e}^{\mathrm{i}k\varphi}] = |R_k(\zeta)|\ \cos(\arg(R_k) + k\varphi) \tag{4.3.14}$$

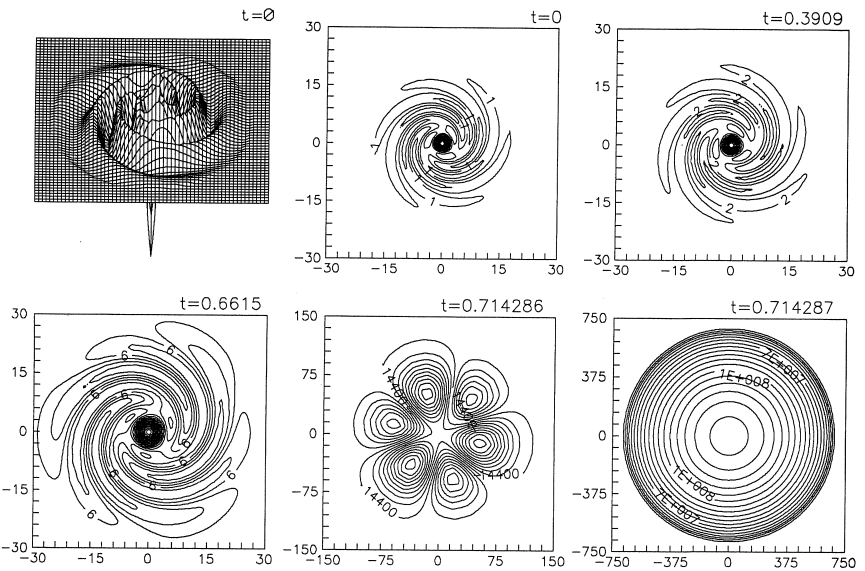

Figure 4.3. Evolution of a three-armed spiral wave for $\delta = 2$, $p = 2.4$, $c_0 = 1$, $k = 3$ from [4.9] with kind permission of the authors.

and for the reflection property (4.3.10) examine only the case $k > 0$. A thorough analysis and complete discussion requires numerical evaluation and has been done by Dimova and Vasileva [4.3] of which we reported the most significant examples. The contour plots of some of the linearized approximations are shown in figure 4.1 while in figure 4.2, the evolution of the shape of $y(x, \phi)$ is shown depending on the parameter $c_0(c_0 = 0, 0.1, 1)$. One-, two- or three-armed spiral structures may appear.

In a more recent paper [4.9], the problem for numerical realization of the exact eigenfunctions is solved for the range $p < \delta + 1$. In figure 4.3 the evolution of a three-armed spiral wave for $\delta = 2$, $p = 2.4$, $c_0 = 1$, $k = 3$ is shown.

References

[4.1] Buckingham E 1914 *Phys. Rev.* **4** 345

[4.2] Dimova S N, Kaschlev M S, Koleva M G and Vasileva D P 1991 Numerical analysis of nonradially-symmetric structures arising in non-linear reaction diffusion processes (Programming and Mathematical Techniques in Physics) *Intern. Conf. Prog. Math. Meth. Solving Phys. Problems* (eds) Yu Yu Lobanov and E P Zhidkov (Singapore: World Scientific)

[4.3] Dimova S N and Vasileva D P 1994 Numerical realization of blow-up spiral wave solutions of a nonlinear heat transfer equation *Int. J. Num. Meth. Heat Fluid Flow* **4** 497

[4.4] Galaktionov V A, Dorodnitsyn V A, Elenin G G, Kurdyumov S P and Samarskii A A 1988 The quasilinear heat conduction equation with a source: enhancement, localization, symmetry, exact solutions, asymptotic forms and structure *J. Soviet Math.* (*JOSMAR*) **41** 1163

[4.5] Groebner W 1973 *Serie di Lie e Loro Applicazioni* (Rome: Cremonese)

[4.6] Jancel R and Wilhelmsson H 1991 Quasilinear parabolic equations: some properties of physical significance *Phys. Scripta* **43** 393

[4.7] Waller S M 1990a A free parameter group similarity solution for a one dimensional non-linear diffusion equation *Phys. Scripta* **41** 193

[4.8] Waller S M 1990b Invariant group similarity solution for a class of reaction–diffusion equations *Phys. Scripta* **42** 385

[4.9] Dimova S, Kashiev M, Koleva M and Vasileva D 1998 Numerical analysis of radially nonsymmetric blow-up solutions of a nonlinear parabolic problem *J. Comp. Appl. Math.* **97** 81

[4.10] Samarskii A A, Galaktionov V A, Kurdyumov S P and Mikhailov A P 1995 *Blow-up in quasilinear parabolic equations* (Berlin: Walter de Gruyter)

Chapter 5

Phase Space Analysis

A substantial advantage gained in reducing the problem of evolution of the state of a system in the problem of evolution of a finite number of 'lumped' variables lies in the possibility of analysing, by topological methods developed for the study of *autonomous systems of differential equations*, the general *qualitative* properties of the solutions, depending on a finite number of control parameters, without need of detailed quantitative calculations. The typical set of n ODE depending on m parameters in the form:

$$\frac{\mathrm{d}Y_i}{\mathrm{d}t} = F_i(Y_1, Y_2, \ldots, Y_n,\ \alpha_1, \alpha_2, \ldots, \alpha_m) \tag{5.1}$$

describes m-fold families of the *characteristic* trajectories of the system of equations in an n-dimensional phase space of co-ordinates $(Y_1, Y_2, \ldots, Y_n)$. Each point vector $\boldsymbol{q}(t) \equiv \{Y_1, Y_2, \ldots, Y_n\}$ in the phase space represents the state of the system at time t and $\boldsymbol{p}(t) \equiv \{\dot{Y}_1, \dot{Y}_2, \ldots, \dot{Y}_n\}$ is the (generalized) momentum vector. The trajectories stemming from an initial point $\boldsymbol{q}_0 = \boldsymbol{q}(t=0)$ with initial velocity $\boldsymbol{p}_0 = \boldsymbol{p}(t=0)$ and a given vector of parameters α are regular (continuous, differentiable) except in the set of points where simultaneously all $F_i(\boldsymbol{Y}, \alpha) \equiv 0,\ i = 1, 2, \ldots, n$. These special points are defined as *singular points* of the system of equations, or fixed points of the dynamical system. The knowledge of the set of fixed points of the system gives a very significant picture of the behaviour of a given system and of all the systems ruled by originally different equations but having the same set of phase space fixed points. The fixed points determine the asymptotic (in time) states of a system and the behaviour of the phase trajectories in their neighbourhood describing the approach or escape of the system from such asymptotic states allows assessment of important properties of periodicity and stability of it. Isolated fixed points are just the zero-dimensional case of more general invariant sets of points (compact invariant manifolds) consisting of the loci of points, which during evolution are mapped onto themselves. In a two-dimensional phase space, they are the famous *limit cycles*.

The dynamic behaviour of even very different complex systems, when reduced to a model such as (5.1) can be promptly identified on the score of typical behaviour of the characteristics in the neighbourhood of the singular points.

Numerous rigorous presentations are available in textbooks on differential equations and analytical mechanics that should be consulted [5.1, 5.2] for completeness.

However, it is useful for the applications of the present text to summarize the basic classification of the singular points in a two-dimensional phase space where equation (5.1) takes the standard form of autonomous system:

$$\begin{aligned} \frac{\mathrm{d}Y_1}{\mathrm{d}t} &= P(Y_1, Y_2) \\ \frac{\mathrm{d}Y_2}{\mathrm{d}t} &= Q(Y_1, Y_2). \end{aligned} \tag{5.2}$$

The variables Y_i are then the components of a two-dimensional 'phase flow' whose momentum vector is $\boldsymbol{p} \equiv \{\dot{Y}_1, \dot{Y}_2\}$. In all the points where the r.h.s. are non-vanishing, (5.2) is equivalent to the equation obtained eliminating the parameter t:

$$\frac{dY_1}{dY_2} = \frac{P(Y_1, Y_2)}{Q(Y_1, Y_2)}. \tag{5.3}$$

But, in general, the latter form includes all the solutions of system (5.2) but there are solutions of (5.3), corresponding to the vanishing of the r.h.s., which *are not* solutions of (5.2). These are the fixed points of the phase flow.

For a study of (5.2) or (5.3) let us consider a linearization of $P(\boldsymbol{Y}) = P(\boldsymbol{Y}_\mathrm{s}) + (\boldsymbol{Y} - \boldsymbol{Y}_s) \cdot \nabla P|_{(Y_{1s}, Y_{2s})}$ and of $Q(\boldsymbol{Y}) = Q(\boldsymbol{Y}_s) + (\boldsymbol{Y} - \boldsymbol{Y}_s) \cdot \nabla Q|_{(Y_{1s}, Y_{2s})}$ around each isolated singular point (Y_{1s}, Y_{2s}) whose co-ordinates are obtained solving the generally *non-linear* algebraic system:

$$\begin{aligned} P(Y_{1s}, Y_{2s}) &= 0 \\ Q(Y_{1s}, Y_{2s}) &= 0. \end{aligned} \tag{5.4}$$

Through an obvious translation of co-ordinates $\boldsymbol{y} = \boldsymbol{Y} - \boldsymbol{Y}_s$, from the system (5.2) the local approximation is obtained:

$$\frac{\mathrm{d}}{\mathrm{d}t} \begin{bmatrix} y_1 \\ y_2 \end{bmatrix} = \begin{bmatrix} a & b \\ c & d \end{bmatrix} \cdot \begin{bmatrix} y_1 \\ y_2 \end{bmatrix} \tag{5.5}$$

equivalent to the local form of equation (5.3)

$$\frac{dy_1}{dy_2} = \frac{ay_1 + by_2}{cy_1 + dy_2} \tag{5.6}$$

where a, b, c and d are constant coefficients resulting from the expansion of P and Q.

Formally, it is convenient to transform system (5.5) through a non-singular matrix $\boldsymbol{T}$

$$\boldsymbol{y} = \boldsymbol{T} \cdot \boldsymbol{z} \tag{5.7}$$

$$\frac{d\boldsymbol{z}}{dt} = \boldsymbol{N} \cdot \boldsymbol{z} \tag{5.8}$$

where $\boldsymbol{N} = \boldsymbol{T}^{-1} \cdot \boldsymbol{M} \cdot \boldsymbol{T}$ is a matrix with the same eigenvalues of

$$\boldsymbol{M} \equiv \begin{bmatrix} a & b \\ c & d \end{bmatrix} \tag{5.9}$$

but cast in a simpler and more useful form.

The eigenvalues are roots of the characteristic equation:

$$\begin{vmatrix} a - \lambda & b \\ c & d - \lambda \end{vmatrix} = 0.$$

The condition necessary to have distinct real roots is then $\Delta = (a - d)^2 + 4bc > 0$.

In this case, the transformation matrix is built with the eigenvectors of $\boldsymbol{M}$ and the equations are

$$\frac{d}{dt} = \begin{bmatrix} z_1 \\ z_2 \end{bmatrix} = \begin{bmatrix} \lambda_1 & 0 \\ 0 & \lambda_2 \end{bmatrix} \cdot \begin{bmatrix} z_1 \\ z_2 \end{bmatrix} \tag{5.10}$$

equivalent to

$$\frac{dz_1}{dz_2} = \frac{\lambda_1 z_1}{\lambda_2 z_2} \tag{5.11}$$

which has as integral curves stemming from the singular point in the plane (z_1, z_2) the family of characteristics

$$z_1 = C|z_2|^{\lambda_1/\lambda_2}. \tag{5.12}$$

For the nature of the curves, for $ad - bc > 0$, the singular (fixed) point is called a stable ($\lambda_1 < \lambda_2 < 0$) node or unstable 'node' $\lambda_1 > \lambda_2 > 0$, and if $ad - bc < 0$ an unstable hyperbolic point ($\lambda_1 < 0 < \lambda_2$).

Alternatively if $\Delta < 0$, the eigenvalues are complex conjugates $\lambda_1 = \mu + \mathrm{i}\nu$ and $\lambda_2 = \mu - \mathrm{i}\nu$ and a convenient transformation

$$\boldsymbol{T} = \begin{bmatrix} c & \mu - a \\ 0 & \nu \end{bmatrix}$$

brings $\boldsymbol{M}$ in

$$\boldsymbol{N} = \begin{bmatrix} \mu & -\nu \\ \nu & \mu \end{bmatrix}.$$

The fixed point is a stable ($\lambda_1 = \lambda_2^*,\ \mu < 0,\ \nu > 0$) or unstable ($\lambda_1 = \lambda_2^*,\ \mu > 0,\ \nu < 0$) spiral point, and finally if the roots are purely imaginary ($\lambda_1 = \mathrm{i}\nu,\ \lambda_2 = -\mathrm{i}\nu$) the singular point of the phase flow is an elliptic point. In this latter case, the phase trajectories are given, in a small neighbourhood of the fixed point, by

$$\frac{\mathrm{d}z_1}{\mathrm{d}z_2} = -\frac{z_2}{z_1} \tag{5.13}$$

that is by a family of concentric circles $z_1^2 + z_2^2 = \rho^2$.

When the roots are distinct, one positive and one negative, the singular point is hyperbolic. If the eigenvalues are real and equal

$$\boldsymbol{N} = \begin{bmatrix} \lambda & 0 \\ 0 & \lambda \end{bmatrix}$$

and the fixed point is either a stable ($\lambda < 0$) or unstable ($\lambda > 0$) star. The determination of the properties of the phase trajectories near the singular points plus the identification of asymptotic lines by various methods is the basis for the construction of phase portraits of dynamic systems described by systems of first-order autonomous equations.

This concise summary of the methods and the properties of most common singularities is sufficient for the purposes of this text. For more advanced topics and concepts, we suggest a number of specialized books.

Sometimes, the formal procedure summarized here, which is always correct, can be speeded up by preliminary changes of dependent variables that can be suggested just by experience or familiarity with known examples in other fields of science.

5.1 Application to the Analysis of Reaction–Diffusion Processes

The cases analysed in chapters 3 and 4 can be seen as particular examples of a more general reaction–diffusion problem described by equations of the type

$$\frac{\partial u}{\partial t} = x^{-\gamma}\frac{\partial}{\partial x}\left[x^{\gamma}D(u)\frac{\partial u}{\partial x}\right] + P(u,x) - Q(u,x) \tag{5.1.1}$$

where the diffusion coefficient is of the type

$$D(u) = au^{\delta}$$

and the source and sink terms are expressed through an ansatz expansion

$$\begin{aligned} P(u,x) &= \sum_r (1 - x^2/b^2)^{\beta_r} c_r u^{p_r} \\ Q(u,x) &= \sum_r (1 - x^2/b^2)^{\mu_r} e_r u^{q_r} \end{aligned} \tag{5.1.2}$$

where $\beta_r, \mu_r, c_r, e_r, p_r, q_r$ are constants and b defines the position of an external boundary where it is required, for instance, that $u(b,t) = 0$. The form factors chosen here to be of the type $(1 - x^2/b^2)^{\beta_r}$ and $(1 - x^2/b^2)^{\mu_r}$ in the source and sink terms can, in principle, be adjusted to fit prescribed or simulated density profiles, while (here) u is meant to be the temperature of the system. For a fusion plasma heated by alpha particles, for instance, $p_r \cong 2 - 3$, while RF heating would give $p_r \cong 1$ and bremsstrahlung radiative losses $q_r \cong 0.5$. For the diffusion coefficient, caused e.g. by drift wave turbulence, $\delta = 3/2$.

Extending the approach presented in the previous paragraphs, for the dynamic variable u one can assume the representation

$$u(x,t) = A(t)G(x/\mathscr{L}(t), \eta(t), \zeta(t)) \tag{5.1.3}$$

where $A(t)$ is a time-varying scaling factor and $\mathscr{L}(t), \eta(t), \zeta(t)$ are width and shape factors and for the profile shape, one may take

$$G = (1 - x^2/b^2)^a[1 - (x/\mathscr{L})^2 + \eta(x/\mathscr{L})^4 - \zeta(x/\mathscr{L})^6] \tag{5.1.4}$$

with $a = 1 + \delta$ that guarantees finite non-vanishing flux

$$D\frac{\partial u}{\partial x} = \frac{a}{1+\delta}\frac{\partial u^{1+\delta}}{\partial x}.$$

The form factor $(1 - x^2/b^2)^a$ allows the consideration of finite boundary effects.

The formal procedure outlined previously leads to three coupled non-linear equations for the amplitude A the width $\mathscr{L}$ and the form factor η assuming here $\zeta = \text{const.}$ for simplicity:

$$\begin{aligned} \frac{\mathrm{d}A}{\mathrm{d}t} &= f(A, \mathscr{L}^2) \\ \frac{\mathrm{d}\mathscr{L}^2}{\mathrm{d}t} &= g(A, \mathscr{L}^2, \eta) \\ \frac{\mathrm{d}\eta}{\mathrm{d}t} &= h(A, \mathscr{L}^2, \eta). \end{aligned} \tag{5.1.4}$$

The expressions for f, g and h are given in Wilhelmsson [5.3]. Here, we describe the results of the phase space methods in discussing the particular case with $\eta = \text{const.}$ The 'cardinal curves' of the dynamic system in the phase plane $(A, \mathscr{L}^2)$ are given by

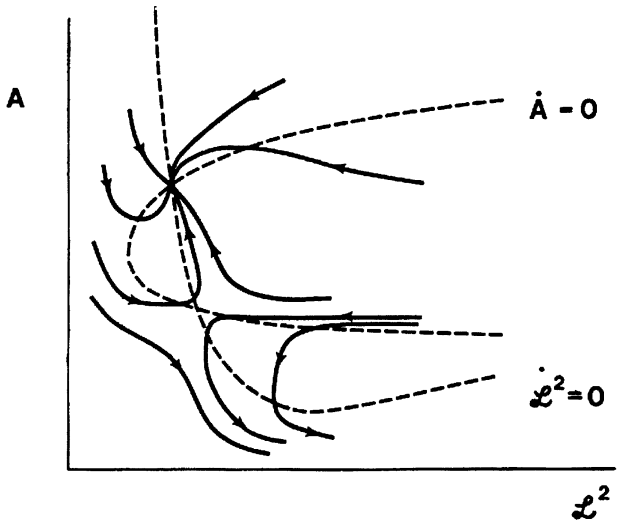

Figrue 5.1. Qualitative phase-plane plot describing the trajectories of the points $(A, \mathscr{L}^2)$ as time increases. The dashed curves are the 'cardinal' curves corresponding to $\mathrm{d}A/\mathrm{d}t = 0$ and $\mathrm{d}L^2/\mathrm{d}t = 0$, the full line curves refer to the point trajectories. The parameters fulfill the inequality for a burning fusion plasma $\delta + 1 > p > q$. The upper (large A) equilibrium is stable (node), the lower unstable (saddle point). By changing the relative influence of the processes, i.e. the losses, cases can be found where the cardinal curves cross in one, two or three points or where they do not cross at all, defining one or several equilibria or none.

$$\frac{dA}{dt} = 0, \quad \frac{d\mathscr{L}^2}{dt} = 0 \tag{5.1.5}$$

and are shown in the figure as dashed lines.

The singular points, at the intersections of the two curves, have the nature of a stable node and an unstable hyperbolic saddle point.

The phase-plane portrait is presented qualitatively in figure 5.1 and in figure 5.2, the corresponding quantitative evolution of the profiles are presented. The results obtained and shown here have been tested by comparison with detailed results of the direct numerical integration of the PDE and of the ODE system obtained by the central expansion technique. The agreement, e.g. for the profiles $u(x,t)$ ('temperature'), is excellent. Furthermore, the direct numerical integration of the ODE system for $A, \mathscr{L}^2$ and η is faster than the numerical solution of the PDE (5.1.1), although the latter provides naturally the finest details.

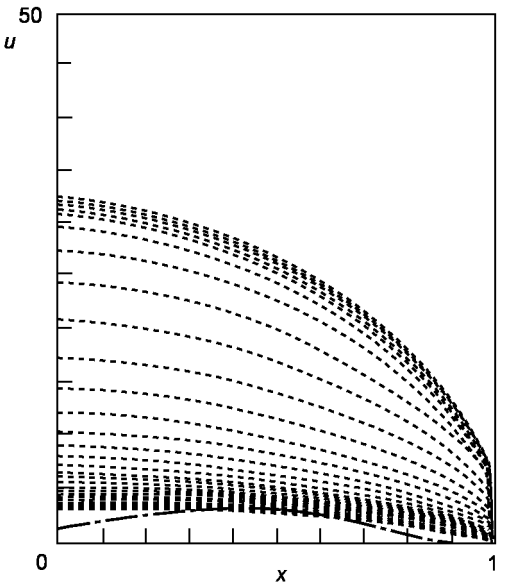

Figure 5.2. Time evolution of a temperature profile for a two-dimensional situation from an arbitrary initial state (dashed line) associated to figure 5.1. One notices two equilibria, an unstable one with $A = T_{eq} = 3.0$ and a stable one with $A = T_{eq} = 32.4$. The stable equilibrium is identical to the one identified in figure 5.1. The time it takes to grow from the initial condition $A = 1$ to the stable equilibrium $A = 32.4$ is 4.7 time units, to be compared with the time of one unit required to grow from $A = 25$ to $A = 32.4$.

The phase space analysis of the evolution of the state of a dynamical system (e.g. the temperature of a bounded burning plasma) can be used very conveniently to determine the accessibility of possible stationary points, the approach to or run-away from equilibria. The trajectories in the phase space *can be traced over long time intervals* in contrast to the description by means of more sophisticated theoretic methods, based for instance on variational principles, which provide results only in a suitably defined neighbourhood of a stationary profile.

The insight provided by even a rough identification of the topology of phase space is invaluable to develop strategies of control of the system and in addition it can be strengthened by rapid *back-of-envelope* estimates of the dominating physical effects through the dependence of the phase space coordinates of the fixed points on the parameters of the system. This often turns out to be invaluable also as a tool to guide the use of complex PDE codes.

References

[5.1] Lakin E W D and Sanchez D A 1970 *Topics in Ordinary Differential Equations* (Boston: Prindle, Weber, Schmidt)

[5.2] Tricomi F G 1961 *Equazioni Differenziali* (Turin: Boringhieri)

[5.3] Wilhelmsson H 1990 Evolution and self-formation in some non-linear systems *Bulletin de la classe des Sciences* vol I p 269 Acad. Royale de Belgique

[5.4] Wilhelmsson H *et al* 1994 Evolution of temperature profiles in a fusion reactor plasma *Phys. Scripta* **45** 184

Chapter 6

Models for Coupled Evolution of Temperature and Density in a Fusion Heat Pinch

The problems related to the transport of energy and particles are central issues in present-day fusion research. The design and operation of large fusion devices based on the tokamak concept of magnetic confinement, such as JET, TFTR and the next generation reactors, require detailed insight in the role played by the various processes responsible for the transport of particles and energy in the plasma approaching thermonuclear fusion conditions. For practical fusion experiments, the confined plasma is subject to a variety of heating power inputs (energetic beams, resonant radiofrequency and fusion produced alpha particles), as well as to a variety of power losses (radiative, convective and due to charge exchange) and the problem consists of reaching an operating regime in the parameter space $(n, \tau_{\mathrm{E}}, T)$, that may be called the Lawson parameter space, in which fusion produced power output overbalances all losses and inputs. So far, only demonstrative experiments have been performed, falling just a little bit short of the simple *balance* of input power.

The physical processes underlying a particular regime of reactor operation are extremely complex and many of the obstacles to reaching a satisfactory performance depend on the boundary conditions for all the physical fluxes entering and leaving the confined plasma (e.g. electromagnetic Poynting flux, multispecies particle fluxes and energy (heat) flux). Therefore, the performance is (at least it has been so far) highly machine-dependent, being related to a number of seemingly parasitic effects, due to the material properties of the plasma facing 'first wall' components, so that an equal effort has to be spent on the basic understanding of 'pure' plasma phenomena and on technical details, which, it should be stressed, rise to the status of *problems of principle* so far as they dictate the boundary conditions for the equations of the problem.

There has, however, been a long-lasting hope in the research community that some sort of robust core of all the various experiments could be identified, from the fundamental and more understood physical models and 'similar' experiments. The word 'similar' indicates the faith in invariance of some key quantity under some general transformation of circumstances (geometry, heating methods, plasma cross-sectional shape) and justifies the search for 'scaling laws' for particles and energy confinement times (suitably defined), heating efficiency and other global properties of a plasma in steady-state conditions, in the spirit of application of Buckingham π theorem.

Both the empirical and the theory-based research in this field must somehow move in a restricted domain of data or models, selected more or less consciously, *a priori*. The results should be then tested for their predictive value, essentially within the same domain, with no surprise if they fail miserably in quite different circumstances.

With these caveats, we explore here the consequences on confinement scaling laws of largely accepted models of the dynamics of plasma temperature (assuming isothermal species) and density in presence of alpha particle fusion power input and heat and particle flux pinches [6.6].

Theory-based energy transport models in tokamak plasmas have so far proven to be unsuccessful in helping the interpretation of experimental observations of the effective energy replacement time and in the prediction of performance, because electrostatic and possibly also magnetic turbulence contribute to an anomalous increase of the heat and particle diffusivities. While from the macroscopic point of view, this translates into a reduction factor of the global confinement time, in terms of heat (and particles) diffusivity the implication is that the diffusivity is no longer a thermodynamic coefficient relating the thermodynamic forces (local temperature gradient) to the heat flux but it may be a complicated function of local parameters (density, temperature, magnetic shear) and temperature gradient.

A number of empirical models have been fitted to a wealth of experimental data and framed within general, albeit undetermined, similarity laws based on dimensionless parameters:

$$\chi = \frac{T}{B} F(\rho^*, \beta^*, v^*) \tag{6.1}$$

where $F(\rho^*, \beta^*, v^*)$ is a generic function of the dimensionless variables (here all starred for uniformity of notation); $\rho^* = \rho_i/a \propto T^{1/2}$, $v^* = na/T^2$, $\beta^* = nT/B^2$. Extracting the dependence on the normalized gyro-radius, the undetermined formula (6.1) can be made more specific with respect to known transport mechanisms [6.1, 6.2].

Particular arrangements of the dimensionless parameters (β^*, v^*) may lead to different, non-linear scaling of χ with the plasma temperature T and its gradient.

A simple but prominent case is the so-called 'offset linear scaling' (Rebut *et al* 1998 [6.13]) of the heat flux with the temperature gradient, which means that the heat flux is non-zero even at vanishing temperature gradient. This offset part is often considered as a convective effect.

It is, however, more instructive to consider the linear transport matrix, see chapter 2, which relates a set of 'canonically conjugate' thermodynamic forces X_i and fluxes Γ_i. The linear transport model assumes that each flux be related linearly to a combination of thermodynamic forces through a matrix of transport coefficients L_{ij}. Diagonal coefficients relate each flux to its main driving mechanism, the gradient of a state variable, and off-diagonal represent the cross-effect of different thermodynamic forces. Here for the most significant formal electron fluxes, we adopt a well-known suggestive notation [6.5]

$$\begin{pmatrix} \vec{\Gamma} \\ \vec{q}_e \\ J_\parallel - \sigma_\parallel E_\parallel^A \end{pmatrix} = \begin{bmatrix} D & L_{12} & L_{\text{ware}} \\ L_{21} & \chi_e & L_{23} \\ L_{\text{boot}} & L_{32} & \sqrt{\varepsilon}\sigma_\parallel \end{bmatrix} \cdot \begin{pmatrix} -\nabla n \\ -\nabla T \\ -E_\parallel^A \end{pmatrix}. \tag{6.2}$$

Within this description, the heat flux in particular has a contribution proportional to the density gradient due to the L_{21} term and to the parallel electric field through L_{23}.

Here, we report a study that illustrates the non-diagonal transport effects, related to drift wave turbulence [6.6, 6.10].

The energy transport equation for a magnetically confined plasma can be cast in the form:

$$\frac{3}{2}\left(\frac{\partial}{\partial t} + \boldsymbol{v}\cdot\nabla\right)T + T\nabla\cdot\boldsymbol{v} = -\frac{1}{n}\nabla\cdot\boldsymbol{q} \tag{6.3}$$

where $\nabla\cdot\boldsymbol{v}$ and the $\boldsymbol{v}_i\cdot\nabla T$ can be expressed in terms of the (turbulent) fluctuation of drift waves electrostatic potential:

$$\begin{aligned} \nabla\cdot\boldsymbol{v}_i &\cong [\omega - \omega_{\text{e}}^*]\frac{e\Phi}{T_{\text{e}}}; \quad \boldsymbol{v}_i\cdot\nabla n_0 = -\text{i}n_0\,\omega_{\text{e}}^*\frac{e\Phi}{T_{\text{e}}}; \\ \boldsymbol{v}_i\cdot\nabla T &\cong -\text{i}\omega^* T\eta_i\frac{e\Phi}{T_{\text{e}}} \end{aligned} \tag{6.4}$$

and considering adiabatic electrons the particles and heat fluxes are eventually expressed as

$$\Gamma_T \equiv -\chi\frac{\text{d}T}{\text{d}r} = -\left(\frac{\text{d}T}{\text{d}r} - \frac{2}{3}\frac{T}{n}\frac{\text{d}n}{\text{d}r}\right)\frac{\gamma}{k_T^2} \tag{6.5}$$

$$\Gamma_n \equiv -D\frac{\mathrm{d}n}{\mathrm{d}r} = -\left(\frac{\mathrm{d}n}{\mathrm{d}r} - \alpha\frac{n}{T}\frac{\mathrm{d}T}{\mathrm{d}r}\right)\frac{\gamma}{k_T^2} \tag{6.6}$$

where γ is the growth rate of the drift waves instability, k_T is the radial wavenumber, α depends on the mode eigenfrequency but is $O(1)$.

The essential form of the one-dimensional transport model for this problem consists, therefore, of two coupled equations for the temperature and density:

$$\frac{\partial T}{\partial t} = \frac{a_T}{x^\gamma}\frac{\partial}{\partial x}\left(x^\gamma T^\delta \frac{\partial T}{\partial x}\right) - \frac{k_T}{x^\gamma}\frac{\partial}{\partial x}\left(x^\gamma T^{\delta+1} n^{-1}\frac{\partial n}{\partial x}\right) + cT^p n^\beta - eT^q n^\beta \tag{6.7}$$

$$\frac{\partial n}{\partial t} = \frac{a_n}{x^\gamma}\frac{\partial}{\partial x}\left(x^\gamma T^\delta \frac{\partial n}{\partial x}\right) - \frac{k_n}{x^\gamma}\frac{\partial}{\partial x}\left(x^\gamma T^{\delta-1} n\frac{\partial T}{\partial x}\right) + S. \tag{6.8}$$

Here $S(x,t)$ represents a source of particles (ions) and we consider the heat conductivity and particle diffusion coefficient of the form $\kappa = a_T T^\delta$ and $D = a_n T^\delta$, respectively, with a_T, a_n, k_T, k_n, c, and e being positive constants. The power-input term is assumed to have the structure $cT^p n$ and the radiative loss term is taken to scale as $eT^q n^\beta$.

It is interesting and instructive to focus the attention on a paradigmatic case of a burning fusion plasma with a distributed heat source term $P_{\mathrm{fus}}/3n \approx cT^2 n$, bremsstrahlung losses $P_{\mathrm{brems}}/3n \approx 0.52 \times 10^{-38} Z_{\mathrm{eff}} T^{1/2} n$ and a turbulent diffusion due to drift waves scaling as $T^{3/2}$. This fixes the exponents to $p = 2$, $q = 1/2$, $\beta = 1$, $\delta = 3/2$, $\gamma = 1$ and the other constants are chosen corresponding to reference plasma of $n(0) = 5 \times 10^{19}\,\mathrm{m}^{-3}$, $T(0) = 10\,\mathrm{keV}$. With a localized density source simulating pellet fuelling

$$S = \begin{cases} 30 & \text{for } 0 \le x \le 0.1 \\ 0 & \text{for } 0.1 < x \le 1 \end{cases}$$

numerical integration of the equations with boundary conditions $T(b,t) = 0$, $n(b,t) = 0$ gives the results shown in figures 6.1–6.10 for simulations of a tokamak 'L mode' of confinement and from figure 6.11 to figure 6.20 for a 'H mode' of confinement.

In figures 6.5a, 6.10, 6.15, 6.20, 'phase space' plots show the existence of attractor equilibrium points and an oscillatory approach or escape from them.

The same results can be obtained by application of the technique of central expansion, where it is absolutely important to incorporate the condition of finite minor radius of the plasma $r = b$, summing up the effect of magnetic confinement and existence of a 'limiter' condition to obtain bounded solutions.

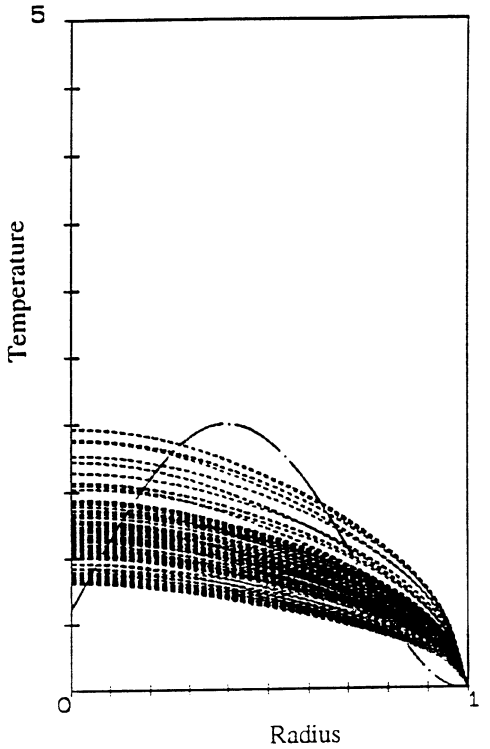

Figure 6.1. Curves describing the time evolution of a temperature profile from an initial state (thin dotted line) to an equilibrium state. The parameter values are: $e = 1$, $\delta = 1.5$, $p = 2.4$, $q = 0.5$, $b = 1$, $c = 5$, $\beta = 1$ and $s = 30$ for $0 < r < 0.1$, $s = 0$ for $0.1 < r < 1$. ('L mode' simulation, neglecting pinch terms).

6.1 Dynamic Evolution of Temperature and Density in Alpha-Particle-Heated Plasmas

With the methods outlined in the previous chapters, we consider the coupled PDEs for the basic model of density and temperature evolution in a cylindrical (i.e. very large aspect ratio) confinement configuration, neglecting bremsstrahlung losses, which is an adequate assumption for a very hot fusion plasma under the very optimistic assumption that conditions of resistive MHD stability for all modes [6.3] can be obtained and maintained during the evolution.

It turns out that several interesting global properties of this model system can be studied in terms of exact solutions of the coupled equations, in a form which expresses time as a function of the temperature through an Abel integral.

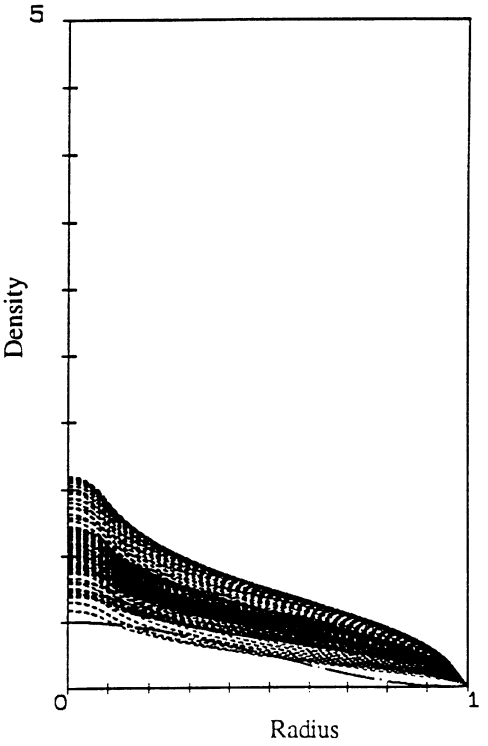

Figure 6.2. Curves describing the time evolution of the density profile from an initial state (thin dotted line) to an equilibrium state, with the parameters of figure 6.1 ('L mode' simulation).

Non-linear oscillations of the temperature, also including the effect of losses, can be studied, obtaining a pattern similar to the relativistic motion of an oscillator with velocity-dependent mass.

This latter application is potentially interesting for a diagnostics of the heat diffusivity. As a matter of fact, the use of pulsed or periodically modulated heat sources is becoming a well-developed technique that has provided intriguing results that will be discussed briefly, from another point of view, in chapter 10.

The model is based on the coupled transport equations for the plasma temperature and density with sinks and sources:

$$\frac{\partial T}{\partial t} = x^{-\gamma}\frac{\partial}{\partial x}\left(x^{\gamma}\chi(T)\frac{\partial T}{\partial x}\right) - x^{-\gamma}\frac{\partial}{\partial x}\left(x^{\gamma}\chi_p(T,n)\frac{\partial n}{\partial x}\right) + cT^p n^{\beta} - eT^q n$$

$$\frac{\partial n}{\partial t} = x^{-\gamma}\frac{\partial}{\partial x}\left(x^{\gamma}D(T)\frac{\partial n}{\partial x}\right) - x^{-\gamma}\frac{\partial}{\partial x}\left(x^{\gamma}D_p(T,n)\frac{\partial T}{\partial x}\right) + S. \qquad (6.1.1)$$

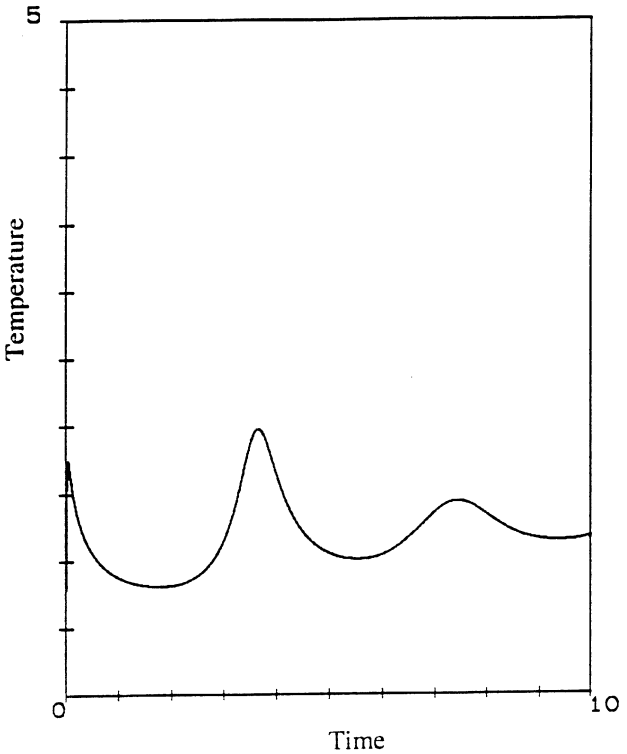

Figure 6.3. Time dependence of the central temperature for the case of figure 6.1.

The 'diagonal' heat conductivity and particle diffusion coefficient are represented by

$$\chi(T,n) = a_T T^{\delta} \qquad D(T,n) = a_n T^{\kappa} \tag{6.1.2}$$

while the 'off diagonal' coefficients representing the heat and particles' pinch effects are assumed to scale as

$$\chi_p(T,n) = k_T n^{-1} T^{\delta+1} \qquad D_p(T,n) = k_n n T^{\kappa-1} \tag{6.1.3}$$

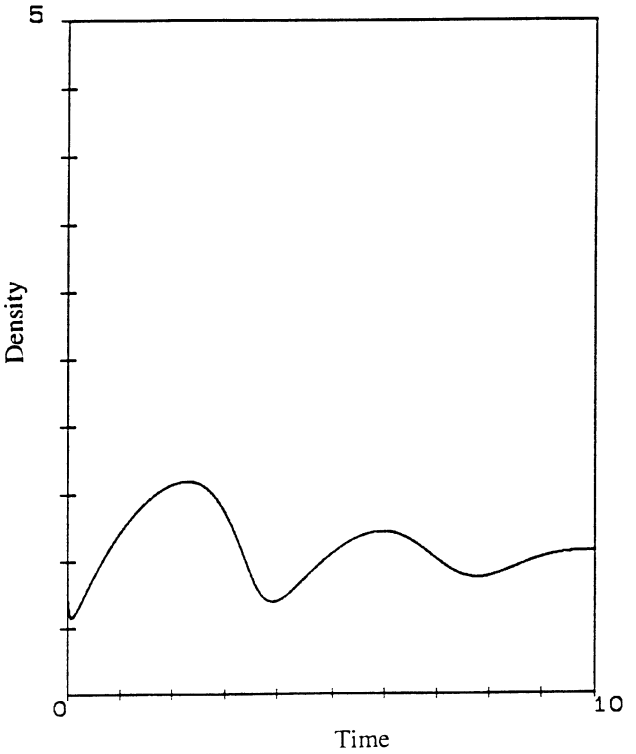

Figure 6.4. Time dependence of the central density for the case of figure 6.1.

where $a_T, a_n, k_T, k_n, \delta$ and κ are constants. The model sink and source terms, scaling as power laws of density and temperature, are weighted by constant coefficients c and e.

Physically, values of $p = 2$ or 3 are appropriate to represent alpha particle heating in a fusion plasma and $p = 1$ a radiofrequency heat source. A value of $\delta = 3/2$ may describe diffusion due to drift wave turbulence. Appropriate boundary conditions for plasma configuration with a limiter at the nominal radius $x = b$ may be

$$\begin{aligned} T(b,t) &= 0 \\ n(b,t) &= 0. \end{aligned} \tag{6.1.4}$$

Also, taking into account the boundary conditions in the procedure of the central expansion leads to non-explosive equilibrium solutions, as will be shown.

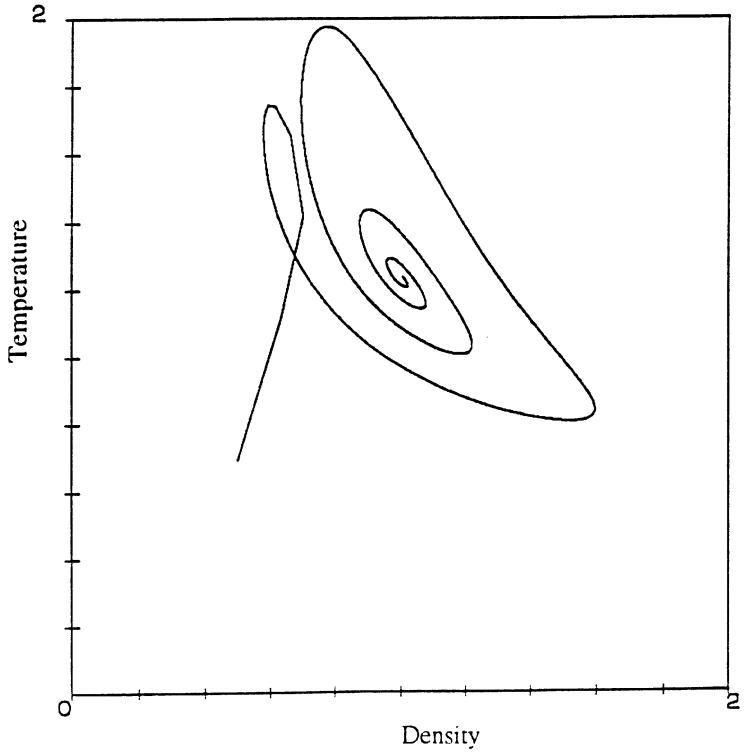

Figure 6.5. Phase-plane curve describing the time evolution of temperature T and density n for the cases of figures 6.1 and 6.2, from an initial state to a final equilibrium (stable spiral point).

The method of central expansion applied to the above equations in the instructive case $\beta = 1$ and constant source term s, assuming once again

$$T(x,t) = A_T(t)\left(1 - \frac{x^2}{b^2}\right)^{\beta} G\left(\frac{x}{\mathscr{L}_T(t)}\right)$$

$$n(x,t) = A_n(t)\left(1 - \frac{x^2}{b^2}\right)^{\beta} G\left(\frac{x}{\mathscr{L}_T(t)}\right)$$

and obtaining the following equations for the amplitudes:

$$\begin{aligned} \frac{\mathrm{d}A_T}{\mathrm{d}t} &= -\mu A_T^{\delta+1} + cA_T^p A_n \\ \frac{\mathrm{d}A_n}{\mathrm{d}t} &= -\nu A_T^{\kappa} A_n + s \end{aligned} \tag{6.1.5}$$

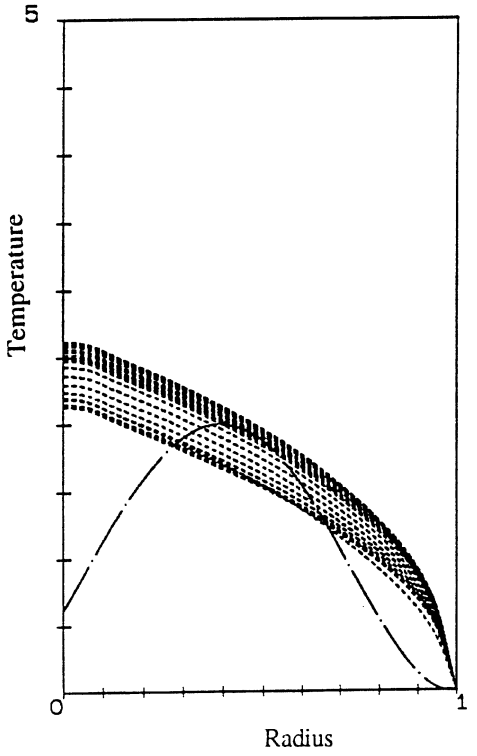

Figure 6.6. Time evolution of a temperature profile from an initial state (thin dotted line) to an equilibrium state, including pinch effect. The parameter values are $k_T = 0.25$ and $k_n = 0.25$ ('L mode' simulation).

where new coefficients are introduced for convenience

$$\begin{aligned} \mu &= 2(\gamma + 1)[a_T/l_T^2 - k_T/l_n^2] \\ \nu &= 2(\gamma + 1)[a_n/l_n^2 - k_n/l_T^2] \end{aligned} \tag{6.1.6}$$

and the effective scale lengths are defined as

$$\begin{aligned} 1/l_T^2 &= 1/\mathscr{L}_T^2 + 1/b^2(1 + \delta) \\ 1/l_n^2 &= 1/\mathscr{L}_n^2 + 1/b^2(1 + \kappa). \end{aligned} \tag{6.1.7}$$

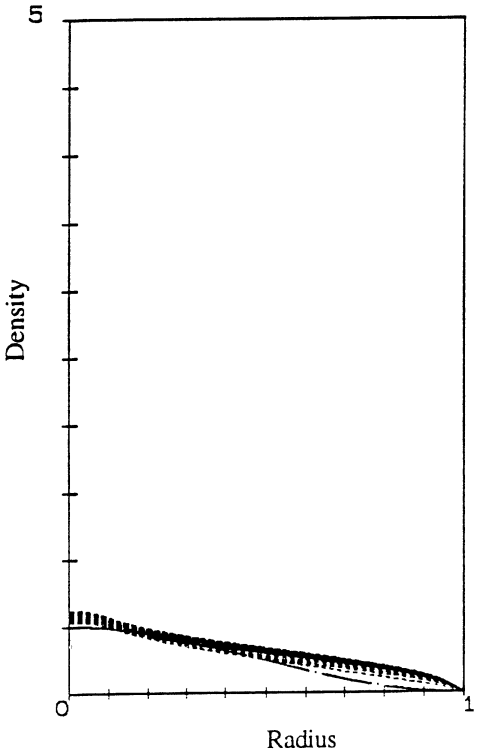

Figure 6.7. Time evolution of the density profile from an initial state (thin dotted line) to an equilibrium state, with the parameters of figure 6.6.

The phase space analysis identifies the fixed points in the plane (A_T, A_n)

$$A_T^{(e)} = \left(\frac{cs}{\mu v}\right)^{1/(\delta+1-p+\kappa)} \tag{6.1.8}$$

$$A_n^{(e)} = \left(\frac{s}{v}\right)^{1-\kappa/(\delta+1-p+\kappa)} \left(\frac{c}{\mu}\right)^{-\kappa/(\delta+1-p+\kappa)}. \tag{6.1.9}$$

For $p = \delta + 1$ and $\kappa = \delta$ and values of practical interest $p = 5/2,\ \delta = 3/2$ the equilibrium fixed point is a spiral point approached asymptotically in time.

The phase trajectory approaches the fixed points in a spiral that corresponds to oscillations in time of temperature and density. Explicitly, this can be seen reducing the system of equations (6.1.5) to a single equation for the variable

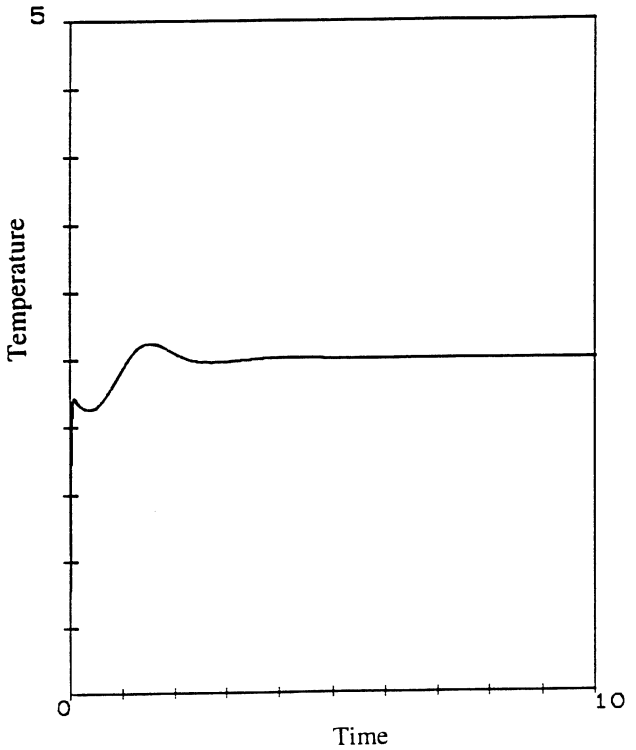

Figure 6.8. Time dependence of the central temperature for the case of figure 6.6.

$X = A_T^{-\delta}$. For the particular choice of parameters indicated, X evolves according to the equation

$$\frac{\mathrm{d}^2X}{\mathrm{d}t^2} + \frac{v}{X}\left(\frac{\mathrm{d}X}{\mathrm{d}t} - \delta\mu\right) = -sc\delta. \tag{6.1.10}$$

The solutions of this non-linear equation have an oscillatory behaviour. Multiplying both sides of the equation by $\mathrm{d}X/\mathrm{d}t$ and integrating, one obtains an Abel-type integral expression for t,

$$t - t_0 = \frac{1}{\sqrt{2\delta}} \int_{X_0}^{X} \frac{\mathrm{d}z}{[\mu v \ln(z/X_m) - sc(z - X_m)]^{1/2}}. \tag{6.1.11}$$

Here the integration constant has been determined from the condition $\mathrm{d}X/\mathrm{d}t = 0$, obtained at X_m.

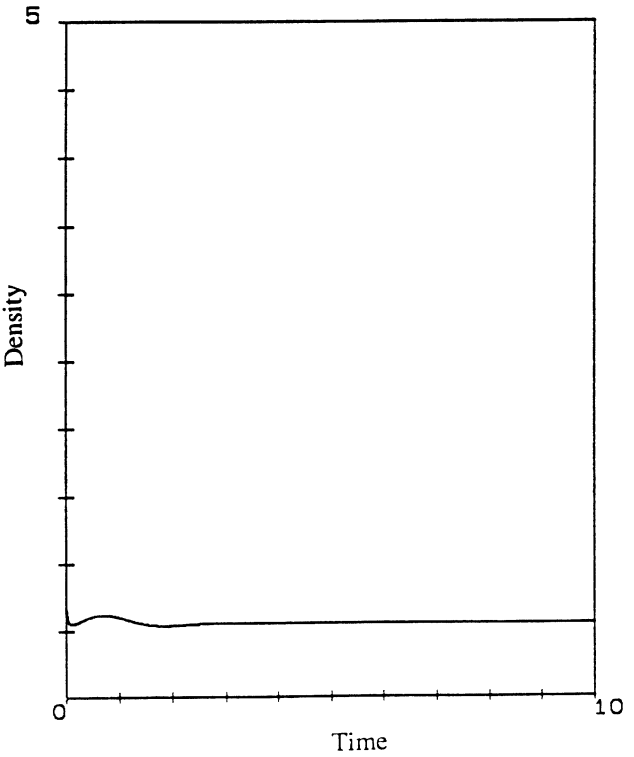

Figure 6.9. Time dependence of the central density for the case of figure 6.6.

This formal result, which is significant as a matter of principle, may appear to be of limited practical use. A more useful procedure is then to rewrite the equation in the equivalent form:

$$X\frac{\mathrm{d}^2X}{\mathrm{d}t^2}+v\frac{\mathrm{d}X}{\mathrm{d}t}+sc\delta X-(v\delta\mu)=0 \tag{6.1.12}$$

which is similar to that of the oscillatory motion of a 'particle' with a relativistically velocity-dependent mass.

Linearizing around the fixed point $X^{(e)}=(v\mu/cs)$, with $X=X^{(e)}+\delta X$ one obtains for the small displacement $\delta X \ll X$ the damped oscillator equation

$$\frac{\mathrm{d}^2\delta X}{\mathrm{d}t^2}+\frac{sc}{\mu}\frac{\mathrm{d}\delta X}{\mathrm{d}t}+\frac{(sc)^2\delta}{v\mu}(\delta X)=0 \tag{6.1.13}$$

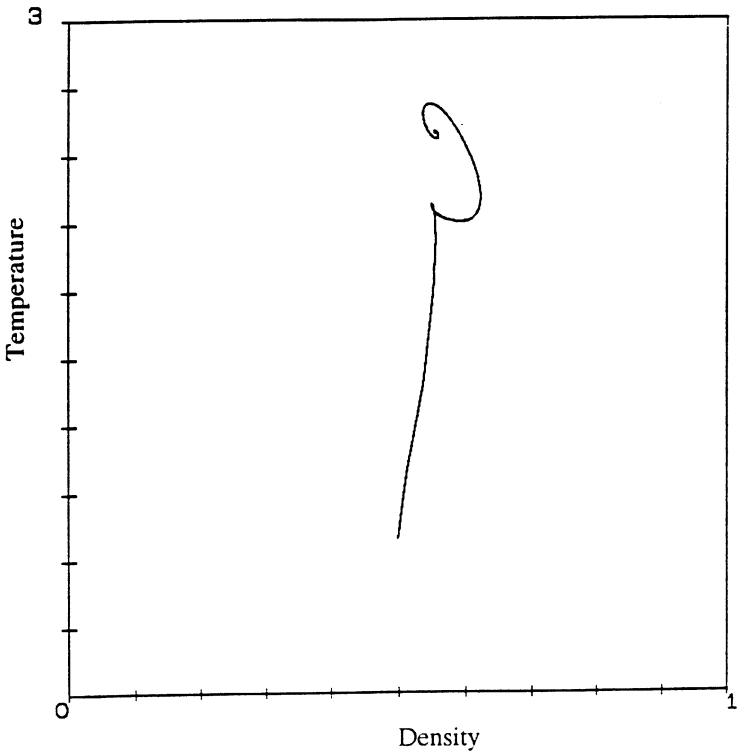

Figure 6.10. Phase-plane curve describing the time evolution of temperature T and density n for the cases of figures 6.6 and 6.9, from an initial state to a final equilibrium (stable spiral point).

which leads to the solution

$$X = X^{(e)} + \delta X_0 \, \mathrm{e}^{-\nu_R t} \cos(\omega t) \tag{6.1.14}$$

where the damping and the oscillation pulsation are

$$\begin{aligned} \nu_R &= sc/2\mu \\ \omega &= \frac{sc}{2\mu}\sqrt{\frac{4\mu\delta}{\nu} - 1}. \end{aligned} \tag{6.1.15}$$

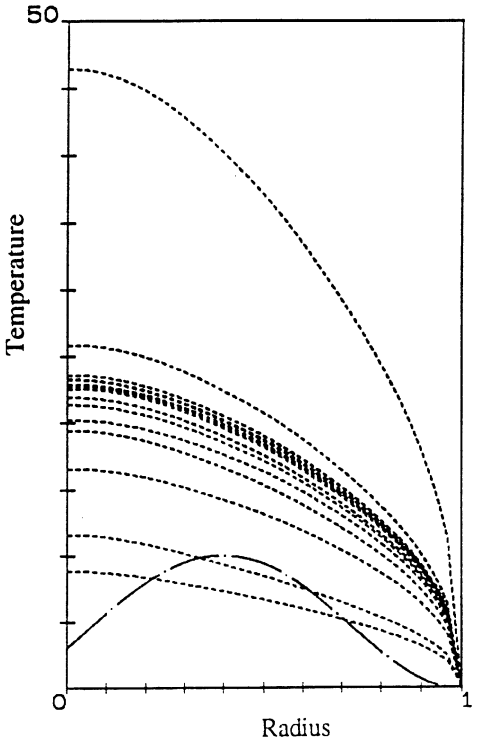

Figure 6.11. Curves describing the time evolution of a temperature profile from an initial state (thin dotted line) to an equilibrium state. The curves refer to a two-dimensional situation. The parameter values are: $e = 1$, $\delta = 1.5$, $p = 2.4$, $q = 0.5$, $a_T = 0.1$, $a_n = 0.001$, $k_T = 0.0$, $k_n = 0.0$, $b = 1$, $c = 5$, $\beta = 1$ and $s = 30$ for $0 < r < 0.1$, $s = 0$ for $0.1 < r < 1$ ('H mode' simulation, neglecting pinch term).

Finally returning to the original amplitudes of temperature and density, one obtains the expressions

$$A_T = \frac{A_T^{(e)}}{\left[1 - \delta \dfrac{\Delta_{T0}}{A_T^{(e)}} \mathrm{e}^{-\nu_R t} \cos(\omega t)\right]^{1/2}} \tag{6.1.16}$$

and for $p = d + 1$,

$$A_n \approx A_n^{(e)} - \frac{\omega}{c} \frac{\Delta_{T0}}{(A_T^{(e)})^p} \mathrm{e}^{-\nu_R t} \left[\sin(\omega t) + \frac{\nu_R}{\omega} \cos(\omega t)\right] \tag{6.1.17}$$

with $\Delta_{T_0} = -\delta X_0 (A_T^{(e)})^{\delta+1} \delta^{-1}$.

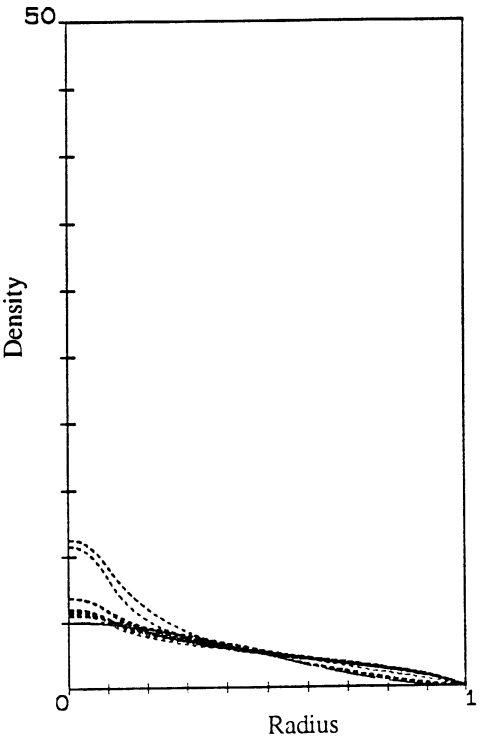

Figure 6.12. Curves describing the time evolution of the density profile from an initial state (thin dotted line) to an equilibrium state, with the parameters of figure 6.11 ('H mode' simulation, neglecting pinch term).

From the point of view of the physical interpretation, it is interesting to note that in the expressions for the oscillation frequency and damping rate the common factor sc/μ is proportional to the particle and heat source strength, s and c, and decreases with the effective temperature diffusion coefficient μ. From the form of the equation for X it is also apparent that when deviation of X from the equilibrium (fixed point) value is in the non-linear regime, the curvature $\left|\mathrm{d}^2X/\mathrm{d}t^2\right|$ has to increase, in comparison with the linear value forming a non-linear peak sharper than the linear one.

Sharp initial non-linear peaking, followed by quick decay, should be expected particularly for strong temperature pinching causing also an increase of the oscillation pulsation (6.1.15). The non-linear peaking effects are, in principle, contained in the integral form (6.1.11) in absence of damping, whereas the other characteristics of the problem are well-described by the

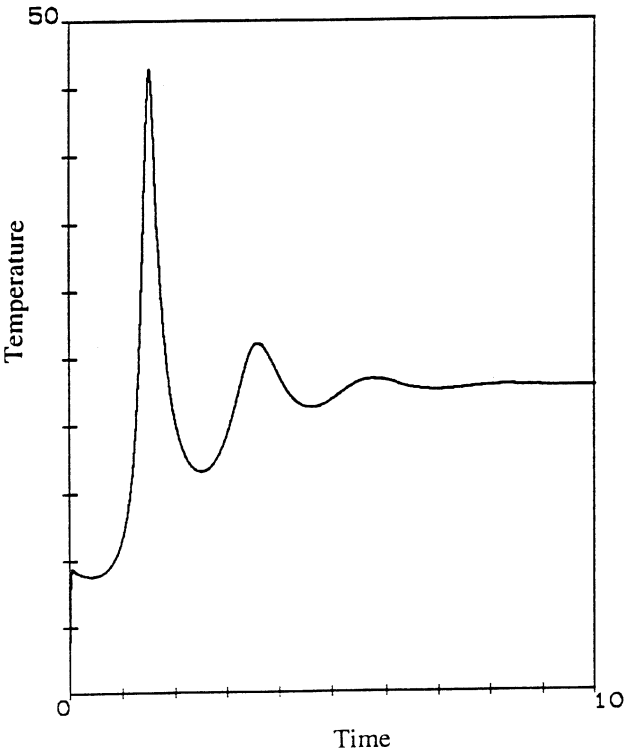

Figure 6.13. Time dependence of the central temperature for the case of figure 6.11.

simple results (6.1.15). It should be emphasized that even in the simple case with constant density n and $e = 0$, therefore with no pinch term and no bremsstrahlung losses, the problem cannot be solved analytically in exact form for arbitrary initial conditions because the governing equation does not satisfy the Painlevé criterion.

The direct numerical integration of equation (6.1.1) gives the results shown in figures 6.21–6.23 for the choice $p = 1 + \delta$, $\beta = 1$, and $e = 0$.

The family of curves of figure 6.21 describe the time evolution of a temperature profile from an initial state (thin dotted line) to an equilibrium state reached after some oscillations of the profile, obtained neglecting the heat and particles pinch effects. Figure 6.22 shows the behaviour of the peak temperature. The oscillations are due to the mechanism of coupling with the density evolution portrayed very effectively in the plane of the state variables (T and n) shown in figure 6.23; here the phase space trajectory winds in a spiral approaching a stable spiral point equilibrium.

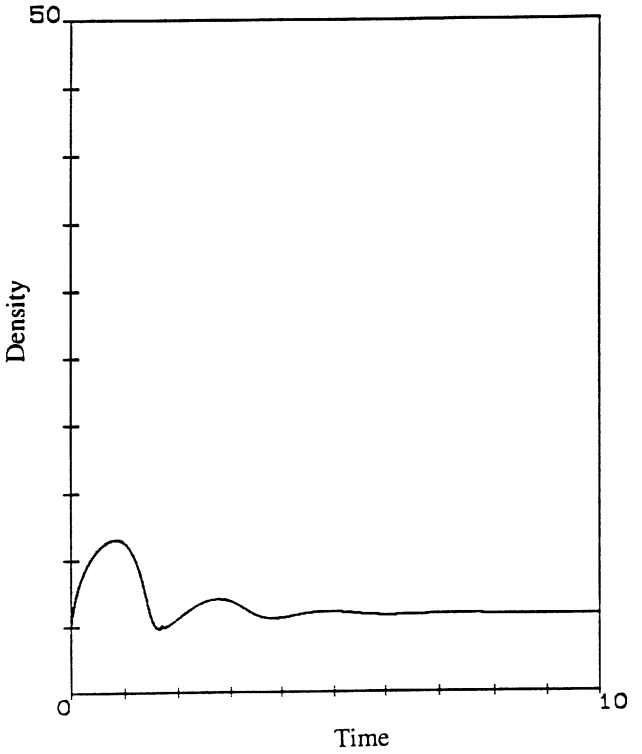

Figure 6.14. Time dependence of the central density for the case of figure 6.11.

In terms of the equilibrium values, it is possible to estimate the so-called energy confinement time

$$\tau_{\mathrm{E}} = \frac{3}{2}\frac{A_n^{(e)} A_T^{(e)}}{P} \tag{6.1.18}$$

where P is the net input powers which may scale as a power of temperature and density.

For instance, in the case of plasma heating by absorption of high-frequency electromagnetic waves, one may consider the input power $P = sA_T^{(e)}$ and the confinement time should then be expected to scale as:

$$\tau_{\mathrm{E}} = \frac{3}{2}\frac{A_n^{(e)}}{s} = \frac{3}{2s}\left(\frac{s}{\nu}\right)^{1-\kappa/(\delta+1-p+\kappa)}\left(\frac{c}{\mu}\right)^{-\kappa/(\delta+1-p+\kappa)}. \tag{6.1.19}$$

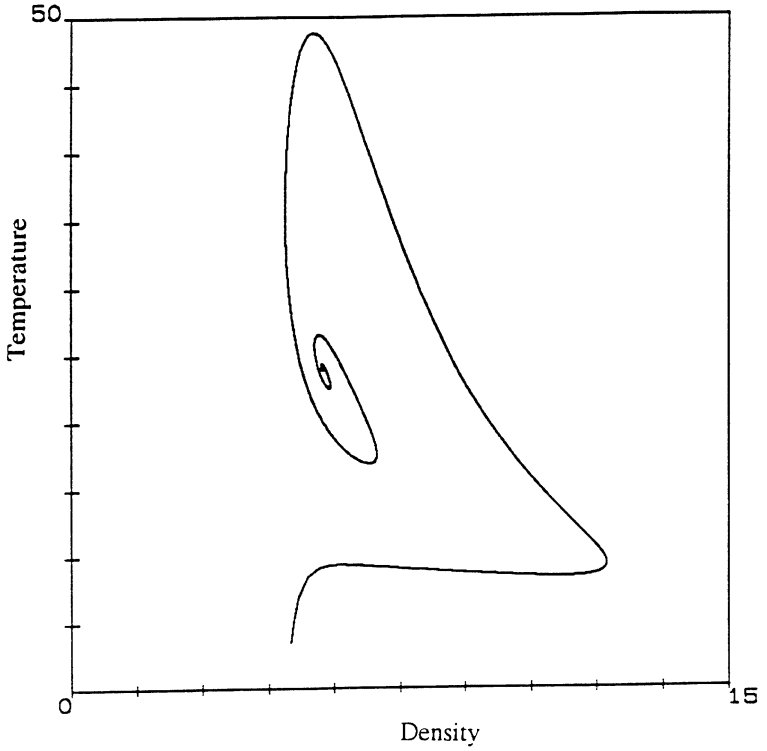

Figure 6.15. Phase-plane curve describing the time evolution of temperature T and density n for the cases of figures 6.14 and 6.15, from an initial state to a final equilibrium (stable spiral point).

For $p = 1 + \delta$, one has

$$\tau_{\mathrm{E}} = \frac{3}{2}\frac{\mu}{sc}. \tag{6.1.20}$$

It is useful to define also a fusion power scaling law $P_{\mathrm{F}} = A_T^{(e)} A_n^{(e)} \tau_E$. From the previous expressions it turns out that for $p = 1 + \delta$

$$P_{\mathrm{F}} = \frac{3}{2}\frac{\mu^2}{c}\left(\frac{1}{cs}\right)^{1-1/\kappa}\left(\frac{1}{\mu v}\right)^{1/\kappa}. \tag{6.1.21}$$

For increasing temperatures, the parameter p in the alpha particle heating term tends to decrease when entering the burning plasma state and reactor conditions.

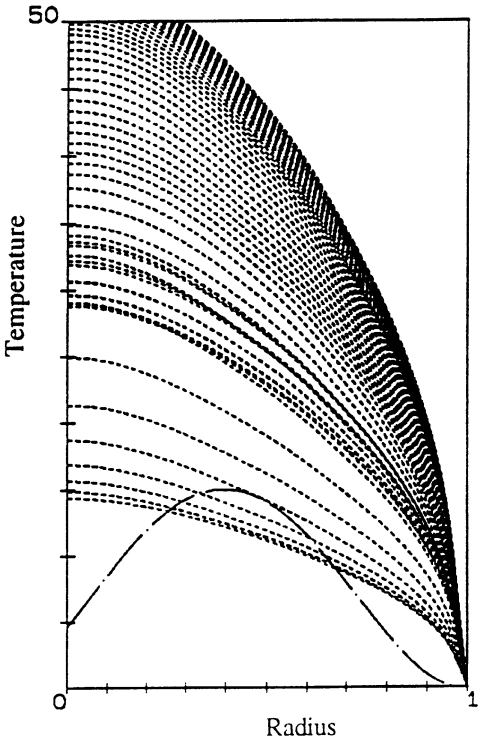

Figure 6.16. Curves describing the time evolution of a temperature profile from an initial state (thin dotted line) to an equilibrium state. The parameter values are: $e = 1$, $\delta = 1.5$, $p = 2.4$, $q = 0.5$, $a_T = 0.1$, $a_n = 0.001$, $k_T = 0.001$, $k_n = 0.001$, $b = 1$, $c = 5$, $\beta = 1$, $s = 30$ for $0 < r < 0.1$, $s = 0$ for $0.1 < r < 1$ ('H mode' simulation).

In the case $p = 1.5$, and $\delta = \kappa = 3/2$, the expression of the confinement time becomes

$$\tau_{\mathrm{E}} \propto \frac{1}{(cs)^{0.6}} \tag{6.1.22}$$

and

$$P_{\mathrm{F}} \propto \frac{1}{c}(cs)^{0.067}. \tag{6.1.23}$$

This energy confinement scaling $(cs)^{-m}$ compares reasonably well with result $m \sim 0.69$ of the H-mode obtained on the JET tokamak [6.4, 6.8].

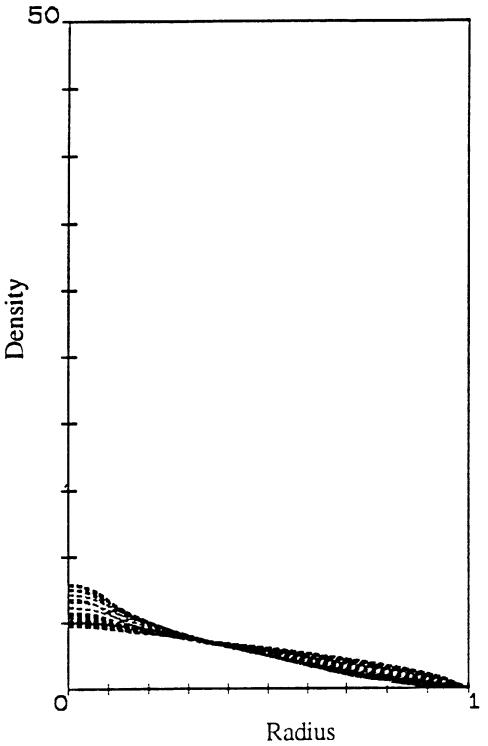

Figure 6.17. Curves describing the time evolution of the density profile from an initial state (thin dotted line) to an equilibrium state, with the parameters of figure 6.16 ('H mode' simulation).

For $p = 2$ and $\delta = \kappa = 3/2$, the scaling is

$$\tau_{\mathrm{E}} \propto \frac{1}{(cs)^{3/4}} \tag{6.1.24}$$

$$P_{\mathrm{F}} \propto \frac{1}{c}(cs)^{-0.083} \tag{6.1.25}$$

in reasonable agreement with the experimental results of the H-mode obtained on the DIII-D tokamak. The projected scaling for the reactor tokamak ITER is slightly lower: $m \sim 0.54$ [6.9]. All these cases illustrate the degradation of the energy confinement with input power, which was discovered experimentally and not predicted by theory, see chapter 2.

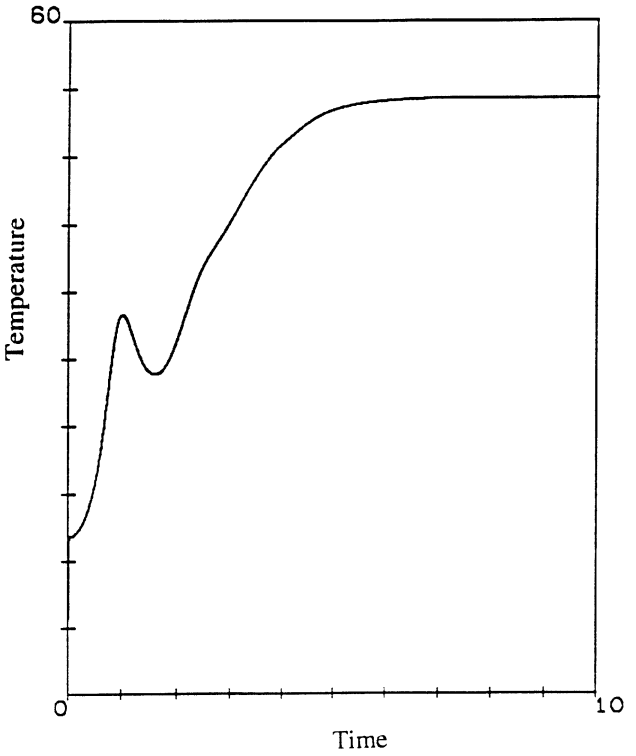

Figure 6.18. Time dependence of the central temperature for the case of figure 6.16.

It should be emphasized that the results expressed by relations (6.1.19)–(6.1.25) are obtained here by direct analytical solution of the coupled reaction–diffusion equation (6.1.1) for the transport of plasma temperature and density (in a one-fluid description and large aspect ration configuration), assuming that the thermal conductivity and particle diffusion coefficient have certain power law dependence on temperature.

An extensive literature exists devoted to the problems of determining from first principles the form of transport coefficients, in terms of the basic physical processes affecting the charged particles confined in the tokamak magnetic configuration. It is by no means accidental or miraculous that a rather satisfactory agreement of the global energy confinement time scaling can be obtained, within a certain range of values of the coefficients, without even having discussed the detailed physics of the transport phenomena. It means only that the structure of equations of the type (6.1.1) reproduces closely enough the dominant physical processes in a (MHD stable) plasma medium, and the confinement time (6.1.25) is an 'effective' index of the medium representing the balance of losses and sources.

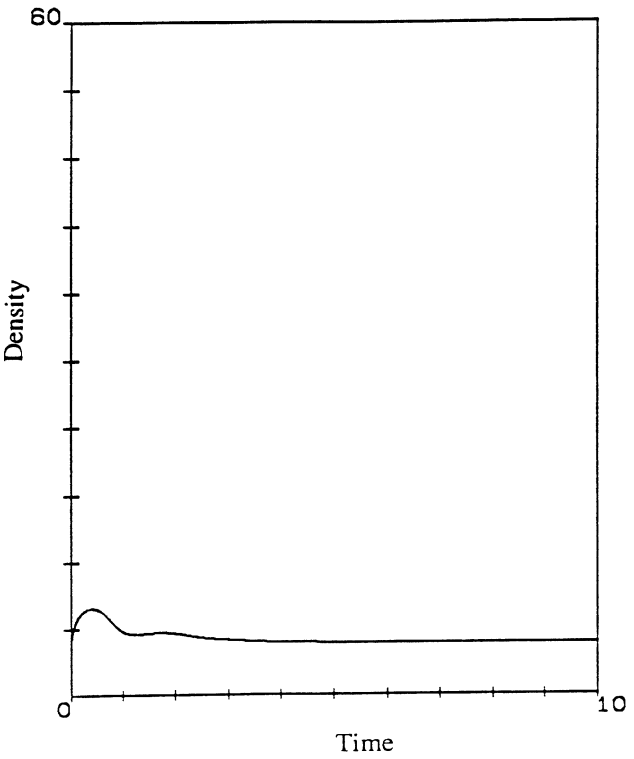

Figure 6.19. Time dependence of the central density for the case of figure 6.16.

For comparison, the following could be said. In the field of classical electromagnetics, the properties of a material medium can be usually defined by a dielectric constant (function), that to the external world helps to describe the overall response of the medium to external sources, for example microwaves, without making known the detailed microstructural responses when, for instance, a strong wave is scattered by a medium.

The interplay among experimental observations, analytic theory and computer simulations is necessary for progress in the understanding of the dynamics of the global processes in hot plasmas.

The examples discussed show how instructive the analysis of the dynamics of the 'lumped' variables can be in describing the profiles of temperature and density. The inspection of the 'phase space' topology for instance gives, to the trained eye, a rather prompt identification of the effects of the various terms of the process, for instance, it sheds light on the role of heat and particle pinches in approching an equilibrium. This procedure can, in fact, be adopted as a diagnostic tool for interpretation of experimental results: it is indeed possible, for

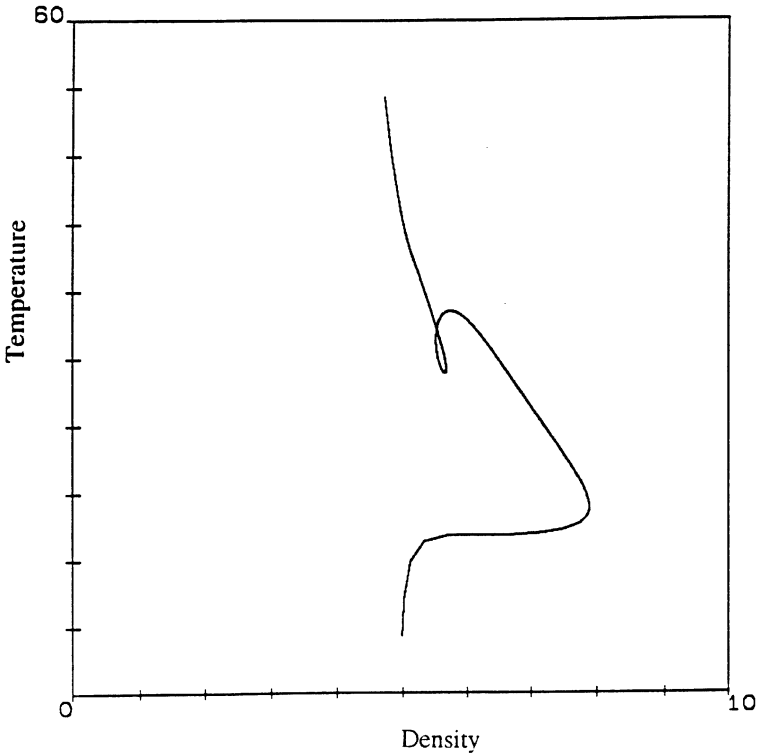

Figure 6.20. Phase-plane curve describing the time evolution of temperature T and density n for the cases of figures 6.16 and 6.17, from an initial state to a final equilibrium (stable spiral point). ('H mode' simulation including pinch term).

instance, to construct from an experiment plots of $T(0)$ versus $n(0)$ and interpret the plots in terms of comparison with the known 'models'.

A further model worth discussing concerns the dynamics of the temperature and density of hypothetical fusion plasma where the alpha particles become thermalized in a finite time τ_T, contributing to heat the plasma. A detailed study on the system of coupled equations for the (one fluid) plasma temperature, density and Ohmic current has been done by Wilhelmsson and Le Roux [6.11] in the usual cylindrical approximation, with the inclusion of Ohmic, auxilary and alpha particle power inputs and bremsstrahlung radiation losses.

Rather than repeating the lengthy derivation of the model equations for the temperature amplitudes and the profile parameters of the various quantities, it is convenient to present and discuss the results, related to the thermalization process of the alpha particles.

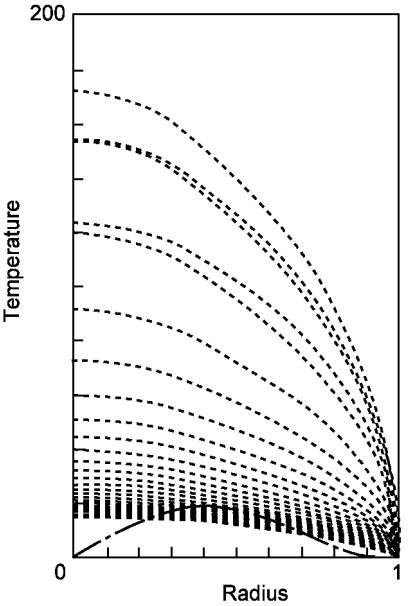

Figure 6.21. Set of curves describing the time evolution of a temperature profile from an initial state (thin dotted line) to an equilibrium state reached after some oscillations of the profile, neglecting pinch effect. The curves refer to a two-dimensional situation. The parameter values are: $e = 0, \delta = 1.5,\ p = 2.5, q = 0.5, a_T = 0.1, a_n = 0.001, k_T = 0.002,$ $k_n = 0.002,\ b = 1,\ c = 0.1,\ \beta = 1$ and $s = 30$ for $0 < r < 0.1,\ s = 0$ for $0.1 < r < 1$. Notice that $p = 1 + \delta$ for the case represented in the figure ('H mode' simulation).

It is just necessary to report the model consisting in coupled equations for temperature density and simple poloidal field diffusion to discuss the role of the thermalization effect and the interpretation of the results:

$$\left(\tau_T \frac{\partial}{\partial t} + 1\right)\left\{\frac{\partial T}{\partial t} - \frac{a_T}{r}\frac{\partial}{\partial r}\left[rT^{\delta}\frac{\partial T}{\partial r}\right] + \frac{k_T}{r}\frac{\partial}{\partial r}\left[rT^{\delta+1}\frac{1}{n}\frac{\partial n}{\partial r}\right] - \frac{1}{3n}(P_{\text{Ohm}} + P_{\text{aux}}) + enT^{q}\right\} = cnT^{p} \tag{6.1.26}$$

$$\left(\tau_n \frac{\partial}{\partial t} + 1\right)\left\{\frac{\partial n}{\partial t} - \frac{a_n}{r}\frac{\partial}{\partial r}\left[rT^{\kappa}\frac{\partial n}{\partial r}\right] + \frac{k_n}{r}\frac{\partial}{\partial r}\left[rT^{\kappa-1}n\frac{\partial T}{\partial r}\right]\right\} = S \tag{6.1.27}$$

$$\frac{\partial B_{\vartheta}}{\partial t} = -\frac{\partial}{\partial r}\left[\frac{\eta}{r}\frac{\partial r B_{\vartheta}}{\partial r}\right]. \tag{6.1.28}$$

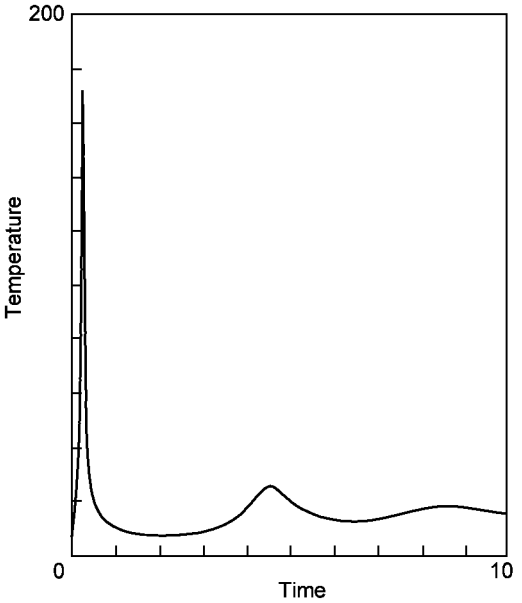

Figure 6.22. Time dependence of the central temperature for the case of figure 6.21. Notice the initial sharp peak of oscillation, a characteristic influence of the pinch effects.

Here, on account of the assumed equality of ion and electron temperatures, $\eta = c_{\rm res} Z_{\rm eff} T^{-3/2}$ and $\tau_T \cong 1.6 \times 10^{16} T^{3/2}/n$ and τ_n are the thermalization time constants of alpha particles and injected particles, respectively; the models for heat diffusivity used in the equations (6.1.26) and (6.1.27) are $\chi_T = 3a_T T^{\delta}$ and $\chi_n = -3k_T T^{\delta}$, respectively, while those for particle diffusion are $D_T = a_n T^{\kappa}$ and $D_n = -k_n T^{\kappa}$. The power input due to alpha particles is $P_\alpha = cnT^p$ with p ranging between 2.5 and 1.5 for a temperature interval between 8 and 20 keV [6.9].

The influence of the thermalization of alpha particles on the dynamic evolution of the plasma can be appreciated by examining the simplest case with neglect of radiation losses $(e = 0)$ and pure alpha heating $(c_{\rm res} = 0, h = 0)$. The equations for the central expansion amplitudes turn out to be:

$$\left(\tau_T \frac{\partial}{\partial t} + 1\right)\left(\frac{\mathrm{d}}{\mathrm{d}t} - \mu_c A_T^{\delta}\right) A_T = c A_T^p A_n$$
$$\left(\tau_n \frac{\partial}{\partial t} + 1\right)\left(\frac{\mathrm{d}}{\mathrm{d}t} - \nu_c A_T^{\kappa}\right) A_n = s_c . \tag{6.1.29}$$

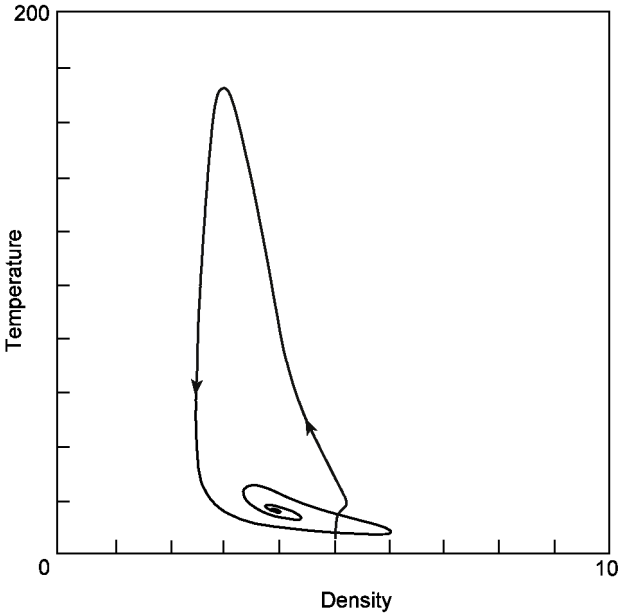

Figure 6.23. Phase-plane curve describing the time evolution of temperature T and density n for the cases of figures 6.21 and 6.22 from an initial state to a final equilibrium (stable spiral point). Arrows indicate the direction of time evolution.

Here the coefficients

$$\mu_c = 4(a_T/\ell_T^2 - k_T/\ell_n^2)[1 - (T_b/T_0)^{\delta+1}]$$
$$\nu_c = 4(a_n/\ell_n^2 - k_n/\ell_T^2)[1 - (n_b/n_0)^{\kappa+1}]$$

embed the all-important boundary conditions representing the effect of the MHD equilibrium configuration. In the following, the subscripts on μ and ν are omitted for simplicity.

This highly non-linear system describes oscillating solutions, around the fixed points given by expressions (6.1.8) and (6.1.9) and the frequency and damping rate can be estimated by linearization:

$$\begin{aligned}\omega^2 = \omega_0^2\Big\{1 + \tfrac{1}{2}(\tau_T + \tau_n)\nu A_T^{(s)}\kappa + \frac{\mu}{2}[\tau_T(\delta + 1 - 3p) \\ + \tau_n(\delta + 1 - p)]A_T^{(s)}\delta - \nu_{R0}\mu\nu[\tau_T(\delta + 1) \\ + \tau_n(\delta + 1 - p + \kappa)]A_T^{(s)\delta+\kappa}\Big\}\end{aligned} \tag{6.1.30}$$

$$v_R = v_{R0} - \tfrac{1}{2}[\kappa\mu v(\tau_T + 2\tau_n)A_T^{(s)\delta+\kappa} + p\mu^2\tau_T(\delta + 1 - p)A_T^{(s)}2\delta]. \tag{6.1.31}$$

In the particular case $p = \delta + 1$ and $\kappa = \delta$, one recovers the results (6.1.15)

$$\omega_0^2 = v_{R0}^2\left(4\frac{\delta\mu}{v} - 1\right)$$

$$v_{R0} = \frac{sc}{2\mu}.$$

Hence it appears that oscillations occur when $4\delta\mu/v > 1$.

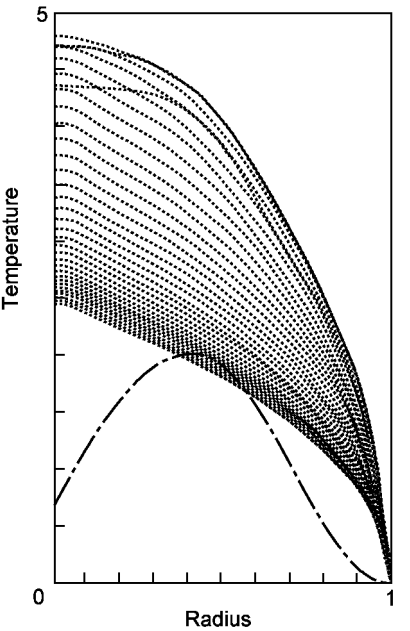

Figure 6.24. Curve describing the time evolution of a temperature profile for pure alpha particle heating including the effect of pinches ($k_T = k_n = 0.25$) and thermalization effects ($\tau_T = 0.5$, $\tau_n = 0.25$), assuming zero boundary conditions ($T_b = n_b = 0$). The parameter values are: $e = 1$, $\delta = 1.5$, $p = 2.4$, $q = 0.5$, $a_T = 1$, $a_n = 0.5$, $b = 1$, $c = 5$ and $s = 30$ for $0 < r < 0.1$, $s = 0$ for $0.1 < r < 1$. ('L mode' simulation with pinch effects). The dash-dotted curve indicates the arbitrary initial distribution that quickly grows to a maximum temperature distribution and then swings back to a lower stable equilibrium profile.

With the values appropriate for a drift-wave turbulence transport model [6.5] and thermonuclear power input $\delta = 3/2$, $p = \delta + 1$ and $\kappa = \delta$, this relation is fulfilled.

Therefore, while under the assumption that the density is constant, the approach of the temperature to the stable equilibrium is non-oscillatory; when the time variation of density is considered together with alpha heating, the approach to equilibrium is oscillatory.

When several heating processes are included at the same time in the description, it turns out that the oscillations are enhanced by increasing the thermonuclear power input, while the approach to equilibrium is non-oscillatory for Ohmic heating.

The effect of heat and particle pinches, if present, is to shorten the time scale of the oscillations.

In figure 6.24, the time evolution of a temperature profile for pure alpha particle heating is illustrated for a case that includes the effect of heat and particle pinches $(k_T = k_n = 0.25)$ and finite thermalization times

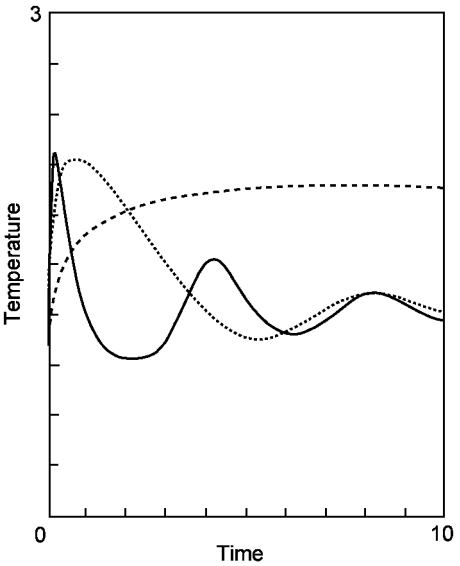

Figure 6.25. Time dependence of the central temperature for a case with parameters $e = 1$, $\delta = 1.5$, $\kappa = 1.5$, $p = 2.4$, $q = 0.5$, $a_T = 1$, $a_n = 0.5$, $b = 1$, $c = 5$, $\beta = 1$ and $s = 30$ for $0 < r < 0.1$, $s = 0$ for $0.1 < r < 1$. Thermalization effects are described by $\tau_T = cT^{3/2}/n$, $c_T = 0.01$ (solid curve), 0.1 (dotted curve), 1 (dashed curve) and $\tau_n = 0.01$. Simulation of L mode with zero boundary values ($T_b = n_b = 0$), neglecting pinch effects, ($k_T = 0$ and $k_n = 0$), for pure alpha particle heating (neglecting Ohmic heating, i.e. $c_{\mathrm{oh}} = 0$ in the Ohmic term $c_{\mathrm{oh}}T^{-3/2}/n$).

($\tau_T = 0.5$ and $\tau_n = 0.25$), assuming zero boundary conditions ($T_b = n_b = 0$). The parameter values are: $e = 1$, $\delta = 1.5$, $p = 2.4$, $q = 0.5$, $a_T = 1$, $a_n = 0.5$, $b = 1$, $c = 5$, and $s = 30$ for $0 < r < 0.1, s = 0$ for $0.1 < r < 1$.

The simulation may be considered that of an 'L mode'. The dash-dotted curve indicates the arbitrary initial profile that quickly grows to a maximum temperature distribution and then swings back to a lower stable equilibrium profile. The role of a finite time scale of thermalization of the alpha particles is shown in the plots of the central temperature, figure 6.25, and central density, figure 6.26, calculated for different temperature thermalization times.

The effect of thermalization of the high-energy alpha particles created by thermonuclear reactions is such as to smoothen the oscillations, i.e. to reduce their frequency and linear damping. The form of the explicit dependence of the thermalization time on temperature seems to have a tendency to support self-control of the oscillations in H mode simulations (with edge temperature pedestal) while for the L mode cases, this trend is much less evident.

6.2 Dynamic Response Treatment of Burning Fusion Plasmas

The existence of oscillatory regimes around the equilibrium values of temperature and density, demonstrated above, gives an interesting suggestion for a diagnostic of the hot plasma state.

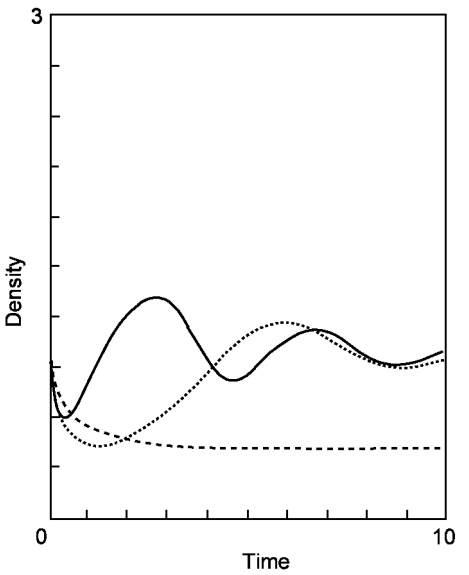

Figure 6.26. Thermal effects on the time evolution of the central density for the case of figure 6.25.

The response of a plasma to periodic variations in the heat and particle sources could give information on the characteristic values of transport coefficients of the plasma for equilibrium parameter domains and perhaps help deciphering the complex structure of the system. More specifically, one could envisage obtaining information on the values of the experiment, for example on the exponents p and δ appearing in the dynamic equations such as (6.1.1).

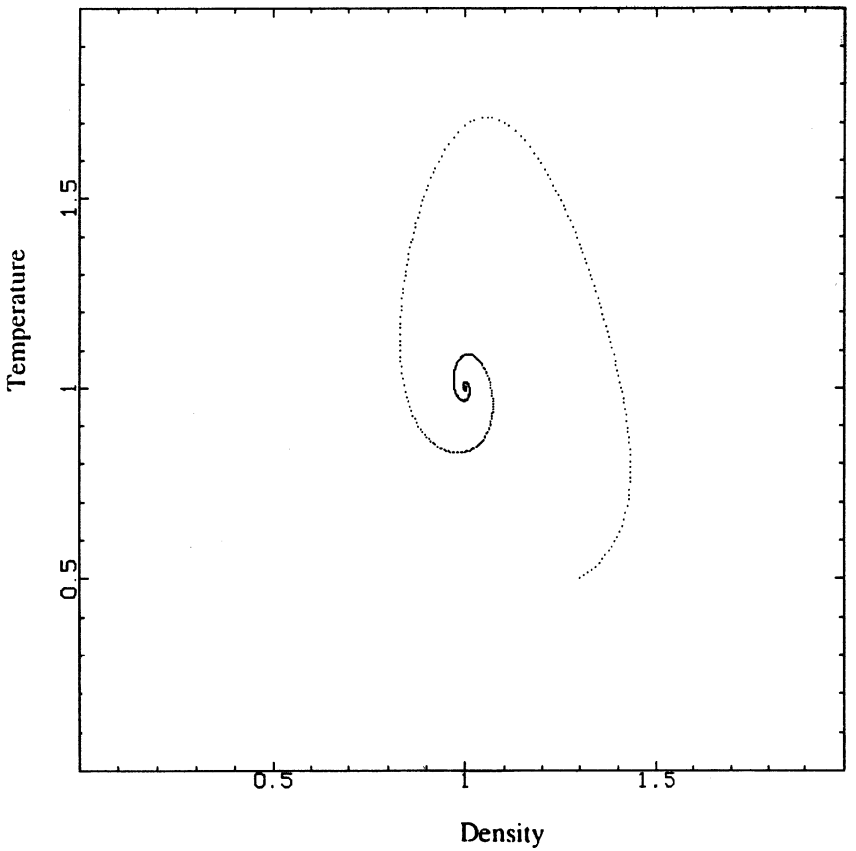

Figure 6.27. Phase-plane curve describing the time evolution of temperature T and density n in the centre of the plasma from an initial state to a final equilibrium (stable spiral point) in the absence of forced periodic variations. The parameters used are: $e = 0$, $\mu = 5$, $\nu = 1$, $\delta = 1.5$, $\kappa = 1.5$, $p = 2.4$, $q = 0.5$, $a_T = 0.1$, $a_n = 0.001$, $k_T = 0.001$, $k_n = 0.001$, $b = 1$, $c = 5$, $\beta = 1$ and $s = 1$; $T_0 = 0.5$, $n_0 = 1.3$. The frequency and damping of the free natural oscillations corresponding to the homogeneous solutions of equation (6) are $\omega_h = 2.85$ and $\lambda_R = 2.5$.

With such questions in mind, the basic problem of the influence of periodic perturbations on the plasma behaviour has been studied analytically and treated by numerical simulation [6.9]. For the domain close to a stable stationary point, the solution consists of a linear superposition of free and forced oscillations. The forced oscillations that remain as response after a sufficiently long time correspond to closed loops of nearly elliptical form in the $T(t) - n(t)$ plots.

When several periodic perturbations of different frequencies are applied simultaneously, the asymptotic state could have sub-loops and complicated structures would be repeated for all times. The numerical calculations confirm

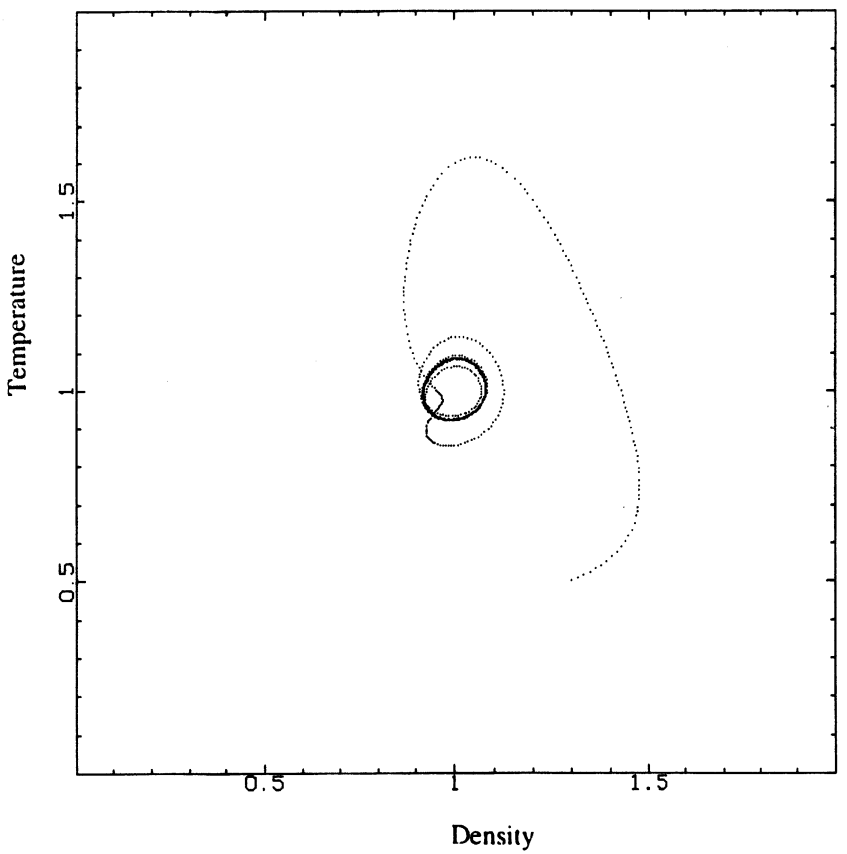

Figure 6.28. Phase-plane curve describing the time evolution of temperature T and density n in the centre of the plasma with the parameters of figure 6.27 in presence of a periodic variation of the particle source with $\varepsilon_s = 0.3$, $\omega_h = 5$ and $\lambda_R = 0$.

the results of the direct analysis and show how the shapes of the ellipses and the direction of their axes depend on the plasma transport and heating parameters, as well as on the applied frequency.

It remains to be settled how these interesting relations describing response of the burning fusion plasma to periodic perturbations (of the fuel source) can be applied for diagnosic purposes.

In figure 6.27, it is shown that free oscillations converge toward a stationary point in the *absence* of periodic perturbations, and in figure 6.28, the effect of such periodic perturpations is apparent.

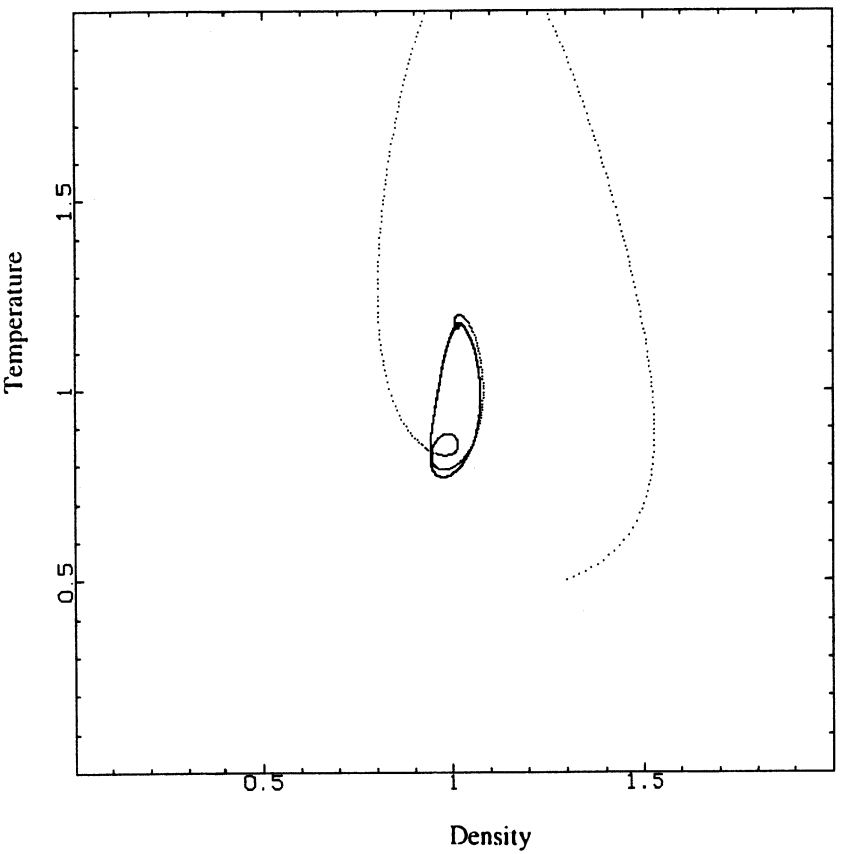

Figure 6.29. Phase-plane curve describing the time evolution of temperature T and density n in the centre of the plasma with the parameters of figure 6.27 in the presence of a periodic variation of the particle source with $\varepsilon_s = 0.3$, $\omega_h = 5$ and $\lambda_R = 0$.

References

[6.1] Connor J W and Taylor J B 1977 Scaling laws for plasma confinement *Nucl. Fus.* **17** 1047; Coppi B 1988 *Phys. Lett. A* **128** 183

[6.2] Cordey J G, Balet B, Campbell D, Challis C D, Christiansen J P, Gormezano C, Gower C, Muir D, Righi E, Saibene G R, Stubberfield P M and Thomsen K 1996 A review of the dimensionless parameter scaling studies *Plasma Phys. Control. Fus.* **38** A67

[6.3] Hazeltine R D and Meiss I D 1991 *Plasma Confinement* (Redwood City, CA: Addison-Wesley)

[6.4] Keilhacker M and the JET team 1991 Scrape-off layer model for the study of impurity retention in the pumped divertor planned for JET *Nucl. Fus.* **33** 1453

[6.5] Kim Y B, Diamond P H and Groebner R J 1991 Neoclassical poloidal and toroidal rotation in tokamaks *Phys. Fluids B* **3** 2050.

[6.6] Le Roux M-N, Weiland J and Wilhelmsson H 1992 Simulation of a coupled dynamic system of temperature and density in a fusion plasma *Phys. Scripta* **46** 457

[6.7] Reidel K S and Kaye S M 1990 Uncertainties associated with extrapolating L-mode energy confinement to ITER and CIT *Nucl. Fus.* **30** 731

[6.8] Schissel D P *et al* 1990 Impurity profiles for H-mode discharges in dIII-D *Nucl. Fus.* **30** 1999

[6.9] Wilhelmsson H, Stenflo L and Engelmann F 1970 Explosive instabilities in the well defined phase description *J. Math. Phys.* **11** 1738

[6.10] Weiland J 1999 Collective modes in inhomogeneous plasmas *Kinetic and Advanced Fluid Theory* (Bristol: IOP)

[6.11] Wilhelmsson H and Le Roux M-N 1993 Self consistent treatment of transport in tokamak plasmas *Phys. Scripta* **48** 735

[6.12] Wilhelmsson H and Gustafsson H-G 1994 Dynamic response treatment of a burning fusion plasma *Phys. Scripta* **49** 715

[6.13] Rebut P H, Lallia P P, Watkins M L 1988 The critical temperature gradient model of plasma transport: applications to JET and future tokamaks Controlled fusion and plasma physics *Proc. 12th Eur. Conf. (Nice 1988)* Vol 1 (Vienna: IAEA) p 191

Chapter 7

Phenomena in Resistive Magnetohydrodynamics

When the plasma can be described as a classical, electrically conducting fluid governed by the classical laws of motion of continua and thermodynamics summarized in chapter 2, one may still distinguish widely different regimes of the interaction with the electromagnetic field.

For low-frequency disturbances, the displacement current term in Maxwell equations can be neglected and the dynamics of two species system of particles interacting with a slowly varying field is given by:

$$\frac{\partial n_\alpha}{\partial t} + \nabla \cdot \boldsymbol{u}_\alpha n_\alpha = 0$$

$$m_\alpha n_\alpha \left[\frac{\partial}{\partial t}\boldsymbol{u}_\alpha + \boldsymbol{u}_\alpha \cdot \nabla \boldsymbol{u}_\alpha\right] = -\nabla p_\alpha + n_\alpha q_\alpha \left[\boldsymbol{E} + \frac{1}{c}\boldsymbol{u}_\alpha \times \boldsymbol{B}\right]$$

$$\nabla \times \boldsymbol{B} = \frac{4\pi}{c}\sum_\alpha q_\alpha n_\alpha \boldsymbol{u}_\alpha$$

$$\nabla \cdot \boldsymbol{B} = 0$$

$$\nabla \times \boldsymbol{E} = -\frac{1}{c}\frac{\partial \boldsymbol{B}}{\partial t}$$

$$\nabla \cdot \boldsymbol{E} = 4\pi \sum_\alpha n_\alpha q_\alpha$$

$$\frac{\partial p_\alpha}{\partial t} + \boldsymbol{u}_\alpha \cdot \nabla p_\alpha + \gamma p_\alpha \nabla \cdot \boldsymbol{u}_\alpha = 0.$$

The occurrence of self-similar evolution with explosive characteristics during processes of resistive reconnection of magnetic field lines around a neutral layer in a two species plasma is discussed in Tajima's book [7.3]. It is interesting to see that the basic approach to the solution of the equations of the model is quite similar to the methods outlined in chapter 2 of this text.

The coalescence instability is an ideal MHD process involving the redistribution of the current density on Alfvénic time scales and evolving later as a non-linear resistive reconnection. In a periodic slab geometry $-L_x \leq x \leq L_x$ and $-L_y \leq y \leq L_y$, let a sheared poloidal field along the y co-ordinate be generated by externally applied current sheets directed along the z co-ordinate and located at $y = 0$ and $y = L_y$ and let a constant magnetic field be along z, so that $\boldsymbol{B} = \nabla\Psi \wedge \boldsymbol{e}_z + B_z\boldsymbol{e}_z$ with a neutral line at $x = 0$ and perturbations due to finite resistivity allowed to grow in the x direction. The reconnection process developing a nearly one-dimensional current sheet is formed at the neutral layer.

Near $x = 0$, there is no specific scale length and one may assume as solutions of the system of governing equations a self-similar form with a single time-dependent scale factor $A(t)$, as the plasma is quasineutral:

$$n_e \approx n_i = \frac{n_0}{A(t)}, \qquad u_{ex} = u_{ix} = \frac{\dot{A}}{A}G(x) \tag{7.1}$$

where $G(x) \sim x$ on account of the local structure of the poloidal magnetic field $B_y(x,t) = B_0(t)x/\lambda$. It is shown after simple but lengthy algebra that the scale factor is governed by the equation

$$\ddot{A} = -\frac{v_A^2}{\lambda^2 A^2} + \frac{c_s^2}{\lambda^2 A^\gamma}. \tag{7.2}$$

The first term corresponds to the $\boldsymbol{J} \wedge \boldsymbol{B}$ force compressing the plasma, while the second term, due to finite pressure, gives the gas dynamic expansion eventually capable of leading to a saturated state. For a nearly one-dimensional compression (one degree of freedom), the equation for A can be integrated once to give

$$\dot{A}^2 = \frac{2v_A^2}{\lambda^2 A} - \frac{c_s^2}{\lambda^2 A^2} + C_0 \tag{7.3}$$

where

$$C_0 = \dot{A}_0^2 - \frac{2v_A^2}{\lambda^2 A_0} + \frac{c_s^2}{\lambda^2 A_0^2}$$

is the initial condition on the scale factor. The determination of the time behaviour of the scale factor leads to the expression of the time behaviour of the electromagnetic field and plasma quantities. The poloidal magnetic field energy density is

$$\frac{B_y^2}{8\pi} = \frac{B_{y0}^2}{8\pi A^4}\left(\frac{x}{\lambda}\right)^2. \tag{7.4}$$

As the scale factor $A(t)$ drops rapidly in time by orders of magnitude, a magnetic 'explosive' collapse occurs. For the details of the analysis, the cited references should be consulted, while here it is sufficient to cite the instructive description of the explosive stage of the coalescence in the limit of negligible plasma pressure. This corresponds to neglecting a possible saturation mechanism. From the first integral of motion with a small initial condition ε one has

$$\dot{A}^2 A = \frac{2v_A^2}{\lambda^2} - \varepsilon \equiv \left(\frac{2}{3}\frac{\mathrm{d}A^{3/2}}{\mathrm{d}t}\right)^2 \tag{7.5}$$

and therefore to leading order

$$A(t) \approx \left(\frac{9}{2}\right)^{1/2}\left(\frac{v_A}{\lambda}\right)^{2/3}(t_0 - t)^{2/3} + O(\varepsilon) \tag{7.6}$$

vanishes at a finite time t_0 and the associated physical quantities have an explosive behaviour, e.g.

$$u_x = -\frac{2}{3}\frac{x}{(t_0 - t)} \tag{7.7}$$

$$\frac{B_y^2}{8\pi} = \frac{B_{y0}^2\lambda^{2/3}}{8\pi v_A^{8/3}}\left(\frac{2}{9}\right)^{4/3}\frac{x^2}{(t_0 - t)^{8/3}}. \tag{7.8}$$

In conclusion, there is a variety of phenomena which can be described through the use of varying scale factors, that is a version of the 'central expansion' procedure suitable for diffusion–reaction problems and related to the similarity transformation of the equations.

Formal similarities of the reaction–diffusion problems (in the special case where the diffusion part is omitted) also exist with another interesting problem, namely that of coherent non-linear interaction of waves in plasmas.

This gives a reason to include in the text a section on coherent non-linear interaction of waves, which also offers an interesting connection with another important problem area, namely the reconnection of magnetic field lines [7.1] and the associated formation and coupling of rotating magnetic islands in a tokamak [7.2], that can lead to deterioration of plasma confinement.

The interaction of three waves also exhibits in particular cases explosive phenomena similar to those referred to in relation (7.8) that may describe the evolution of a solar flare due to the coalescence instability of two merging current carrying loops [7.3].

References

[7.1] Leboeuf J N, Tajima T and Dawson J M 1982 Dynamic magnetic X points *Phys. Fluids* **25** 784

[7.2] Pritchett P L and Wu C 1979 Coalescence of magnetic islands *Phys. Fluids* **22** 2140

[7.3] Tajima T 1989 *Computational Plasma Physics: with Applications to Fusion and Astrophysics* (Redwood City, CA: Addison-Wesley)

Chapter 8

Coherent Non-linear Interaction of Waves in Plasmas

In a plasma, a wide spectrum of waves can exist. If certain waves attain large amplitude and if certain kinematic relations of congruence among the wave vectors and frequency occur, then strong dynamic coupling is possible among multiplets of waves. This type of coupling is non-linear, involving products of the amplitudes of the interacting waves, and the lowest order, most important case is that of three-waves interaction. A comprehensive derivation of the governing equations and their treatment for transverse and longitudinal waves in a plasma is given in the book by Weiland and Wilhelmsson [8.9] to which we refer for the main concepts and notation. Here we present and discuss a selected number of topics related to the subject of the previous chapters. However, a brief introduction is necessary to illustrate the essence of the problem for our specific purposes. We recall that the propagation of electromagnetic waves, transverse and longitudinal in a plasma in specific regimes of equilibrium parameters (density, temperature and ambient magnetic field) can be studied at the linear level from the knowledge of the 'dispersion relation', which for *initial value problems* relates the possible (complex) wave frequencies to real propagation vectors (or refraction indices) and for *boundary value problems* relates real wave frequency to the possible complex propagation vectors.

The procedure of constructing the plasma response to electromagnetic field perturbations in terms of a dispersion relation in specific plasma regimes (fluid, kinetic) is a vast and fascinating subject, well established and treated in classical textbooks to which we refer the interested reader [8.1, 8.11, 8.12] for the details of the general derivation, of which we are here content to summarize the logical steps. The closure of the system of Maxwell equations for a plasma can be given by associating the evolution equations for the first two moments of the distribution functions of the charged particles, $\rho_\alpha = n_\alpha q_\alpha$ and $\boldsymbol{u}_\alpha$, illustrated in chapter 1:

$$
\begin{aligned}
\nabla \times \boldsymbol{E} &= -\frac{1}{c}\frac{\partial \boldsymbol{B}}{\partial t} \\
\nabla \times \boldsymbol{B} &= \frac{4\pi}{c}\sum_{\alpha} q_\alpha n_\alpha \boldsymbol{u}_\alpha + \frac{1}{c}\frac{\partial \boldsymbol{E}}{\partial t} \\
\nabla \cdot \boldsymbol{E} &= 4\pi \sum_{\alpha} n_\alpha q_\alpha \\
\nabla \cdot \boldsymbol{B} &= 0.
\end{aligned}
\tag{8.1}
$$

The basic approach to the study of this system of equations is to consider through a technique of linearization a class of solutions infinitesimally close to an exact, albeit trivial, equilibrium solution with uniform background parameters. Generalization to slightly inhomogeneous equilibrium conditions is possible so long as the ratio of the typical wavelength of interest is much smaller than the scale length of the relevant equilibrium quantity. For the treatment of such cases by appropriate asymptotic techniques, we refer to the specialized literature.

It is convenient to introduce a formal smallness parameter $\varepsilon \ll 1$ as a reminder of the ordering of the perturbation with respect to the equilibrium quantities and look for a solution of the form

$$
\begin{aligned}
n_\alpha &= N + \varepsilon \tilde{n}_\alpha(x,t) \qquad & \boldsymbol{E} &= \varepsilon \tilde{\boldsymbol{E}}_\alpha(\boldsymbol{x},t) \\
\boldsymbol{u}_\alpha &= \varepsilon \tilde{\boldsymbol{u}}_\alpha(\boldsymbol{x},t) \qquad & \boldsymbol{B} &= \boldsymbol{B}_0 + \varepsilon \tilde{\boldsymbol{B}}_\alpha(\boldsymbol{x},t).
\end{aligned}
\tag{8.2}
$$

Applying the procedure and retaining the leading order contributions in ε, one obtains a linearized version of the original set of equations for the twiggled variables that is space and time dependent. The simplest approach is to consider a particular form for each of these unknown perturbations fields $\tilde{\varphi}_\alpha(\boldsymbol{x},t)$ as 'normal modes', with space and time harmonic dependence $\tilde{\varphi}_\alpha(\boldsymbol{x},t) = \tilde{\varphi}_{\alpha,\boldsymbol{k},\omega} \mathrm{e}^{\mathrm{i}[\boldsymbol{k}\cdot\boldsymbol{x}-\omega t]}$ the PDE system of equations is reduced to a single algebraic system for a single unknown, say the electric field perturbation $\tilde{\boldsymbol{E}}(\boldsymbol{x},t) = \tilde{\boldsymbol{E}}_{\boldsymbol{k},\omega} \mathrm{e}^{\mathrm{i}[\boldsymbol{k}\cdot\boldsymbol{x}-\omega t]}$, in the form:

$$
\left[\boldsymbol{k}\boldsymbol{k} - k^2 \overleftrightarrow{\boldsymbol{I}} + \frac{\omega^2}{c^2}\overleftrightarrow{\varepsilon}(\omega,\boldsymbol{k})\right] \cdot \tilde{\boldsymbol{E}}_{\boldsymbol{k},\omega} = 0 \tag{8.3}
$$

where $\overleftrightarrow{\varepsilon}(\omega,\boldsymbol{k})$ is the dielectric tensor of the medium (plasma), a complex entity depending on the wave vector and frequency as well as on the plasma equilibrium parameters (density, temperature and ambient magnetic field), which summarizes the macroscopic response of matter to the external electromagnetic perturbation by an effect of polarization, which tends to decrease the total field in the medium, i.e. to produce a screening effect to the applied field. This effect may be due, for instance, to a displacement of the electron shells in neutral

atoms or to changes in orientation of permanent electric dipoles in the material medium. In a plasma where the charged particles may move freely, the screening effect is due to induced currents. The finite inertia of the moving particles, albeit very small, requires a finite time to set up the response polarization field. The response time scale is related to a characteristic frequency of the medium which for a plasma is the well-known 'plasma frequency' $\omega_{p\alpha}^2 = 4\pi q_\alpha^2 n_\alpha / m_\alpha$ proportional to the density of particles.

The causal response between the applied field and the induced polarization field $\tilde{\boldsymbol{P}}(\boldsymbol{x},t)$ at point $\boldsymbol{x}$ at time t can be formally postulated as the integral operator relation $\tilde{\boldsymbol{P}}(\boldsymbol{x},t) = \iint \overleftrightarrow{\chi}(\boldsymbol{x}-\boldsymbol{x}',t-t') \cdot \tilde{\boldsymbol{E}}(\boldsymbol{x}',t)\,\mathrm{d}\boldsymbol{x}'\,\mathrm{d}t'$ connecting it to the driving field at earlier times in different points through the medium susceptivity response tensorial kernel $\overleftrightarrow{\chi}(\boldsymbol{x},t)$.

This is the phenomenon of space and time dispersion. The convolution relation between $\tilde{\boldsymbol{P}}(\boldsymbol{x},t)$ and $\tilde{\boldsymbol{E}}(\boldsymbol{x},t)$ is conveniently treated through integral transforms. Typically, when applicable, a Fourier transform yields the closure relation $\tilde{\boldsymbol{D}}_{k,\omega} = \overleftrightarrow{\varepsilon}(\omega,\boldsymbol{k}) \cdot \tilde{\boldsymbol{E}}_{\boldsymbol{k},\omega}$ between the Fourier amplitude of the electric displacement vector in the medium and the Fourier amplitude of the electric field, having used the standard definitions $\tilde{\boldsymbol{D}}_{\boldsymbol{k},\omega} = \tilde{\boldsymbol{E}}_{\boldsymbol{k},\omega} + 4\pi\tilde{\boldsymbol{P}}_{\boldsymbol{k},\omega}$ and a tensorial permittivity $\overleftrightarrow{\varepsilon}(\omega,\boldsymbol{k}) = \overleftrightarrow{\boldsymbol{I}} + 4\pi\overleftrightarrow{\chi}(\omega,\boldsymbol{k})$.

An alternative form of the response of matter to electromagnetic fields is given in terms of the current density fields driven by the electric field. In the following it will be of interest to consider the non-linear current response, which in a spatially homogeneous, time-independent medium can be written in general as:

$$\begin{aligned}\tilde{\boldsymbol{J}}(\boldsymbol{x},t) = &\iint \underline{\underline{\sigma}}(\boldsymbol{x}-\boldsymbol{x}',t-t') \cdot \tilde{\boldsymbol{E}}(\boldsymbol{x}',t')\,\mathrm{d}\boldsymbol{x}'\,\mathrm{d}t' \\ &+ \int \mathrm{d}\boldsymbol{x}' \int \mathrm{d}t' \int \mathrm{d}\boldsymbol{x}'' \int \mathrm{d}t'' \underline{\underline{\sigma}}(\boldsymbol{x}-\boldsymbol{x}',t-t',\boldsymbol{x}-\boldsymbol{x}'',t-t''): \\ &\times \tilde{\boldsymbol{E}}(\boldsymbol{x}',t')\tilde{\boldsymbol{E}}(\boldsymbol{x}'',t'') + \cdots \end{aligned} \tag{8.4}$$

where the linear and dominant non-linear contributions are displayed separately

$$\tilde{\boldsymbol{J}}(\boldsymbol{x},t) = \tilde{\boldsymbol{J}}_L(\boldsymbol{x},t) + \tilde{\boldsymbol{J}}_{NL}(\boldsymbol{x},t) \tag{8.5}$$

and the neglected terms are *assumed* to be of higher order in some small parameter specific of a given system.

However, the *linear* and *non-linear* contributions to the response are not to be confused with ordering, for instance in an expansion of the field amplitudes

$$\tilde{\boldsymbol{E}}(\boldsymbol{x},t) = \tilde{\boldsymbol{E}}_1(\boldsymbol{x},t) + \varepsilon\tilde{\boldsymbol{E}}_2(\boldsymbol{x},t) + \varepsilon^2\tilde{\boldsymbol{E}}_3(\boldsymbol{x},t) + \cdots \tag{8.6}$$

In fact, at the same order in ε, we may have both a *linear* and a *non-linear* response current density contribution.

The convolution structure of the causal expression for $\tilde{\boldsymbol{J}}(\boldsymbol{x},t)$ allows the use of Fourier transforms (or a 'normal mode' ansatz) obtaining the relation $\tilde{\boldsymbol{J}}_{\boldsymbol{k},\omega} = \overleftrightarrow{\sigma}(\omega,\boldsymbol{k})\tilde{\boldsymbol{E}}_{\boldsymbol{k},\omega}$ that implies that the conductivity tensor $\overleftrightarrow{\sigma}(\omega,\boldsymbol{k})$ is related to the permittivity tensor by $\overleftrightarrow{\sigma}(\omega,\boldsymbol{k}) = (\mathrm{i}\omega/4\pi)[\overleftrightarrow{\boldsymbol{I}} - \overleftrightarrow{\varepsilon}(\omega,\boldsymbol{k})]$.
The tensor

$$\overleftrightarrow{\mathscr{D}} \equiv \left[\boldsymbol{k}\boldsymbol{k} - k^2\overleftrightarrow{\boldsymbol{I}} + \frac{\omega^2}{c^2}\overleftrightarrow{\varepsilon}(\omega,\boldsymbol{k})\right]$$

or

$$\overleftrightarrow{\mathscr{D}} \equiv \left[\left[\frac{\omega^2}{c^2} - k^2\right]\overleftrightarrow{\boldsymbol{I}} + \boldsymbol{k}\boldsymbol{k} + \frac{4\pi i}{\omega}\frac{\omega^2}{c^2}\overleftrightarrow{\sigma}(\omega,\boldsymbol{k})\right]$$

is the dispersion dyadic governing the relations among wave vector and wave frequency, through the condition, called the dispersion relation

$$\mathscr{D}(\omega,\boldsymbol{k}) = \det[\overleftrightarrow{\mathscr{D}}] = 0. \tag{8.7}$$

The discussion of wave properties in terms of the dispersion relation, which is generally a complex function of $(\omega,\boldsymbol{k})$, can often become quite subtle, although in the simplest cases it is very explicit.

For the considerations to follow, it is mainly of interest to consider the formulation of the so called initial value problem in which the wave vector should be considered an 'assigned' real vector and the dispersion relation

$$\mathscr{D}(\omega,\boldsymbol{k}) = \mathscr{D}_{\mathrm{R}}(\omega,\boldsymbol{k}) + \mathrm{i}\mathscr{D}_{\mathrm{I}}(\omega,\boldsymbol{k}) = 0 \tag{8.8}$$

is solved for the frequency $\omega(\boldsymbol{k}) = \omega_{\mathrm{R}}(\boldsymbol{k}) + \mathrm{i}\omega_{\mathrm{I}}(\boldsymbol{k})$, a complex quantity, function of the wave vector $\boldsymbol{k}$. The real part of the frequency is related to the wave phase and group velocities defined as $\boldsymbol{v}_{\mathrm{ph}} = \omega_{\mathrm{R}}/\boldsymbol{k}$ and $\boldsymbol{v}_{\mathrm{g}} = \partial\omega_{\mathrm{R}}/\partial\boldsymbol{k}$, respectively. The imaginary part $\omega_{\mathrm{I}}(\boldsymbol{k}) = \gamma(\boldsymbol{k})$ is related to the damping or amplification rate of the wave amplitude in time, according to its sign. Therefore, it is related to the exchange of energy between the wave and the dielectric medium. When it can be considered small relative to the real part of the frequency, it can be estimated from equating real and imaginary parts of the complex dispersion relation expanded in Taylor series to leading order:

$$\gamma(\boldsymbol{k})\frac{\partial\mathscr{D}_{\mathrm{R}}(\omega_{\mathrm{R}},\boldsymbol{k})}{\partial\omega} + \mathscr{D}_{\mathrm{I}}(\omega_{\mathrm{R}}(\boldsymbol{k}),\boldsymbol{k}) = 0. \tag{8.9}$$

In fact, a wave propagating in a dielectric medium (here a plasma) is a systematic variation of field and particle energy, which can be conveniently ex-

pressed in terms of the dielectric tensor $\overleftrightarrow{\varepsilon}(\omega, \boldsymbol{k})$. In order to simplify the discussion, we shall limit the consideration of the 'time dispersion' case.

To progress, we need a discussion of Poynting theorem for a real quasi-monochromatic field of the form $\vec{\mathscr{E}}(\boldsymbol{x}, t) = \frac{1}{2}\tilde{\boldsymbol{E}}_\omega(\boldsymbol{x}, \tau)\mathrm{e}^{-\mathrm{i}\omega t} + \text{c.c.}$, where c.c. denotes the complex conjugate and $\tau = \varepsilon t$ is a time scale of variation of the amplitude, slow compared to the time scale of variation of the phase. Furthermore, to avoid the difficulty associated with the unphysical fact that at $t \to -\infty$ monochromatic fields do not vanish, it is expedient to assume $\tilde{\boldsymbol{E}}_\omega(\boldsymbol{x}, \tau) = \boldsymbol{E}(\boldsymbol{x})\mathrm{e}^{-\nu t}$, which amounts to the device of considering formally a complex frequency $s = \omega - \mathrm{i}\nu$ with $\nu \ll \omega$. Then the real Poynting vector $\vec{\mathscr{P}} = (c/4\pi)(\vec{\mathscr{E}} \times \vec{\mathscr{B}})$ is written as

$$\begin{aligned}\vec{\mathscr{P}} = &\frac{c}{16\pi}[\boldsymbol{E}(\boldsymbol{x}) \times \boldsymbol{B}^*(\boldsymbol{x}) + \boldsymbol{E}^*(\boldsymbol{x}) \times \boldsymbol{B}(\boldsymbol{x})]\mathrm{e}^{-2\nu t} \\ &+ \frac{c}{16\pi}[\boldsymbol{E}(\boldsymbol{x}) \times \boldsymbol{B}(\boldsymbol{x})\mathrm{e}^{-\mathrm{i}2\omega t} + \boldsymbol{E}(\boldsymbol{x}) \times \boldsymbol{B}(\boldsymbol{x})\,\mathrm{e}^{+\mathrm{i}2\omega t}]\,\mathrm{e}^{-2\nu t}. \qquad (8.10)\end{aligned}$$

Averaging over the quasiperiod $T = 2\pi/\omega$, the oscillating terms give zero contributions and the result is a slowly varying average

$$\langle\vec{\mathscr{P}}\rangle_T = \frac{c}{16\pi}[\boldsymbol{E}(\boldsymbol{x}) \times \boldsymbol{B}^*(\boldsymbol{x}) + \boldsymbol{E}^*(\boldsymbol{x}) \times \boldsymbol{B}(\boldsymbol{x})]\mathrm{e}^{-2\nu t}. \qquad (8.11)$$

The Maxwell system applied to fields of the form

$$\begin{aligned}&\vec{\mathscr{E}}(\boldsymbol{x}, t) = \tfrac{1}{2}\boldsymbol{E}(\boldsymbol{x})\mathrm{e}^{-\mathrm{i}st} + \text{c.c.}, \quad \vec{\mathscr{E}}(\boldsymbol{x}, t) = \tfrac{1}{2}\boldsymbol{E}(\boldsymbol{x})\mathrm{e}^{-\mathrm{i}st} + \text{c.c.}, \\ &\vec{\mathscr{D}}(\boldsymbol{x}, t) = \tfrac{1}{2}\vec{\boldsymbol{D}}(\boldsymbol{x})\mathrm{e}^{-\mathrm{i}st} + \text{c.c.}\end{aligned}$$

gives

$$\nabla \times \boldsymbol{E} = -\frac{\mathrm{i}s}{c}\boldsymbol{B}, \quad \nabla \times \boldsymbol{B} = -\frac{\mathrm{i}s}{c}\boldsymbol{D} = -\frac{\mathrm{i}s}{c}\overleftrightarrow{\varepsilon} \cdot \boldsymbol{E} \qquad (8.12)$$

and therefore the divergence of Poynting vector is

$$\nabla \cdot \langle\vec{\mathscr{P}}\rangle_T = \frac{\mathrm{i}\mathrm{e}^{-2\nu t}}{16\pi}\{\boldsymbol{E}^*(\boldsymbol{x}) \cdot [s\overleftrightarrow{\varepsilon}(s) - s^*\overleftrightarrow{\varepsilon}^*(s)] \cdot \boldsymbol{E}(\boldsymbol{x}) - 2\mathrm{i}\nu\boldsymbol{B} \cdot \boldsymbol{B}^*\}. \qquad (8.13)$$

Since $\nu \ll \omega$ expanding around ω gives

$$s\overleftrightarrow{\varepsilon}(s) - s^*\overleftrightarrow{\varepsilon}(s) = -2\mathrm{i}\nu\frac{\partial\omega\overleftrightarrow{\varepsilon}(\omega)}{\partial\omega} \qquad (8.14)$$

therefore, since $-2\nu e^{-2\nu t} = (de^{-2\nu t}/dt)$, one obtains the Poynting theorem for quasimonochromatic fields in a time dispersive medium

$$-\nabla \cdot \langle \vec{\mathscr{P}} \rangle_T = \frac{\partial}{\partial t} \left\{ \frac{1}{8\pi} \boldsymbol{E}^* \cdot \frac{\partial \omega \overleftrightarrow{\varepsilon}(\omega)}{\partial \omega} \cdot \boldsymbol{E} + \frac{\|B\|^2}{8\pi} \right. \tag{8.15}$$

Since

$$\frac{\partial \omega \overleftrightarrow{\varepsilon}(\omega)}{\partial \omega} = c^2 \frac{\partial \overleftrightarrow{\mathscr{D}}(\omega, \boldsymbol{k})}{\partial \omega}$$

equation (8.15) can be rewritten as

$$-\nabla \cdot \langle \vec{\mathscr{P}} \rangle_T = \frac{\partial}{\partial t} \left\{ \frac{c^2}{8\pi} \boldsymbol{E}^* \cdot \frac{\partial \overleftrightarrow{\mathscr{D}}(\omega, \boldsymbol{k})}{\partial \omega} \cdot \boldsymbol{E} \right\}. \tag{8.16}$$

8.1 Formalism for Non-linear Wave Coupling

As anticipated, the characteristic waves satisfying the plasma dispersion relation may meet conditions of frequency and wavenumber matching too, whereby a resonant interaction is possible with another wave compatible with the dispersion relation.

To visualize the meaning of the kinematic conditions, which allow coupling between waves with transfer of energy among them, it is useful to consider a particular direction of propagation, say along an ambient magnetic field, and represent each interacting wave by vectors of components (ω_j, k_j) in the plane (ω, k) where separate branches $\omega(k)$ of the dispersion relation $\mathscr{D}_{\mathrm{R}}(\omega, k) = 0$ are also plotted.

Three wave coupling is allowed if they form a closed parallelogram of representative vectors with their tips lying on (necessarily distinct) branches of the dispersion curves. The kinematic conditions are therefore

$$\begin{aligned} \omega_1 &= \omega_2 + \omega_0 \\ \boldsymbol{k}_1 &= \boldsymbol{k}_2 + \boldsymbol{k}_0 \end{aligned} \tag{8.1.1}$$

and they involve two waves on the high-frequency branch and the other (decay wave) on the low-frequency one.

The energy exchange among waves occurs because physically perturbed currents generated by each wave act as sources for the other.

Here we shall outline as a matter of principle a procedure for the calculation of the coupling interaction for the simplest case of an isotropic plasma without

external magnetic field. In practice, in concrete cases, more agile *ad hoc* methods can be used. The specialized literature offers numerous instructive examples.

The coupling term is generally proportional to product of the amplitudes on the interacting waves and, to be specific, it is necessary to examine the particular linear models for the various waves.

It is convenient to separate the electromagnetic wave field as $\widetilde{\boldsymbol{E}}_{\boldsymbol{k},\omega} = \widetilde{\boldsymbol{E}}_{L,\omega} + \widetilde{\boldsymbol{E}}_{T,\omega}$ where $\widetilde{\boldsymbol{E}}_{L,\omega} = \widetilde{E}_{L,\omega} k^{-1}\boldsymbol{k}$, with $\widetilde{E}_{L,\omega} = k^{-1}(\boldsymbol{k} \cdot \boldsymbol{E}_{\boldsymbol{k},\omega})$, represents the longitudinal waves with the field along the propagation vector and $\widetilde{\boldsymbol{E}}_{T,\omega} = \widetilde{\boldsymbol{E}}_{\boldsymbol{k},\omega} - k^{-2}(\boldsymbol{k} \cdot \widetilde{\boldsymbol{E}}_{\boldsymbol{k},\omega})\boldsymbol{k}$ are the transverse waves for which $\boldsymbol{k} \cdot \widetilde{\boldsymbol{E}}_{\boldsymbol{k},\omega} = 0$. The Fourier transformed *linear* wave equation is then rewritten as

$$\left(\varepsilon_T(\omega,\boldsymbol{k}) - \frac{c^2k^2}{\omega^2}\right)[\overleftrightarrow{\boldsymbol{I}} - k^{-2}\boldsymbol{k}\boldsymbol{k}] \cdot \widetilde{\boldsymbol{E}}_{k,\omega} + [\varepsilon_L(\omega,\boldsymbol{k})\overleftrightarrow{\boldsymbol{I}}] \cdot \widetilde{\boldsymbol{E}}_{L,\omega} = 0. \quad (8.1.2)$$

By scalar multiplication with k the equation (8.1.2) for longitudinal waves becomes

$$\varepsilon_L(\omega,\boldsymbol{k})\widetilde{E}_{L,\omega} = 0 \quad (8.1.3)$$

and, for instance, in the case of a 'warm' plasma in the fluid description one can write:

$$\varepsilon_L = 1 - \sum_\alpha \frac{\omega_{p\alpha}^2}{\omega^2 - k^2 v_{th\alpha}^2} = 0 \quad (8.1.4)$$

where ω is the longitudinal wave frequency and $v_{th,\alpha}$ is the thermal velocity of species α. For transverse waves $\widetilde{\boldsymbol{E}}_{T,\omega} = [\overleftrightarrow{\boldsymbol{I}} - k^{-2}\boldsymbol{k}\boldsymbol{k}] \cdot \widetilde{\boldsymbol{E}}_{\boldsymbol{k},\omega} \neq 0$ and the equation (8.1.2) takes the form

$$\left\{\frac{c^2k^2}{\omega^2} - \varepsilon_T(\omega,\boldsymbol{k})\right\}\widetilde{E}_{T,\omega} = 0 \quad (8.1.5)$$

which, for example, for a plasma in the fluid description means

$$\varepsilon_T = 1 - \sum_\alpha \frac{\omega_{p\alpha}^2}{\omega^2} \quad (8.1.6)$$

where ω is the frequency of the transverse waves .

Let us consider now the case in which the wave equation (8.3) in the Fourier space has non-linear source terms (current densities related non-linearly to the field amplitude)

$$\overleftrightarrow{\mathscr{D}}(\omega,\boldsymbol{k}) \cdot \widetilde{\boldsymbol{E}}_{\boldsymbol{k},\omega} = -\mathrm{i}\varepsilon\boldsymbol{J}_{NL} \quad (8.1.7)$$

where ε is a smallness tag.

Then the non-linear equation (8.1.7), split in longitudinal (L) and transverse (T) parts, takes the form

$$\overleftrightarrow{\mathscr{D}}_T(\omega,\boldsymbol{k}) \cdot \widetilde{\boldsymbol{E}}_{T,\omega} + \overleftrightarrow{\mathscr{D}}_L(\omega,\boldsymbol{k}) \cdot \widetilde{\boldsymbol{E}}_{L,\omega} = -\mathrm{i}\varepsilon\boldsymbol{J}_{NL}. \quad (8.1.8)$$

Since $\vec{\mathscr{D}}_L(\omega, \boldsymbol{k}) = D_L k^{-2} \boldsymbol{k}\boldsymbol{k}$ projecting along the wavevector by scalar multiplication of (8.1.8) with $\boldsymbol{k}/k$ leads to

$$D_L(\omega, \boldsymbol{k}) \widetilde{E}_{L,\omega} = -\mathrm{i}\varepsilon k^{-1} \boldsymbol{k} \cdot \boldsymbol{J}_{NL} \tag{8.1.9}$$

and similarly projection on the transverse direction leads to

$$D_T(\omega, \boldsymbol{k}) \widetilde{E}_{T,\omega} = -\mathrm{i}\varepsilon [\vec{\boldsymbol{I}} - k^{-2} \boldsymbol{k}\boldsymbol{k}] \cdot \boldsymbol{J}_{NL}. \tag{8.1.10}$$

The r.h.s. of equations (8.1.9) and (8.1.10) are the appropriate non-linear longitudinal or transverse components of currents induced by the interacting waves. In both cases the general form of the non-linear dispersion equation is

$$D_\alpha(\omega, \boldsymbol{k}) \widetilde{E}_{\alpha,\omega} = -\mathrm{i}\varepsilon j_{\alpha NL} \tag{8.1.11}$$

with $\alpha = L, T$.

Let us assume that the field is a quasimonochromatic field with slowly varying amplitude $\widetilde{\boldsymbol{E}}_\omega(\boldsymbol{x}, \tau) = \boldsymbol{E}(\boldsymbol{x}) \mathrm{e}^{-\nu t}$ so that we may consider the Taylor expansion of (8.1.11) around the roots of the linear dispersion relation $D_\alpha(\omega, \boldsymbol{k}) = 0$ so that

$$\left[(\omega - \omega_j) \left. \frac{\partial D_\alpha}{\partial \omega} \right|_{\omega_j} + \frac{1}{2} (\omega - \omega_j)^2 \left. \frac{\partial^2 D_\alpha}{\partial \omega^2} \right|_{\omega_j} + \ldots \right] \widetilde{E}_{\alpha,\omega} = -\mathrm{i}\varepsilon j_{\alpha NL}. \tag{8.1.12}$$

On account of the slow time variation of the amplitude we may introduce a slow time derivative operator $\omega - \omega_j = -\mathrm{i}\varepsilon(\partial/\partial t)$ which, to leading order in ε, leads to a system of non-linear evolution equations for the field amplitudes

$$\left[\left. \frac{\partial D_\alpha}{\partial \omega} \right|_{\omega_j} \frac{\partial}{\partial t} - \mathrm{i} \frac{\varepsilon}{2} \left. \frac{\partial^2 D_\alpha}{\partial \omega^2} \right|_{\omega_j} \frac{\partial^2}{\partial t^2} + \ldots \right] \widetilde{E}_{\alpha,\omega} = j_{\alpha NL}. \tag{8.1.13}$$

It is convenient to cast equation (8.1.13) in the form of 'normal mode' equations through a suitable transformation

$$A_{\alpha,\omega} = T(\omega) \widetilde{E}_{\alpha,\omega} \tag{8.1.14}$$

so that to leading order in ε

$$\left[\left. \frac{\partial D_\alpha}{\partial \omega} \right|_{\omega_j} T(\omega) \right] \frac{\partial A_{\alpha,\omega}}{\partial t} = j_{\alpha NL}. \tag{8.1.15}$$

To eliminate all the terms in (8.1.13) with higher-order derivatives on the slow time scale the requirement is that $[(\partial D_\alpha/\partial\omega)|_{\omega_j} T(\omega)] = C$ with C independent of ω. This prescribes $T(\omega) = C((\partial D_\alpha/\partial\omega)|_{\omega_j})^{-1}$ and therefore the normal mode amplitude evolves as

$$\frac{\partial}{\partial t} A_{\alpha,\omega} = C^{-1} j_{\alpha,NL}. \tag{8.1.16}$$

For the case of three interacting waves with matching wavevectors and frequencies, the second order non-linear source terms in the evolution equation (8.1.16) take the form

$$j^{(2)}_{\alpha,NLj} = \sum_{k_i + k_k = k_j} \sigma_{ij} E_i E_k \tag{8.1.17}$$

and the equations for the evolution of the normal mode amplitudes on a time scale much longer than the wave period are of the general form

$$\frac{\partial A_{\alpha,\omega_j}}{\partial t} = \sum_{k_i + k_k = k_j} \frac{\sigma_{ij}}{C \left.\dfrac{\partial D_\alpha}{\partial \omega}\right|_{\omega_i} \left.\dfrac{\partial D_\alpha}{\partial \omega}\right|_{\omega_k}} A_{\alpha,\omega_i} A_{\alpha,\omega_k}. \tag{8.1.18}$$

It is interesting to observe the relation of the normal mode amplitude to the wave energy density

$$A_{\alpha,\omega} E^*_{\alpha,\omega} = \left.\frac{\partial D_\alpha}{\partial \omega}\right|_{\omega} |\widetilde{E}_{\alpha,\omega}|^2 = 8\pi W. \tag{8.1.19}$$

For a system in thermal equilibrium $(\partial D_\alpha / \partial D)|_\omega$ will always be positive. In the case of non-equilibrium, however, the sign of the coupling factor may be reversed. This has a significant influence on the wave interaction, as shall be shown in the next paragraphs.

In the case of a magnetized plasma, the plasma is anisotropic and separation of the wave field in transverse and longitudinal components cannot be done in general, except for special directions of propagation relative to the magnetic field. In this case the general ideas for constructing coupled mode equations should be extended to the matrix form of equation (8.1.7) using diagonalization transformations. However, in practice it is more convenient to address each particular problem with direct *ad hoc* calculations.

8.2 Coupled Mode Equations

The interaction of three (or more) waves can become a strong process only when each wave 'belongs' to the dispersion relation of the medium (plasma) and it is resonant in the sense just described of satisfying a matching relation among frequencies and wave vectors. Here we limit consideration to the case of three waves where the excitation of each one depends on the product of the amplitudes of the other two. The three-wave interaction is sufficiently complex to exhibit features that may occur in more general situations where many waves interact, as in plasma turbulence. On the other hand, for the coupling mechanism it is sufficiently simple from an analytical point of view to allow for exact solutions and for the construction of interesting conservation laws that shed light on the basic physical mechanisms. In the process of developing such analysis, suitable normalization of the amplitudes of the waves is made and the coupling

coefficients turn out to be generally complex, to account for the presence of linear dissipation and growth of the interacting waves.

It can be anticipated that the three-wave interaction can be an unstable process, a simple example of non-linear instability. A necessary condition for this to happen is the availability of free energy in the medium. This is the case, for instance, of a plasma penetrated by an electron beam, in which case the free energy is the kinetic energy of the beam.

Such a combined medium of background plasma and electron beam also has the interesting property that one of the three interacting waves carries *negative* wave energy.

The concept of negative wave energy has a paradoxical meaning except when other waves, that carry positive wave energy, are present simultaneously, which makes positive or null the overall energy content of the system. Since this is, in fact, the case for the other two waves in the three-wave interaction considered, a most extraordinary phenomenon may occur, namely that all the three waves grow in amplitude simultaneously and conserve the total wave energy of the system in the process of growth of the amplitudes. It turns out that the process will be an explosive phenomenon in which all three waves tend to diverge in a finite time.

Other cases of three-wave interaction are not of the explosive type. It has been demonstrated that such cases may, however, lead to other interesting situations. Consider one wave that has a linear growth (i.e. for small amplitudes) and the other two are damped. If the growth rate is much higher than the damping of the other two, *a chaotic* behaviour of the system is caused as result of the competition between the non-linearly coupled waves, and the solution breaks up into numerous new branches and leads to chaotic solutions [8.3, 8.4].

It should be mentioned that the method of coherent wave interaction used here allows for studies of the phase dynamics, which also influences the evolution of amplitudes. It is therefore more detailed than another method, namely the random phase method (taken from solid state physics), where the phases are smeared out according to certain procedures [8.5, 8.6].

Since a unified description of non-linear interactions occurring in different physical situations can be obtained from the same formalism, we forego the details of the derivation of the coupling coefficients referring to the existing vast literature and address the problem of the evolution of the amplitudes $a_0,\ a_1,\ a_2,\ a_j = A_j(t)\,\mathrm{e}^{\mathrm{i}\,\mathrm{Re}(\omega_j)t}$ of the coupled modes written in the rather 'universal' form [8.7–8.10]:

$$\begin{aligned}
&\frac{\mathrm{d}a_0}{\mathrm{d}t} - \mathrm{i}\omega_0 a_0 = c_{12}^* a_1 a_2 \\
&\frac{\mathrm{d}a_1}{\mathrm{d}t} - \mathrm{i}\omega_1 a_1 = c_{02} a_1 a_2^* \\
&\frac{\mathrm{d}a_2}{\mathrm{d}t} - \mathrm{i}\omega_2 a_2 = c_{02} a_0 a_1^*.
\end{aligned} \tag{8.2.1}$$

Once again it is convenient to change notation, introducing new definitions of the mode amplitudes, coupling coefficients and linear damping:

$$A_j = u_j(t)\mathrm{e}^{\mathrm{i}\varphi_j}, \quad c_{ij} = \kappa_{ij}\mathrm{e}^{\mathrm{i}\theta_{ij}}, \quad \nu_j = \mathrm{Im}(\omega_j) \tag{8.2.2}$$

with $u_j = |A_j|$ and $\kappa_{ij} = |c_{ij}|$.

In the new variables, the system of equations for the coupled mode amplitudes in terms of real variables can be instructively related to the mechanism of energy exchange among modes

$$\begin{aligned}
\frac{\mathrm{d}u_0}{\mathrm{d}t} + \nu_0 u_0 &= \kappa_{12} u_1 u_2 \cos(\phi + \theta_{12}) \\
\frac{\mathrm{d}u_1}{\mathrm{d}t} + \nu_1 u_1 &= \kappa_{02} u_0 u_2 \cos(\phi + \theta_{02}) \\
\frac{\mathrm{d}u_2}{\mathrm{d}t} + \nu_2 u_2 &= \kappa_{01} u_0 u_1 \cos(\phi + \theta_{01})
\end{aligned} \tag{8.2.3}$$

and an equation for the evolution of the phase shift $\phi = \phi_0 - \phi_1 - \phi_2 + \Delta\omega t$ between the waves

$$\begin{aligned}
\frac{\mathrm{d}\phi}{\mathrm{d}t} =& \Delta\omega - \kappa_{12}\frac{u_1 u_2}{u_0}\sin(\phi + \theta_{12}) - \kappa_{02}\frac{u_0 u_2}{u_1}\sin(\phi + \theta_{02}) \\
& - \kappa_{01}\frac{u_0 u_1}{u_2}\sin(\phi + \theta_{01}).
\end{aligned} \tag{8.2.4}$$

The quantity $\Delta\omega = \mathrm{Re}(\omega_0) - \mathrm{Re}(\omega_1) - \mathrm{Re}(\omega_2)$ denotes a frequency mismatch between the waves, which is assumed small.

In the dissipation-free limit, the energy should be conserved and the coupling coefficients will be real. This implies that the phase angles θ_{ij} can be put to zero. If the amplitudes u_i are then rescaled to be the absolute values of the ith wave electric field $u_i = |E_i|$, then the wave energy density corresponding to u_i can be written in the form:

$$\langle W_i \rangle = \frac{1}{4}\frac{\partial \mathscr{D}_i}{\partial \omega_i} u_i^2. \tag{8.2.5}$$

From the system, the following relation is obtained for the expression of the total wave power density:

$$\frac{\mathrm{d}W}{\mathrm{d}t} = 2\left\{\kappa_{12}\frac{\partial \mathscr{D}_0}{\partial \omega_0} + \kappa_{02}\frac{\partial \mathscr{D}_1}{\partial \omega_1} + \kappa_{01}\frac{\partial \mathscr{D}_2}{\partial \omega_2}\right\} u_0 u_1 u_2 \cos(\phi). \tag{8.2.6}$$

The condition for conservation of energy is therefore:

$$\kappa_{12}\frac{\partial \mathscr{D}_0}{\partial \omega_0}+\kappa_{02}\frac{\partial \mathscr{D}_1}{\partial \omega_1}+\kappa_{01}\frac{\partial \mathscr{D}_2}{\partial \omega_2}=0. \tag{8.2.7}$$

For longitudinal waves where

$$\frac{\partial D_i}{\partial \omega_i}=\omega_i\frac{\partial \varepsilon_i}{\partial \omega_i}$$

the energy conservation statement is equivalent to the conditions

$$\kappa_{kl}=\mp\frac{c}{(\partial\varepsilon_i/\partial\omega_i)} \quad \text{and} \quad [-\omega_0+\omega_1+\omega_2]c=0. \tag{8.2.8}$$

The discussion of the properties of the solutions of this dynamical system is further simplified with the renormalizations

$$u_0\rightarrow(\kappa_{01}\kappa_{02})^{1/2}u_0, \quad u_1\rightarrow(\kappa_{01}\kappa_{12})^{1/2}u_1, \quad u_2\rightarrow(\kappa_{02}\kappa_{12})^{1/2}u_2. \tag{8.2.9}$$

The transformed set of mode coupling equations with unitary coupling coefficients is now:

$$\begin{aligned}
\frac{\mathrm{d}u_0}{\mathrm{d}t}+v_0u_0&=u_1u_2\cos(\phi+\theta_{12})\\
\frac{\mathrm{d}u_1}{\mathrm{d}t}+v_1u_1&=u_0u_2\cos(\phi+\theta_{02})\\
\frac{\mathrm{d}u_2}{\mathrm{d}t}+v_2u_2&=u_0u_1\cos(\phi+\theta_{01})
\end{aligned} \tag{8.2.10}$$

$$\begin{aligned}
\frac{\mathrm{d}\phi}{\mathrm{d}t}=\Delta\omega&-\frac{u_1u_2}{u_0}\sin(\phi+\theta_{12})-\frac{u_0u_2}{u_1}\sin(\phi+\theta_{02})\\
&-\frac{u_0u_1}{u_2}\sin(\phi+\theta_{01}).
\end{aligned} \tag{8.2.11}$$

It is noticed immediately that the explosive growth can occur only if the nonlinear terms in all the amplitude equations are positive and therefore the amplitudes of all the waves are growing. The condition is then that all the $\cos(\phi+\theta_{kl})$ must be positive which requires all the θ_{kl} to be in the same half of the trigonometric plane. When all the $\phi+\theta_{kl}$ are in the right half plane $\mathrm{d}\phi/\mathrm{d}t\rightarrow 0$ since for diverging amplitudes the dissipate terms v_iu_i and the frequency mismatch $\Delta\omega$ become negligible. The asymptotic form of the solution may be of the form

$$u_j=\frac{f_j(t)}{t_\infty-t} \tag{8.2.12}$$

where $f_j(t)$ is assumed to be varying more slowly than the denominator near the explosion time.

Substituting this ansatz in the rate equations one obtains

$$f_0^2(t_\infty) = [\cos(\phi(t_\infty) + \theta_{02})\cos(\phi(t_\infty) + \theta_{01})]^{-1} \tag{8.2.13}$$

$$f_1^2(t_\infty) = [\cos(\phi(t_\infty) + \theta_{01})\cos(\phi(t_\infty) + \theta_{12})]^{-1} \tag{8.2.14}$$

$$f_2^2(t_\infty) = [\cos(\phi(t_\infty) + \theta_{02})\cos(\phi(t_\infty) + \theta_{12})]^{-1}. \tag{8.2.15}$$

Furthermore, using the latter expressions for $f_j(t)$ in the equation for the phase difference one gets:

$$\tan(\phi(t_\infty) + \theta_{02}) + \tan(\phi(t_\infty) + \theta_{12}) + \tan(\phi(t_\infty) + \theta_{01}) = 0. \tag{8.2.16}$$

The dissipative terms $v_i u_i$ and the frequency mismatch $\Delta\omega$ have the effect of introducing *threshold* values for the initial amplitudes, above which explosion can occur.

The threshold introduced by the terms $v_i u_i$ can be understood as a result of competition of these damping effects with the non-linear driving terms. When the latter dominate amplitude will start growing, more and more unimpeded.

The influence of $\Delta\omega$ is to contribute a secular term $\Delta\omega t$ to ϕ. If in a characteristic time of the interaction this contribution changes the sign of the $\cos(\phi + \theta_{kl})$ terms, one may expect a significant frequency mismatch. The time of explosion can be used to estimate an upper limit to $\Delta\omega$:

$$\Delta\omega \leq \frac{\pi}{t_\infty}\,. \tag{8.2.17}$$

For a dissipation-free medium for which all the $\theta_{kl} = 0, \pi$, the coupled equations take the form

$$\begin{aligned} \frac{\mathrm{d}u_0}{\mathrm{d}t} &= s_{12}u_1u_2\cos(\phi) \\ \frac{\mathrm{d}u_1}{\mathrm{d}t} &= s_{02}u_0u_2\cos(\phi) \\ \frac{\mathrm{d}u_2}{\mathrm{d}t} &= s_{01}u_0u_1\cos(\phi) \end{aligned} \tag{8.2.18}$$

$$\frac{\mathrm{d}\phi}{\mathrm{d}t} = \Delta\omega - \left[s_{12}\frac{u_1u_2}{u_0} + s_{02}\frac{u_0u_2}{u_1} + s_{01}\frac{u_0u_1}{u_2}\right]\sin(\phi) \tag{8.2.19}$$

and the evolution of the system of waves occurs with the constraints of the following constants of motion (Manley–Rowe):

$$\begin{aligned} s_{12}u_0^2 - s_{02}u_1^2 &= M_1 \\ s_{02}u_1^2 - s_{01}u_2^2 &= M_2 \end{aligned} \tag{8.2.20}$$

and

$$u_0 u_1 u_2 \sin(\phi) - \frac{\Delta\omega}{2} u_j^2 = \Gamma. \tag{8.2.21}$$

The signs $s_{ij} = \mathrm{sign}(c_{ij}) = \pm$ for $\theta_{kl} = 0$ or π are decisive for the nature of the solutions.

The case $s_{12} = s_{02} = s_{01}$ corresponds to an explosively unstable case (all amplitudes diverge simultaneously to infinity in a finite time), whereas the case $s_{02} = s_{01} = -s_{12}$ has oscillating behaviour.

The possible role of the explosively unstable case for astrophysical applications, e.g. solar flares, has already been mentioned. The case of three oscillating waves with a periodic mutual exchange of energy has numerous applications, e.g. in laser and ionospheric physics where stimulated Raman and stimulated Brillouin scattering is of considerable interest.

They represent interaction of two transverse electromagnetic waves, one incident and a reflected wave with one longitudinal wave, a plasma wave or ion acoustic wave, respectively. In this connection, computer simulation studies are used to treat situations with laser pulse energies higher than those available at present in the laboratories.

References

[8.1] Akhiezer A I, Akhiezer I A, Polovin R V, Sitenko A G and Stepanov K N 1967 *Collective Oscillations in Plasmas* (Oxford: Pergamon)

[8.2] Oraevskii V N *et al* 1973 The stabilisation of explosive instabilities by non-linear frequency shifts *Phys. Rev. Lett.* **30** 49

[8.3] Ott E 1981 Strange attractors and chaotic motions of dynamic systems *Rev. Mod. Phys.* **53** 655

[8.4] Weiland J and Wilhelmsson H 1983 Transition to chaos for ballooning modes stabilised by finite Larmor radius effects *Phys. Scripta* **28** 217

[8.5] Tsytovich V N 1970a *Nonlinear Effects in Plasmas* (New York: Plenum)

[8.6] Tsytovich V N 1972 *An Introduction to the Theory of Plasma Turbulencee* (Oxford: Pergamon)

[8.7] Wilhelmsson H 1969 Nonlinear coupling of waves in a magnetised plasma with particle drift motions *J. Plasma. Phys.* **3** 215

[8.8] Wilhelmsson H, Stenflo L and Engelmann F 1970 Explosive instabilities in the well defined phase description *J. Math. Phys.* **11** 1738

[8.9] Weiland J and Wilhelmsson H 1977 *Coherent Non-linear Interaction of Waves in Plasmas* (Oxford: Pergamon)
[8.10] Louisell W H 1960 *Coupled Mode and Parametric Electronics* (New York: Wiley)
[8.11] Stix T H 1962 *The Theory of Plasmic Waves* (New York: McGraw Hill)
[8.12] Krall N A and Trivelpiece A W 1973 *Principles of Plasma Physics* (New York: McGraw Hill)

Chapter 9

Non-linear Coupling of Magnetohydrodynamic Resistive Modes

The physics of magnetic confinement devices conceived for thermonuclear fusion experiments (tokamaks, reverse field pinches, stellarators) is an endless source of problems of non-linear dynamics that occur on several widely different time and space scales. On one hand, this fact allows a separation of the problems and therefore more lucid methods of addressing them; on the other hand, however, all the problems occurring on all the time scales have the same importance for the final goal of dominating the fast microscopic processes of a thermonuclear plasma on the practical long time scale of a reliable power plant.

The essential physical model of the plasma confinement process is magnetohydrodynamic, which means that it is concerned with relatively low frequencies and long wavelength phenomena, as compared with electromagnetic ones involving charge separation. Within the general picture of confinement problems, the two foremost questions are realization of steady-state equilibrium conditions and stability.

The significant developments in the performance of tokamaks in the approach of thermonuclear reactor conditions with high-temperature plasma equilibria, lasting potentially many energy replacement times, has stimulated the research of improved reliability of the tokamak discharge, namely conceiving means for controlling the stability of the plasma with respect to the resistive tearing modes that deteriorate the nested isobaric magnetic surfaces configuration into a multiconnected topology. Rotating finite size magnetic islands grow where the magnetic surfaces that have closed field lines are 'torn' resistively by diffusion of helical field perturbations with the same pitch of the equilibrium lines of force. Prevention of sudden collapse (called disruption) of a tokamak current carrying discharge, and limitation of adverse effects on the confinement of plasma thermal energy, depend on the avoidance of formation of such 'islands' by excitation by resonant external 'error' helical fields, and depend also

on the successful control of intrinsic plasma effects such as the neo-classical drive of unfavourable flattening of bootstrap current profiles on surfaces with closed field lines (q-rational surfaces). A relatively vast literature has grown around the subject of the possible feedback control schemes of this type of rather slow growing instabilities, based mostly on a model of response of the physical system obtained systematically in the tokamak and reverse field pinch (RFP) ordering for perturbations of a single helicity. Isolating the problem of a single perturbation is certainly a sound scientific procedure when the goal is to understand the basic mechanism of the complex process of onset of the linear instability first and of its consequent non-linear evolution toward either saturation or explosion. However, other aspects of the dynamics of these modes, related to their mutual interaction or 'coupling', have been treated only sporadically but deserve more attention, both because they are 'unavoidable' and difficult to 'order out' in a realistic problem and because their study might be facilitated by comparison with similar phenomena in other fields. Here, in fact, it is interesting to report just one such example, where a formal link appears to exist with the well-developed subject of coherent wave interaction outlined in the previous paragraphs and well presented in the specialized literature.

9.1 Reconnection and Magnetic Islands

In the large aspect ratio ($R/a \gg 1$) limit of circular cross-section tokamaks, a single helical magnetic field perturbation can be expressed in terms of a magnetic stream function (flux)

$$\delta\vec{B}_{mn} = \nabla \times (\Psi_{mn}\vec{b}_{mn}) = \delta\vec{B}_{mn}(r)\ \mathrm{e}^{\mathrm{i}(m\theta-(n/R)z+\zeta_{mn})} + c.c.$$

where $\vec{b}_{mn}$ is the unit vector along the magnetic field line on a magnetic surface on which field lines have a rational winding number $q = rB_\phi/RB_\vartheta = m/n$ (and are therefore closed). This representation, appropriate to MHD problems with some symmetry (here helical), reduces the partial differential problem for vector fields to one for scalar functions [9.12].

Such a perturbation is associated with a current density perturbation $\mu_0\delta J_{zk} = -\nabla^2_{*k}\psi_k\ \mathrm{e}^{\mathrm{i}(m\theta-(n/R)z+\zeta_k)} + c.c.$ In general, on a rational $q = m/n$ surface (field line) the current continuity equation $\nabla\cdot\vec{J} = 0$ (quasineutrality condition) has a singularity, which indicates the presence of a boundary layer across which the flux function has a discontinuity of its logarithmic derivative (indicated by Δ'), equivalent to the appearance of a surface current, which tears the topology of the nested tokamak equilibrium magnetic surfaces.

Due to resistive diffusion in a narrow layer around the rational surface, the magnetic perturbation reconnects field lines and grows non-linearly as a struc-

ture of finite radial size $W_{mn} = 8(\psi_{mn}/nB_\theta q')^{1/2}$ and periodic in $m\theta - (n/R)^2$. Such a magnetic island of helicity numbers m and n, as it grows, traps more and more plasma increasing its mechanical inertia, and is subject to the electrodynamical and mechanical forces due to external fields and the action of other islands. As a consequence of torques and of dissipation, the magnetic islands rotate and the evolution equations for the width W_{mn} and the angular frequency ω_w derive from the rate of flux reconnection obtained from the Faraday–Ohm law and from momentum balance, in the essential form:

$$\begin{aligned} &\frac{\mathrm{d}W_{mn}}{\mathrm{d}t} = \frac{r_s^2}{\tau_{R,m}} \operatorname{Re} \Delta'_{mn} \\ &\frac{\mathrm{d}}{\mathrm{d}t}(I_{\phi w}\omega_w/n + [C - I_{\phi w}]\omega_\mathrm{p}) = T_{\phi,E.M.,\mathrm{wall}} \end{aligned} \tag{9.1}$$

with $C = I_{\phi w} + I_p = \text{const.}$ as the sum of the toroidal effective moments of inertia of the island and of the rest of the plasma [9.15].

The last equation can be split in two equations, one for the island rotation frequency and another for the plasma bulk rotation frequency ω_p. The viscous torque between the island and the plasma connects these two equations so that through viscosity the total angular momentum balance between plasma and island is maintained.

However, for illustration purposes, it is sufficient to consider the limiting case of islands immersed in a substantially larger and more massive plasma through which relative motion of the islands is made possible by a low viscosity such that, however, $T_{\phi,\mathrm{visc}} \approx 0$.

The driving terms are the real and imaginary part (due to out-of-phase current perturbations) of the logarithmic derivative Δ'_{mn} of ψ_{mn} and the damping is due to (anomalous) perpendicular viscosity $\mu_\perp$. Here we outline an extension of the theory to include the mutual electrodynamic and viscous coupling of a triplet of rotating magnetic islands of different helicities arranged to realize a 'resonant wavenumber matching'. This mechanism of coupling is different from that studied elsewhere, arising from the multiplicity of poloidal harmonics generated by toroidal geometry. For a single mode the tearing parameter is calculated from the 'outer' solution of the quasineutrality condition $\vec{B} \cdot \nabla(\delta J_\parallel/B) \cong 0$, which must hold at all times. From the expression of the perturbed field and current density we have the form

$$\vec{B}_0 \cdot \vec{\nabla}\left(\frac{\delta J_{\parallel k}}{B}\right) + \delta\vec{B}_k \cdot \vec{\nabla}\left(\frac{J_{0\parallel}}{B}\right) = 0 \tag{9.2}$$

where k is a mode label standing for the couple of mode numbers (m, n).

We consider an extension of this equation, in which presently we ignore inertial (polarization) effects, including current and field perturbations due to two other islands with mode labels k' and $k-k'$:

$$\vec{B}_0 \cdot \vec{\nabla}\left(\frac{\delta J_{\|k}}{B}\right) + \delta\vec{B}_k \cdot \vec{\nabla}\left(\frac{J_{0\|}}{B}\right) = -\sum_{k'} \delta\vec{B}_{k'} \cdot \vec{\nabla}\left(\frac{\delta J_{\|k-k'}}{B}\right) + \delta\vec{B}_{k-k'} \cdot \vec{\nabla}\left(\frac{\delta J_{\|k'}}{B}\right). \tag{9.3}$$

Note that, due to the choice of the other two modes, on both sides of this equation we will have phasors $\mathrm{i}(m\theta - (n/R)z)$. Now, for the equations of the (m', n') and $(m-m', n-n')$ modes, the r.h.s. will contain a similar expression, which is a function of the remaining two modes (or more if one considers the summation). Each physical quantity is real and therefore has a phasor and its complex conjugate.

For a triplet of 'wavenumbers' k, k' and q fulfilling a matching condition $q = k - k'$ equation (9.3) yields a system of coupled non-linear equations for the corresponding helical magnetic flux functions Ψ_k.

The coupled mode equations can be written symbolically in operator form as:

$$\begin{cases} \hat{\Lambda}_k \psi_k = Q_k(\psi_{k'}, \psi_{k-k'}) \\ \hat{\Lambda}_{k'} \psi_{k'} = Q_{k'}(\psi_k, \psi_{k-k'}) \\ \hat{\Lambda}_{k-k'} \psi_{k-k'} = Q_{k-k'}(\psi_{k'}, \psi_k) \end{cases} \tag{9.4}$$

with the kth linear differential operator $\hat{\Lambda}_k$ defined as

$$\hat{\Lambda}_k \equiv \left(\frac{\partial}{\partial r} r \frac{\partial}{\partial r} - \frac{m_k^2}{r}\right) - \frac{k_\perp r \mu_0 q \sigma'}{(m_k - n_k q)}$$

with

$$\sigma' \equiv R \frac{\mathrm{d}}{\mathrm{d}r}\left(\frac{J_{0\|}}{B}\right) = \frac{\mathrm{d}}{\mathrm{d}r}\left(\frac{1}{r}\frac{\mathrm{d}}{\mathrm{d}r}\left(\frac{r^2}{q(r)}\right)\right)$$

and the source terms are modelled here as localized current sheets

$$Q_k(\psi_{k'}, \psi_{k-k'}) = \tilde{Q}_k^{k-k'} \frac{\delta(r - r_{k-k'})}{r_{k-k'}} + \tilde{Q}_k^{k'} \frac{\delta(r - r_{k'})}{r_{k'}} \tag{9.5}$$

with the amplitudes $\tilde{Q}_j^i$ depending non-linearly on $\psi_{i \neq j}$.

Then, in principle, a Picard scheme of successive approximations may be used for the system of equations in which the solutions are sought as limit of

sequences $\{\psi_k^n\}$ where the first element ψ_k^0 is the solution of the uncoupled equations and the successive elements are calculated from a recurrence scheme of the type [5.2]:

$$\begin{cases} \hat{\Lambda}_k \psi_k^{(n)} = Q_k(\psi_{k'}^{(n-1)}, \psi_{k-k'}^{(n-1)}) \\ \hat{\Lambda}_{k'} \psi_{k'}^{(n)} = Q_{k'}(\psi_k^{(n-1)}, \psi_{k-k'}^{(n-1)}) \\ \hat{\Lambda}_{k-k'} \psi_{k-k'}^{(n)} = Q_{k-k'}(\psi_k^{(n-1)}, \psi_{k'}^{(n-1)}) \end{cases} \tag{9.6}$$

associated with the boundary conditions. At the first iteration each equation can then be solved using the Lagrangian method of variation of parameters (or an equivalent Green function formulation) where the complete solution has the form:

$$\begin{aligned} \psi_k(r) =& C_{+k} F_{+k}(r) + C_{-k} F_{-k}(r) \theta(r - r_k) \\ &+ \int_0^r \frac{\begin{vmatrix} F_{+k}(\rho) & F_{-k}(\rho) \\ F_{+k}(r) & F_{-k}(r) \end{vmatrix}}{\widehat{W}[F_{+k}(\rho), F_{-k}(\rho)]} Q_k(\rho)\, \mathrm{d}\rho \end{aligned} \tag{9.7}$$

where $\widehat{W}$ is the Wronskian of the basis solutions of the homogeneous equations $\psi_j^0 = C_+ F_{+j}(r) + C_- F_{-j}(r)$.

Imposition of a regularity constraint at $r = 0$ eliminates one constant for $r - r_k < 0$.

The shifting properties of the delta distribution and the imposition of the appropriate continuity and derivative jump conditions at $r = r_{k'}$ and $r = r_{k-k'}$ allow the representation of each $\psi_k(r)$ in terms of 'filamentary current' source terms and of the amplitude of the reconnected flux $\widehat{\psi}_k \equiv \psi_k(r_k)$.

Then the corresponding generalized (complex) tearing stability parameter

$$\Delta'_{\alpha(\beta \neq \alpha \neq 1)} = \Delta'_{\mathrm{mode}_\alpha} + \frac{r_{s1} C_{23}}{r_{s\alpha}} \frac{h_1 h_\beta}{h_\alpha} \frac{W_1^2 W_\beta^2}{W_\alpha^2}\, \mathrm{e}^{\mathrm{i}\Delta\phi(-1)^{\alpha-1}}$$

for each mode can be obtained with $h_\alpha = B r_{s\alpha} q'/16Rq^2$. Here it is sufficient to illustrate the dissipation-free case involving no other sources besides mode coupling.

The system of coupled equations for the width and frequency of each island is then obtained in the suggestive form [9.1]:

$$\frac{\mathrm{d}W_p}{\mathrm{d}t} = \frac{r_{sp}^2}{\tau_{R,m}} \frac{r_{s1} C_{23}}{r_{sp}} \frac{h_r h_q}{h_p} \frac{W_r^2 W_q^2}{W_p^2} \cos \Delta\phi \tag{9.8}$$

$$\frac{\mathrm{d}}{\mathrm{d}t}\left(I_{\phi j} \frac{\omega_{wj}}{n_j^2} \right) = (-1)^{j-1} \left(\frac{2\pi^2 R r_{s1}}{\mu_0} \right) C_{23} h_1 h_2 h_3 W_1^2 W_2^2 W_3^2 \sin \Delta\phi \tag{9.9}$$

where p, q, and r take in turns the values 1, 2, 3. This system of six equations has four constants of motion c_i, $i = 1, \ldots, 4$:

$$\begin{aligned} W_1^5 - \frac{r_{s2}}{r_{s1}}\left(\frac{h_2}{h_1}\right)^2 W_2^5 &= W_1^5(0) - \frac{r_{s2}}{r_{s1}}\left(\frac{h_2}{h_1}\right)^2 W_2^5(0) \equiv c_1 \\ W_3^5 - \frac{r_{s2}}{r_{s3}}\left(\frac{h_2}{h_3}\right)^2 W_2^5 &= W_3^5(0) - \frac{r_{s2}}{r_{s3}}\left(\frac{h_2}{h_3}\right)^2 W_2^5(0) \equiv c_2 \end{aligned} \tag{9.10}$$

$$\begin{aligned} I_{\phi 1}\frac{\omega_{w1}}{n_1^2} + I_{\phi 2}\frac{\omega_{w2}}{n_2^2} &= c_3 \\ I_{\phi 3}\frac{\omega_{w3}}{n_3^2} + I_{\phi 2}\frac{\omega_{w2}}{n_2^2} &= c_4 . \end{aligned} \tag{9.11}$$

Using these constants of motion the evolution of, say, the width and frequency of island W_2 can be written formally in terms of the interaction of one island with an effective 'potential' due to the other two islands in a way similar to a classic treatment of three waves interaction [9.10, 9.14]

$$\left(\frac{\mathrm{d}W_2}{\mathrm{d}t}\right)^2 + \Pi(W_2, \omega_2) = 0 \tag{9.12}$$

where the effective potential

$$\Pi(W_2, \omega_2) = \frac{c_5}{W_2^8}\left[\frac{\mathrm{d}}{\mathrm{d}t}\left(\frac{I_{\phi 2}\omega_2}{n_2^2}\right)\right]^2 - c_6\frac{[W_2^5 - c_7]^{4/5}[W_2^5 - c_8]^{4/5}}{W_2^4} \tag{9.13}$$

depends on the rotational kinetic energy of the island under consideration and on the initial conditions. The additional constants c_{i+4}, $i = 1, \ldots, 4$ are obtained with simple but tedious algebra from the equations (9.8)–(9.11).

For a fixed phase difference between the modes there are no bounded states, and therefore one expects instability for $\pi/2 < |\Delta\phi| \leq \pi$. However, since the equations for the island growth have all the same sign this is a case where there is no possibility of triggering an explosive type of instability. Nevertheless, for all destabilizing $\Delta\phi$, the growth rate of the island triplet is an increasing function of time, going asymptotically to infinite amplitudes. For a stabilising $\Delta\phi$ it is possible to determine from the effective potential the initial conditions, which lead to final vanishing island widths. According with the sign of the roots of the effective potential function one can obtain initial conditions, which leads to one island width vanishing while the others remain finite, or to the vanishing of two islands with the third finite or, asymptotically in time, to the vanishing of all three.

References

[9.1] Coelho R, Lazzaro E, Nave M F and Serra F 1999 Nonlinear coupling of rotating magnetic islands *Phys. Plasmas* **4** 1304

[9.2] Manley J M and Rowe H E 1956 Some general properties of nonlinear elements – part I. General energy relations *Proc. I.E.E.* **44** 904

[9.3] Furth H P *et al* 1973 Tearing mode in the cylindrical tokamak *Phys. Fluids* **16** 1054

[9.4] Hazeltine R D and Meiss I D 1991 *Plasma Confinement* (Redwood City, CA: Addison-Wesley)

[9.5] Hegna C C *et al* 1996 Toroidal coupling of ideal magnetohydrodynamic instabilities in tokamak plasmas *Phys. Plasmas* **3** 584

[9.6] Lazzaro E and Nave M F 1988 Feedback control of rotating resistive modes *Phys. Fluids* **31** 1623

[9.7] Murtaza *et al* 1985 Nonlinear destabilisation of tearing modes *Phys. Fluids* **28** 427

[9.8] Ortolani S and Schnack D D 1993 *Magnetohydrodynamic of Plasma Relaxation* (Singapore: World Scientific)

[9.9] Rutherford P H 1973 Nonlinear growth of the tearing mode *Phys. Fluids* **16** 1903

[9.10] Sitenko A and Malnev V 1995 *Plasma Physics Theory* (London: Chapman and Hall)

[9.11] Spatschek K H 1990 *Theoretische Plasmaphysik* (Stuttgart: Teubner Studienbücher)

[9.12] Strauss H R 1976 Nonlinear three-dimensional magnetohydrodynamics of noncircular tokamaks *Phys. Fluids* **19** 134

[9.13] Tsytovich V N 1970a *Non-linear Effects in Plasmas* (New York: Plenum)

[9.14] Weiland J and Wilhelmsson H 1977 *Coherent Nonlinear Interaction of Waves in Plasmas* (Oxford: Pergamon)

[9.15] Lazzaro E *et al* 2000 Dynamics of tearing modes during strong electron cyclotron heating on the FTU tokamak *Phys. Rev. Lett.* **84** 6038

[9.16] Chang Z *et al* 1995 Observation of nonlinear neoclassical pressure-gradient-driven tearing modes in TFTR *Phys. Rev. Lett.* **74** 4663

Chapter 10

Non-linear Heat Propagation Phenomena

The methods of similarity transformation are well known in the applications to the equation of heat propagation, and the fundamental Fourier solution of the one-dimensional heat equation is a classical example treated in most textbooks [10.15].

Here we consider some less common problems of non-linear heat propagation phenomena appearing in the physics of laser plasma interaction and in the physics of heat transport in the magnetically confined plasmas of thermonuclear fusion experiments.

We consider, for simplicity, a one-dimensional problem for $x > 0$ with the equation of heat propagation in the classical diffusive form:

$$\frac{\partial T}{\partial t} = \frac{\partial}{\partial x}\left[\chi \frac{\partial T}{\partial x}\right] \tag{10.1}$$

associated with boundary conditions on the heat flux:

$$\Phi_0 = -\chi \frac{\partial T}{\partial x}\bigg|_{x=0} = h_0 t^n. \tag{10.2}$$

Here, however, we choose the heat diffusivity as a non-linear function of T of the type

$$\chi = \kappa_0 T^{\alpha}, \quad \kappa_0 = \chi_0 T_0^{-\alpha}. \tag{10.3}$$

For heat conduction in a plasma $\alpha = 5/2$; in the case of turbulent transport and in other cases of radiative transport the values of α are different [10.12].

Phenomena which can be described by positive values of α have a finite heat propagation front. It is instructive to work out in some detail the approach to the solution of this problem with the methods of dimensional analysis and similarity

transformation, which have the double merit of linking together strongly the physical insight of the problem and the mathematical method, leading actually to significant simplifications.

The input quantities of the problem lead to the expectation that the temperature is a function $T = T(h_0, \kappa_0, x, t)$ where the intensity of the incoming heat flux h_0, as can be seen from equation (10.1), has physical dimensions $[h_0] = [t^{-(1+n)}xT]$. According to the Buckingham theorem [10.1], there is a product of powers of the four dimensioned quantities (h_0, κ_0, x, t) that has the physical 'dimensions' of T: $T \propto [h_0^{\mu}\kappa_0^{\nu}x^{\lambda}t^{\kappa}]$ in some definite system of units.

The four exponents are to be determined from the condition $[T] = [xTt^{-(1+n)}]^{\mu}[x^2t^{-1}T^{-\alpha}]^{\nu}[x^{\lambda}t^{\kappa}]$, which leads to *three* equations in *four* unknowns. Therefore, one must be left undetermined. The system of equations for $(\mu, \nu, \kappa, \lambda)$ is therefore

$$\begin{bmatrix} 1 & -\alpha & 0 \\ 1 & 2 & 0 \\ (n+1) & 1 & -1 \end{bmatrix} \cdot \begin{bmatrix} \mu \\ \nu \\ \kappa \end{bmatrix} = \begin{bmatrix} 1 \\ -\lambda \\ 0 \end{bmatrix}. \tag{10.4}$$

The result is

$$\begin{aligned} \mu &= \frac{2}{2+\alpha} - \frac{\alpha}{2+\alpha}\lambda, \quad \nu = -\frac{1}{2+\alpha} - \frac{1}{2+\alpha}\lambda \\ \kappa &= -\frac{1+2n}{2+\alpha} - \frac{1+(1+n)\alpha}{2+\alpha}\lambda. \end{aligned} \tag{10.5}$$

At this point one can write

$$T \propto h_0^{2/(2+\alpha)-(\alpha/(2+\alpha))\lambda}\kappa_0^{1/(2+\alpha)-(1/(2+\alpha))\lambda}x^{\lambda}t^{-(1+2n)/(2+\alpha)-((1+(1+n)\alpha)/(2+\alpha))\lambda} \tag{10.6}$$

that can be rearranged as

$$T \propto \left(\frac{h_0^2 t^{(1+2n)}}{\kappa_0}\right)^{1/(2+\alpha)} \left(\frac{x}{\left(h_0^{\alpha}\kappa_0\right)^{1/(2+\alpha)} t^{(1+(1+n)\alpha)/(2+\alpha)}}\right)^{\lambda}. \tag{10.7}$$

It is remarkable that this has the form predicted by the Buckingham theorem

$$T(x,t) \propto \left(\frac{h_0^2 t^{1+2n}}{\kappa_0}\right)^{1/(2+\alpha)} f(\zeta) \tag{10.8}$$

where one can identify the time-dependent peak amplitude

$$T_0(t) = \left(\frac{h_0^2 t^{1+2n}}{\kappa_0}\right)^{1/(2+\alpha)} = t^n \left(\frac{h_0^2 t^{1-\alpha n}}{\kappa_0}\right)^{1/(2+\alpha)} \tag{10.9}$$

and the *unique* dimensionless variable

$$\zeta = \frac{x}{(h_0^\alpha \kappa_0)^{1/(2+\alpha)} t^{(1+(1+n)\alpha)/(2+\alpha)}} = \frac{x}{(h_0^\alpha \kappa_0)^{1+(2+\alpha)} t^m} \tag{10.10}$$

setting

$$m = \frac{1+(1+n)\alpha}{2+\alpha}.$$

At this point the 'front' of the peak temperature $T_0(t)$ can be identified in general as

$$\xi(t) = Ct^m \tag{10.11}$$

with the constant C to be determined by compatibility conditions. Assuming $T(x,t) = T_0(t)f(\zeta)$ and changing variables from (x,t) to $\zeta = x/Ct^m$ in the heat equation through chain differentiation, the PDE equation

$$\frac{\partial T}{\partial t} = \frac{\partial}{\partial x}\left[\chi \frac{\partial T}{\partial x}\right]$$

for $T(x,t)$ is transformed into a non-linear ODE for $f(\zeta)$:

$$\frac{\kappa_0}{C^2}\left(\frac{h_0^2}{\kappa_0}\right)^{\alpha/(2+\alpha)} \frac{\partial}{\partial \zeta}\left[f^\alpha \frac{\partial f}{\partial \zeta}\right] + m\zeta \frac{\partial f}{\partial \zeta} - pf = 0 \tag{10.12}$$

with the notation $p = (1+2n)/(2+\alpha)$ and $m = (1+\alpha p)/2$, that is identical to

$$m = \frac{1+(1+n)\alpha}{2+\alpha}.$$

For the particular case $m = -p$ that gives $p = -1/(2+\alpha)$, $m = 1/(2+\alpha)$ equation (10.12) becomes:

$$\frac{(2+\alpha)\kappa_0}{C^2}\left(\frac{h_0^2}{\kappa_0}\right)^{\alpha/(2+\alpha)} \frac{\partial}{\partial \zeta}\left[f^\alpha \frac{\partial f}{\partial \zeta}\right] + \frac{\partial \zeta f}{\partial \zeta} = 0. \tag{10.13}$$

Determining C from the relation

$$C^2 = (2+\alpha)\kappa_0 \left(\frac{h_0^2}{\kappa_0}\right)^{\alpha/(2+\alpha)}$$

it is possible to verify that a function of type $f(\zeta) = (1-\zeta^2)^\rho$ with $\rho = 1/\alpha$ satisfies equation (10.13) leading to a solution of the type [10.20]

$$T(x,t) = T_0(t)\left(1 - \frac{x^2}{\xi^2(t)}\right)^{1/\alpha} \tag{10.14}$$

with

$$T_0(t) = \left(\frac{h_0^2}{\kappa_0 t}\right)^{1/(2+\alpha)}.$$

Expression (10.14) has a remarkable resemblance to the 'central expansion' ansatz, which should be interpreted as an extension of the similarity technique applicable when exact solutions cannot be found.

At the beginning, the diffusion time scale tends to zero and soon after it increases drastically. For the same boundary conditions another interesting case is obtained, with the choice $m = 1$, corresponding to $p = 1/\alpha$ and $n = 1/\alpha$.

The equation becomes

$$\frac{\kappa_0}{C^2}\left(\frac{h_0^2}{\kappa_0}\right)^{\alpha/(2+\alpha)} \frac{\partial}{\partial\zeta}\left[f^\alpha \frac{\partial f}{\partial\zeta}\right] + \zeta\frac{\partial f}{\partial\zeta} - \alpha^{-1} f = 0 \tag{10.15}$$

and it can be seen that setting

$$C^2 = \kappa_0 \left(\frac{h_0^2}{\kappa_0}\right)^{\alpha/(2+\alpha)}$$

equation (10.15) can be satisfied by a function of the type $f(\zeta) = (1-\zeta)^{1/\alpha}$, that corresponds a *propagating wave* solution with constant velocity C and amplitude

$$T_0(t) = \left(\frac{h_0^2 t^{(2+\alpha)/\alpha}}{\kappa_0}\right)^{1/(2+\alpha)}$$

$$T(x,t) = T_0(t)\left(1 - \frac{x}{Ct}\right)^{1/\alpha}. \tag{10.16}$$

A result of the same form is obtained also with different boundary conditions for equation (10.1), namely assigning the temperature at $x = 0$

$$T(0,t) = u_0 t^n \tag{10.17}$$

with the same application of the Buckingham theorem one obtains

$$\begin{bmatrix} 1 & -\alpha & 0 \\ 0 & 2 & 0 \\ -n & -1 & 1 \end{bmatrix} \cdot \begin{bmatrix} \mu \\ \nu \\ \kappa \end{bmatrix} = \begin{bmatrix} 1 \\ -\lambda \\ 0 \end{bmatrix}$$

and therefore $T_0(t) = u_0 t^n$, $\zeta = x/Ct^{(1+n\alpha)/2}$. With $n = 1/\alpha$, $m = 1$ and

$$\frac{\kappa_0 u_0^\alpha}{C^2} \frac{\partial}{\partial \zeta} \left[f^\alpha \frac{\partial f}{\partial \zeta} \right] + \zeta \frac{\partial f}{\partial \zeta} - \alpha^{-1} f = 0.$$

Therefore, the solution has the propagating wave structure similar to equation (10.16), with $C^2 = u_0^\alpha \kappa_0 / \alpha$,

$$T(x,t) = u_0 t^n \left(1 - \frac{x}{Ct}\right)^{1/\alpha}$$

for $x < Ct$ and $T(x,t) = 0$ for $x > Ct$ [10.15].

10.1 More on Travelling Wave Solutions of Non-linear Diffusion Equations

It is a remarkable fact, often overlooked, that both linear and non-linear parabolic (e.g. heat diffusion) equations admit classes of *travelling wave* solutions with finite velocity. The basic structure of these solutions is outlined in many books of mathematical physics [10.15] and interesting recent investigations in this field have been carried out by Herrera and coauthors [10.7], from whom we take the following very instructive examples.

Let us consider the one-dimensional non-linear diffusion equation with non-linear source terms:

$$\frac{\partial T}{\partial t} = \chi_0 T_0^{-\delta} \frac{\partial}{\partial x} \left[T^\delta \frac{\partial T}{\partial x} \right] + T^p - \lambda T^k \tag{10.1.1}$$

with $\delta > 0$, $k > p > 0$. The solutions $T = \lambda^{1/(p-k)}$ are stable and there are travelling wavefronts connecting the asymptotic constant states. To identify a travelling phase front, let us consider a particular case with $\delta = 1$, $k = 4$, $p = 2$, $\chi_0 T_0^{-1} = 1$ which admits simple exact solutions.

A propagating wave solution of equation (10.1.1) must be a function $T(z)$ of the argument (phase front label) $z = x - ct$, where c is a phase velocity to be determined. Introducing an auxiliary function $V(z) = \mathrm{d}T/\mathrm{d}z$ equation (10.1.1) is transformed in the non-linear ordinary differential system:

$$\begin{aligned} T' &= V \\ TV' &= -V^2 - cV - T^2 + \lambda T^4 \end{aligned} \tag{10.1.2}$$

where the prime indicates differentiation with respect to z.

The methods of phase plane analysis can be usefully applied to (10.1.2) after the variable transformation,

$$\frac{\mathrm{d}\tau}{\mathrm{d}z} = \frac{1}{T(\tau(z))}$$

valid for $T > 0$.

The system in the new variables has three singular points: the saddle points $(\lambda^{1/(p-k)}, 0)$ and $(0, -c)$ and the degenerate node $(0, 0)$. Orbits in the phase plane, which start at $(\lambda^{1/(p-k)}, 0)$ and decrease to $T = 0$, correspond to travelling wave solutions. If we consider for instance $\lambda = 1$ for a given value of the parameter c, a trajectory starting at (1, 0) can go to the origin, connect the other saddle point $(0, -c)$ or go to $(0, \infty)$, and crossing of the $T = 0$ axis is forbidden. A particularly interesting case is that described by the orbits which go to $(0, -\infty)$. The original system (10.1.2) can be put in the form

$$(TT')' + cT' + T^2 - \lambda T^4 = 0 \tag{10.1.3}$$

and integrated twice with the conditions $|T'| = |V| \to \infty,\ T \to 0$. The solution (with $\lambda = 1$), parametrized by two integration constants a and b is

$$T_\infty(z) = 2az + b \tag{10.1.4}$$

and represents the asymptotic form of solutions with bounded support, decreasing from $T = 1$ to $T = 0$.

A second class of solutions is described by orbits that approach (0, 0). Their asymptotic behaviour is

$$T_\infty(z) = c/(z + d) \tag{10.1.5}$$

and represents decreasing solutions with infinite support.

A third possibility is represented by the orbits which, for special values of c, connect the two saddle points. For these orbits $T \to 0$ asymptotically in τ, with exponential decay. Since the phase front variable is $z = \int_0^\tau T(\zeta)\mathrm{d}\zeta$, it varies only

in the half line $z > 0$, the asymptotic solution $T_\infty(z)$ has bounded support and a sharp front, therefore the solution has a finite support in the variable $z = x - ct$.

The phase space analysis can also be applied to a more general choice of parameters. Consider the general form of (10.1.1)

$$T^\delta T'' + \delta T^{\delta-1} + cT'^2 + T^p - \lambda T^k = 0 \tag{10.1.6}$$

and take $T' = \alpha T^\gamma + \beta T$, with α, β and γ to be determined by substitution in (10.1.6) and inspection of the required balance condition of exponents.

This leads to $k = 2p + \delta - 1$, $\gamma = 1 - \delta$ and the two possible choices $\alpha = 0$ or $\alpha = -c$. The first gives physically uninteresting unbounded solutions, but in the second case the equation for T' has equilibrium points at $(\lambda^{1/(p-k)}, 0)$ and equating equal powers of T one obtains:

$$\alpha = -1/\sqrt{\lambda(p+\delta)} = -c, \quad \beta = \sqrt{\lambda/(p+\delta)}. \tag{10.1.7}$$

Setting $v = -\frac{1}{2}(\delta - p + 1)/(p + \delta - 1)$ and $U = \lambda^{1/(p+\delta-1)}T$ one obtains

$$\frac{\mathrm{d}z}{\mathrm{d}U} = -\sqrt{(p+\delta)}\frac{U^{(\delta-1)}}{1 - U^{(p+\delta-1)}} \tag{10.1.8}$$

and explicit particular solutions can be obtained in terms of elementary functions integrating (10.1.8) for some choice of parameters.

Instructive examples are obtained for $\delta = 1$, that is for a diffusion coefficient linear in T. With $p = 2$ and $k = 4$ one has

$$T(z - ct) = \begin{cases} -\lambda^{-1/2}\tanh(1/\sqrt{3})(x - ct) & x \le ct \\ 0 & x > ct \end{cases}. \tag{10.1.9}$$

When $p = 1$ and $k = 2$,

$$T(z - ct) = \begin{cases} \lambda^{-1}\{1 + \exp[\sqrt{\lambda/2}(x - ct - z_0)]\} & z \le z_0 \\ 0 & z > z_0 \end{cases}. \tag{10.1.10}$$

Other exact solutions with $\delta = 2$ are reported in [10.7] but in the context of heat transport in fusion plasmas an interesting case is given by the parameters $\delta = -1/2$, which is appropriate for the neoclassical cross-field heat diffusion processes in a tokamak, and $k = 1/2$, corresponding to the scaling of bremsstrsahlung losses, and $p = 1$, representing an energy input source scaling linearly with temperature, as it happens e.g. with RF heating. The solution has the form of an inward propagating bell-shaped pulse

$$T(z - ct) = \begin{cases} \lambda^2\left(\dfrac{\exp[\sqrt{\lambda/2}(x - ct - z_0)]}{1 + \exp[\sqrt{\lambda/2}(x - ct - z_0)]}\right)^2 & z \le z_0 \\ 0 & z > z_0 \end{cases}. \tag{10.1.11}$$

This type of solution may also be relevant for the interpretation of recent observation of puzzling heat transport phenomena in tokamaks, which have attracted much attention and stimulated numerous conjectures, some of which are bizarre.

10.2 Fast Heat Pulse Propagation in Hot Plasmas

Experiments show new evidence of ultra-fast propagation of heat pertubations, on time scales much shorter than allowed by known or acceptable diffusion processes ($t_{\text{pulse}} \ll \tau_{\text{Diff}}$) in magnetically confined fusion plasmas. Various attempts to account for the phenomena in terms of heat diffusion equations assuming various heat conductivity models have failed to explain the experimental results.

A pulse dynamic approach based on the mutually depending non-linear evolutions of the amplitude width and drift velocity of the pulse and/or a background gradient fails to describe the fast propagation of the heat disturbance. Furthermore recent experimental observations [10.6, 10.8, 10.10, 10.19] show the striking effect of sign reversal of the propagating pulse, whereby a 'hot' (positive) heat pulse reaches the inner regions of the (tokamak or stellarator) plasma a 'cold' (negative) perturbation!

It is shown here that solutions of propagating type of the heat diffusion equation embodying accepted tokamak transport models may provide a basic framework for interpretation of such observations without violating the causality principle. The travelling solutions have a specific velocity determined by a 'dispersion relation' involving the scale length of the pulse and the thermal diffusivity of the plasma. This type of solution can account for pulse times-of-flight shorter than diffusive times and even for a change of sign of the amplitude. The solutions may therefore be related to the experimental observations of 'non-local heat transport', where heat disturbances generated at the plasma edge (e.g. by pellet injection) are nearly instantaneously observed in the central region with opposite sign [10.10]. In an attempt to reconcile acceptable physics of heat transport to this type of observation, it is convenient to start from fundamental scaling of the heat diffusivity in a tokamak, summarized by the approriate similarity laws [10.3, 10.5] that give the expression for the thermal diffusivity in the form, discussed in chapter 6, equation 6.1:

$$\chi = \frac{T}{B} F(\rho^*, \beta^*, v^*) \tag{10.2.1}$$

where $F(\rho^*, \beta^*, v^*)$ is a function of the dimensionless variables $\rho^* = \rho_i/a \propto T^{1/2}$, $v^* = na/T^2$, $\beta^* = nT/B^2$. This form encompasses different, non-linear scaling of χ with the plasma temperature T and its gradient.

For the purpose of the present example, we conjecture an effective temperature diffusivity of the form:

$$\chi_{\text{eff}} = \chi_\beta (T)^{\delta-\beta} (\nabla T)^\beta \tag{10.2.2}$$

with $\chi_\beta = \chi_0 T_0^{-\delta} L^\beta$, where L is a scale length characterizing the width of the temperature perturbation we are considering, β and δ are appropriate exponents, and χ_0 is the thermal diffusivity for $\beta = 0$. If L is 'large' compared with the plasma minor radius a, the gradient contribution is negligible; otherwise the dependence is closer to a Zhang–Mahajan [10.18] scaling (ZhMa $\beta = 1$, $\delta = 1$). The non-linear form (10.2.2) of the heat conductivity also includes alternative transport models such as those based on radiative collisionality [10.12] where $\chi^{\text{rad}} \propto T^{3/2}/n_e \lambda_D^4$ and appear appropriate to provide a physical mechanism for the pulse propagation anomalies via the externally driven variations of the Debye length

$$\lambda_D = \left(\sum_s \frac{n_s e_s^2}{T_s} \right)^{-1/2}.$$

Considering then a plausible non-linear dependence of χ on temperature and its gradient, the problem is focussed on the properties of a concise one-dimensional form of the non-linear diffusion equation:

$$\frac{\partial T}{\partial t} = (-1)^\beta \chi_0 L^\beta \frac{\partial}{\partial x} \left[T^{\delta-\beta} \left(\frac{\partial T}{\partial x} \right)^\beta \frac{\partial T}{\partial x} \right]. \tag{10.2.3}$$

We focus the analysis on particular propagating solutions of equation (10.2.3) with initial conditions corresponding to a generic small pulse and a mildly inhomogeneous equilibrium background. The geometry of the problem is a one-dimensional plasma slab in the interval $0 \le x \le a$, and $T(x,t) = T_0 - \alpha x + \tilde{T}(x,t)$, where $\tilde{T}(x,t) = A(t,x) G(\xi)$ and $\xi = x - \int^t v(t')\,\mathrm{d}t'$. Assuming a background profile such that $|\alpha x|/T_0 \ll 1$, a power expansion in ξ can be used conveniently to produce a system of equations for the amplitude $A(x,t) \cong \tilde{A}(t) + \alpha A_1(t,x)$ and the width $L(t)$ of the profile of the perturbation. Introducing the expansion for $\tilde{T}$ in equation (10.2.3) with

$$G(\xi) \cong G_0 \left[1 - \frac{\xi^2}{L^2} + \eta_a \frac{\xi^3}{L^3} + \eta_s \frac{\xi^4}{L^4} \right] \tag{10.2.4}$$

and equating equal powers in ξ, one obtains two coupled non-linear ODEs and a non-linear 'dispersion relation' for the velocity of the pulse. The ξ and x dependence is eliminated up to second order in α, with the choice $A(t,x) \cong \tilde{A}(t)[1 + (\alpha x/T_0)(\delta - \beta)]$, obtaining:

$$\frac{\partial \tilde{A}}{\partial t} \cong (-1)^{\beta} T_0^{-\delta} \chi_0 L^{\beta} \left\{ \frac{4\tilde{A}(t)}{L^2} + \alpha \frac{4\tilde{A}^2(t)}{L^2} \frac{(\delta - \beta)}{T_0} - \alpha^2 \frac{(\delta - \beta)}{T_0} \right\} \tag{10.2.5}$$

$$\begin{aligned} \frac{\partial L}{\partial t} = & \frac{3}{2} T_0^{-\beta} \chi_0 \alpha^{\beta} L^{\beta - 1} \\ & \times \left\{ 4(\beta + 1)\eta_s + 2\tilde{A} \frac{(\delta - \beta)}{T_0} [2(1 + \beta)\eta_s + \beta(1 + \beta) + 2] \right. \\ & + 2\tilde{A}^2 \frac{(\delta - \beta)(\delta - \beta - 1)}{T_0^2} [(1 + \beta)\eta_s + \beta(1 + \beta) + 2] \\ & \left. - 3\alpha^2 L^2 \frac{(\delta - \beta)(\delta - \beta - 1)}{T_0^2} \right\} \end{aligned} \tag{10.2.6}$$

$$v = (-1)^{\beta} T_0^{-\beta} \chi_0 L^{\beta} \left\{ \frac{4}{L^2} \left(\frac{\tilde{A} + \tilde{A}^2(\delta - \beta)}{T_0} \right) - 5\alpha \frac{(\delta - \beta)}{T_0} \right\}. \tag{10.2.7}$$

The diffusion equation (10.2.3) can also be integrated directly to obtain particular solutions in integral form ($\alpha = 0$):

$$k(z - z_0) = \int_{y_0}^{y} \frac{\mathrm{d}y}{[y_0^{(\delta+1)/(\beta+1)} - y^{(\delta+1)/(\beta+1)}]^{1/(\beta+1)}} \tag{10.2.8}$$

where:

$$k = \left(\frac{v}{\chi_{\beta}} \right)^{1/(\beta+1)} \left(\frac{\delta + 1}{\beta + 1} \right) \tag{10.2.9}$$

$$T = y^{(\delta+1)/(\beta+1)}, \quad z = x - vt. \tag{10.2.10}$$

Certain explicit solutions are instructive, e.g. for $\beta = 1$ and $\delta = 0$

$$\frac{T}{\tilde{T}|_{z=z_0} + T_0} = \cos^2 \left[\frac{1}{2} \left(\sqrt{|v/\chi_1|}(z - z_0) \right) \right] \tag{10.2.11}$$

where the velocity v and the width of the pulse are related by $v = 4\chi_0/T_0 L$.

The important fact is that the pulse moves, non-diffusively, more rapidly the smaller the width L. With data of Galli *et al* [10.6], and $L \sim 2$ cm, one obtains $v \sim 260$ m/s, in good agreement with experiments which measure 600 μs for transport across $a \sim 0.16$ m with an estimated $\chi_0 \approx 1.3\,\mathrm{m}^2/\mathrm{s}$. Comparing the particular form with the expression for v from the dynamic equations (10.2.5)–(10.2.7) one obtains (for $\alpha \approx 0$) the relation for $\tilde{A}(t)$ which characterizes the particular solution ($\beta = 1,\ \delta = 0$), namely

$$\frac{\tilde{A}}{T_0}\left(\frac{\tilde{A}}{T_0} - 1\right) = 1 \tag{10.2.12}$$

which has two different roots

$$\frac{\tilde{A}}{T_0} = \frac{1 \pm \sqrt{5}}{2}$$

with opposite signs. For $\beta = 1, \delta$ arbitrary, one obtains the more general relation

$$\frac{\tilde{A}}{T_0} = \frac{1}{2(1-\delta)}\left(1 \pm \sqrt{1 + \frac{4(1-\delta)}{(1+\delta)^2}}\right) \tag{10.2.13}$$

showing that two opposite signs are possible. In particular for a resistive ballooning turbulence transport model (with $\delta = 1/2$) one gets one *positive* root $\tilde{A}/T_0 = 2.4$ and one *negative* root $\tilde{A}/T_0 = -0.4$. The transition from a negative amplitude (e.g. at the plasma edge) to a positive one in the center ($x = 0$) can be shown from equations (10.2.5) and (10.2.6), enforcing the dispersion relation (10.2.7) for the case (10.2.10) of the exact pulse, $v(\tilde{A}, L) = 4\chi_0/L$, $\beta = 1$, $\delta = 0$, $\eta_s = 1/3$. One obtains:

$$\frac{\partial \tilde{A}}{\partial t} = \chi_0 L\alpha\left(\frac{4}{L^2} - \frac{\alpha^2}{T_0^2}\right) \geq 0 \tag{10.2.14}$$

for $L\alpha \leq T_0$ and

$$\frac{\partial L}{\partial t} \cong 12 T_0^{-1}\chi_0\alpha\left\{\eta_s - \tilde{A}(1+\eta_a) + (2+\eta_s)\frac{\tilde{A}^2}{T_0^2}\right\} \geq 0. \tag{10.2.15}$$

In figures 10.1 and 10.2 integration of equations (10.2.5) and (10.2.6) with condition (10.2.7) shows that during the wave-like propagation phase with high

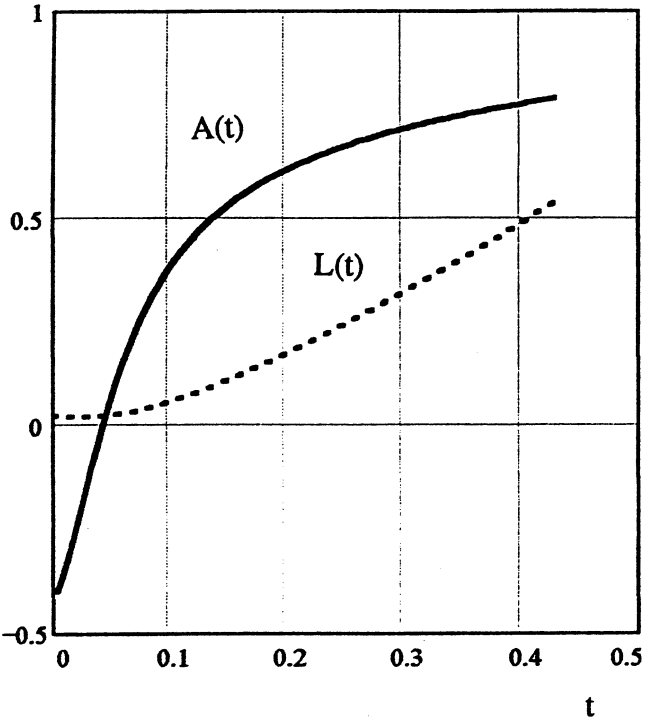

Figure 10.1. Evolution of the amplitude $A(t)$ (full line) and width $L(t)$ (dashed line) of a pulse: $L_0 = 0.025$, $\chi_0 = 0.2$, $\beta = 1$, $\delta = 5/2$, $\eta_a = 0$, $\eta_s = 1/3$, $A(0) = -0.4$, $\mathrm{v}(0) = 10.52$ on a background with $a = 1$, $T_0 = 1$ and $\alpha = 0.3$.

speed v, the width L of the pulse is slowly growing or nearly constant and later it increases significantly entering a diffusive regime (figure 10.1). These preliminary elementary numerical results indicate that the scalings with $\delta > \beta$ exhibit the more dramatic change of sign of the propagating pulses. The simple arguments we have used here and the qualitative behaviour of the examples shown are sufficient to argue that a plausible description of heat transport phenomena appearing as 'non-local response' can be given in terms of excitation of travelling wave solutions, which can have 'flight times' much shorter than the diffusion time. An essential feature of the example presented is that the speed of propagation of the temperature pulse is definitely a property of the pulse shape as it is of the medium. Experiments performed with power pulses (e.g. with electron cyclotron heating (ECH)) with known time and space localization could verify the 'dispersion relation' (10.2.9). The measurement of the propagation speed v of pulses with different space and time localization, complemented by the *expected* scaling of heat diffusivity (with the temperature

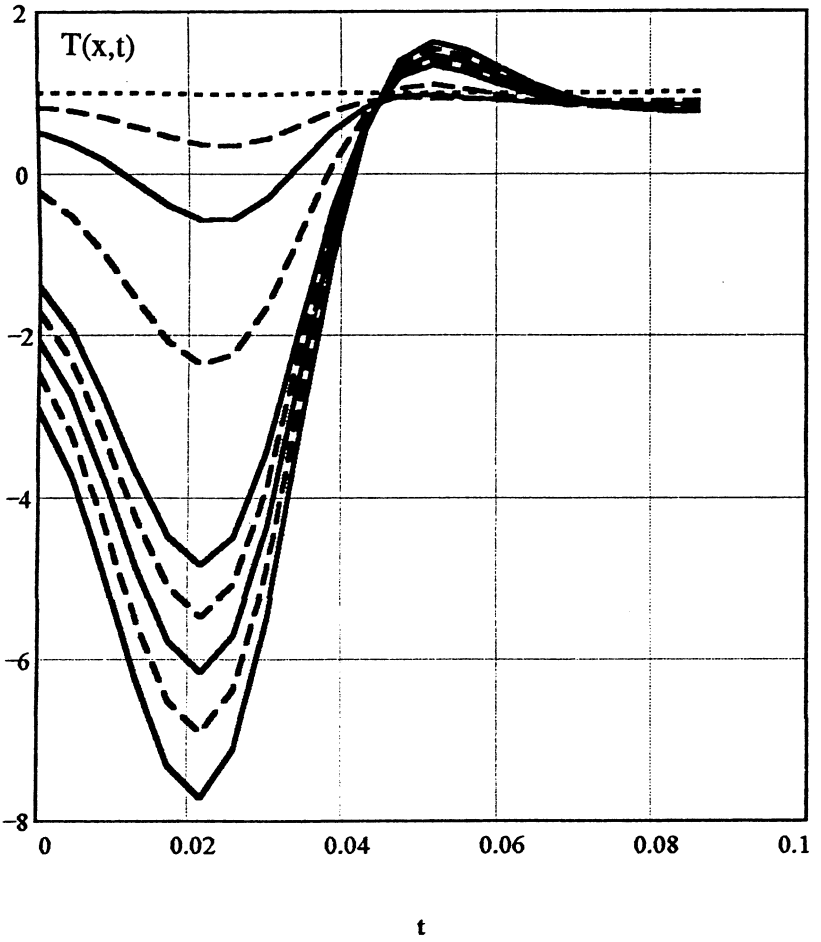

Figure 10.2. Evolution of the $T(x,t)$ profile vs t at nine positions $1 > x > 0$. The change of sign of the propagating temperature perturbation $\tilde{T}(x,t)$ of a pulse with the data of figure 10.1 is apparent.

profile properties), can provide information on the heat transport coefficient. In general, within the scheme of the diffusion equation used here, the inverse problem for pulse propagation should relate the three unknowns (β, δ, χ_0) with three measurable quantities, speed v, amplitude A and width L.

In figure 10.3, an example is shown of the experimental observation of the fast pulse propagation with sign inversion.

The general observed characterics of apparently 'non-local' heat pulse propagation are related to the 'local' non-linear plasma causal response through

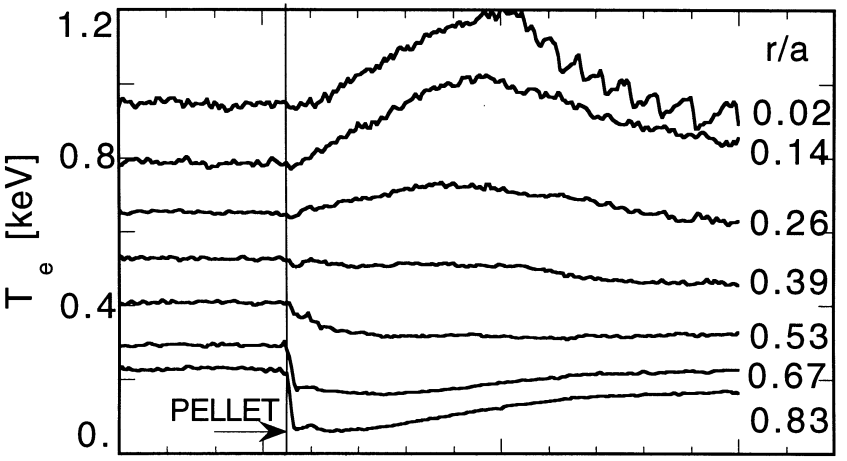

Figure 10.3. Time evolution of an experimental temperature pulse which changes sign. The electron temperature at different radial positions for RTP tokamak discharge R19970224.024 [10.10]. A hydrogen pellet is injected at $t = 0.2054$ s to induce edge cooling in a target Ohmic plasma with safety factor $q(a) = 5.23$, and density $n_e = 1.4 \times 10^{19}$ m^{-3}. (with kind permission of the authors).

mechanisms depending on local temperature and its gradient. The physical origin of non-linearity can be attributed to a variety of phenomena related either to spontaneous turbulence or to externally driven perturbations involving wave-plasma momentum exchange, as suggested recently [10.12]. Further work on this fascinating subject is still required to include realistic physical mechanisms such as convection effects, and the relation with the topology of magnetic confinement configuration.

References

[10.1] Buckingham E 1914 On the physically similar systems – illustrations of the use of dimensional equations *Phys. Rev.* **4** 345

[10.2] Callen J D and Jahns G L 1977 Experimental measurement of electron heat diffusivity in tokamaks *Phys. Rev. Lett.* **9** 491

[10.3] Connor J W and Taylor J B 1977 Scaling laws for plasma confinement *Nucl. Fus.* **17** 1047

[10.4] Coppi B 1988 Profile consistency: global and nonlinear transport *Phys. Lett. A* **128** 183

[10.5] Cordey J G, Balet B, Campbell D, Challis C D, Christiansen J P, Gormezano C, Gowers C, Muir D, Righi E, Saibene G R, Stubberfield P M and Thomsen K

1996 A review of the dimensionless parameter scaling studies *Plasma Phys. Control. Fus.* **38** A67

[10.6] Galli P, Cherubini A, De Angelis R, De Luca F, Erba M, Giannella R, Gorini G, Jacchia A, Häckel J, Mantica P, Parail V V, Porte L and Taroni A 1997 Transient transport studies using laser ablated impurity injection in JET *JET Report JET-P(97)27*

[10.7] Herrera J J E, Minzoni A and Ondarza R 1992 Reaction–diffusion equation in particular solutions and relaxation *Physica D* **57** 249

[10.8] Hogeweij G M D, Chu C C, da Cruz D F, De Luca F, Gorini G, Jacchia A, Lopes Cardozo N J, Mantica P, Oomens A A M, Peeters M, Pijper F J and Polman R W 1996 Evidence of inhomogeneous thermal transport in RTP *Nucl. Fusion* **36** 535

[10.9] Lazzaro E and Wilhelmsson H 1998 Fast heat pulse propagation in hot plasmas *Phys. Plasmas* **8** 2830

[10.10] Mantica P *et al* 1999 Evidence of inhomogeneous thermal transport in RTP *Phys. Rev. Lett.* **82** 5048

[10.11] Minardi E 1996 Model of nonlocal transport in tokamaks *J. Phys. Soc. Jpn* **65** 1891

[10.12] Puri S 1998 Enhanced transport via Kirchhoff *Phys. Plasmas* **8** 2932

[10.13] Rebut P H, Lallia P P and Watkins M L 1988 The critical temperature gradient model of plasma transport: applications to JET and future tokamaks Controlled fusion and plasma physics *Proc. 12th Eur. Conf. (Nice 1988)* Vol 2 (Vienna: IAEA) p 191

[10.14] Romanelli F and Zonca F 1993 The radial structure of the ion-temperature gradient-driven mode *Phys. Fluids B* **5** 4081

[10.15] Tikhonov and Samarskii A A 1977 *Uravnenjie Matematiceskoi Fiziki* (Moscow: Nauka)

[10.16] Weiland J and Nordman H 1993 Drift wave model for inward energy transport in tokamak plasmas *Phys. Fluids B* **5** 1669

[10.17] Wilhelmsson H, Ottaviani M and Le Roux M-N 1998 Propagation and dynamics of heat pulses in hot plasmas *Proc. Int. Workshop on Magnetospheric Plasmas* Altair Souza de Assis and Carlos Augusto Azevedo (eds) (Brasil: XEROX do Brasil Ltda, Rio de Janeiro) March 1998

[10.18] Zhang Y Z and Mahajan S M 1988 Observations on energy transport in tokamaks: a new formula for turbulent transport Comments on plasma *Phys. Contr. Fusion* **11** 243

[10.19] Jacchia A *et al* 1995 Nonlocal diffusivity: impact on transcient and transport studies *Phys. Plasmas* **2** 4589

[10.20] Zeldovich Ya B and Raizer Yu P 1966 Physics of shockwaves and high-temperature hydrodynamic phenomena

Chapter 11

11.1 Concluding Remarks

The material presented in this book covers a wide range of subjects that have in common the fact that they are described by non-linear models of the generic reaction–diffusion type.

It was the purpose of the authors to collect a number of important and not always readily available mathematical problems with their solutions that have unusual properties, and are applicable, with careful choice of the relevant parameters, to model many physical situations, especially in fluid plasmas.

A mathematical procedure (central expansion) related to similarity transformations with varying scale factors and phase space analysis has been suggested for analytical work that provides powerful insight into this field.

Background material has been provided to support the reader in following the mathematical formalization of physical concepts and in providing a link with well-established models of plasma physics.

The main topics addressed in the book concern special solutions of heat and particle transport models in reacting hot plasmas, non-linear electromagnetic wave interaction and special non-linear MHD modes interaction. They all share a possibility of description in terms of 'concentrated' variables. i.e. amplitudes and profile parameters.

The challenge posed by the variety of mechanisms affecting equilibrium and stability of physical systems such as plasmas obviously cannot be met by a single approach, but the description in terms of global quantities of easy interpretation is always of great help in stimulating an inventive approach to new problems.

Glossary and Symbols Used

Notation for reaction–diffusion equations and central expansion treatment

a	coefficient of the heat diffusion term
b	minor radius of the confined plasma in the cylindrical approximation
c	source term coefficient, usually used for heating terms
c	light velocity, chapter 9
e	damping coefficient, usually used for bremsstrahlung losses
p	exponent of the temperature dependence of heat source term
q	exponent of the temperature dependence of heat loss term
s	source term coefficient, usually used for particles
a_n	coefficient of the particles diffusion term
a_T	coefficient of the temperature diffusion term
k_n	coefficient of the particles pinch term
k_T	coefficient of the heat pinch term
T_b	value of temperature at the edge $r = b$
T_0	value of temperature on axis $r = 0$
T_{eq}	value of equilibrium temperature
m_α	mass of particles of species α
n_α	density of particles of species α
n_b	value of density at the edge $r = b$
n_0	value of density on axis $r = 0$
$\boldsymbol{u}_\alpha$	mean (Eulerian) velocity field of fluid of species α
v_{th_α}	thermal velocity particles of species α
P_b	$= 1.57 \times 10^{-38} Z_{\mathrm{eff}} n^2 T^{1/2}$ power density loss by bremsstrahlung radiation
P_{Ohm}	$= 5.23 \times 10^{-5} Z_{\mathrm{eff}} \ln \Lambda T^{-3/2} J^2$ Ohmic heating power in MKS units except T in eV
P_α	$= P_{\mathrm{DT}} = 5.6 \times 10^{-13} n_\mathrm{D} n_\mathrm{T} \langle \sigma v \rangle_{\mathrm{DT}}$ [erg s^{-1}] fusion power density released by D–T reaction $\mathrm{D} + \mathrm{T} \rightarrow \mathrm{He}^4(3.5\ \mathrm{MeV}) + n(14\ \mathrm{MeV})$ with $\langle \sigma v \rangle_{\mathrm{DT}} = 3.68 \times 10^{-12} T^{-2/3} \mathrm{e}^{-19.94 T^{-1/3}}$ [cm^3 s^{-1}] for $T < 25$ keV

D	coefficient of the particles diffusion term
$A(t)$	central value (amplitude) of profile; time varying scaling factor
$L(t)$	width of profile in central expansion formulation $\mathscr{L}^2 = L^2(p-1)$, $\gamma = 0$
γ	$= d - 1$ parameter decribing the space dimensionality of the problem; $d = 1, 2, 3$ in the dimension
κ	coefficient of heat conductivity in coupled T, n equations
α_{r}	recombination coefficient (chapter 3)
β	exponent of the temperature dependence of thermal conduction term
δ	exponent of the density dependence of heating and loss terms
ε_{s}	perturbation in source term
λ_R	natural damping of oscillations of coupled temperature and density
τ_n	thermalization times for injected alpha particles
τ_{T}	$= c_{\mathrm{T}} T^{3/2}/n$ thermalization time of alpha particles
ω_h	natural frequency of oscillations of coupled temperature and density
ω^*	drift frequency
$\rho_{\mathrm{e,i}_\vartheta}$	electron, (ion) poloidal larmor radius
B_T^2	$= b^2(1+\delta)$ rescaled width of temperature channel
B_n^2	$= b^2(1+\kappa)$ rescaled width of density channel
$\ell_{\mathrm{T_c}}^{-2}$	$= 1/L_T^2 + 1/B_T^2$ rescaled characteristic width of temperature profile
$\ell_{n_{\mathrm{c}}}^{-2}$	$= 1/L_n^2 + 1/B_n^2$ rescaled characteristic width of density profile
μ_c	$= 4[a_T \ell_{T_{\mathrm{c}}}^{-2} - k_T \ell_{n_{\mathrm{c}}}^{-2}][1 - (T_b/T_0)^{1+\delta}]$
ν_c	$= 4[a_n \ell_{n_{\mathrm{c}}}^{-2} - k_n \ell_{T_{\mathrm{c}}}^{-2}][1 - (n_b/n_0)^{1+\kappa}]$

Notation for wave coupling equations

$\boldsymbol{B}$	magnetic induction field vector
$\boldsymbol{E}$	electric field vector
$\boldsymbol{J}$	current density vector
$\boldsymbol{k}$	wave propagation vector
c	speed of light
$\bar{\bar{\varepsilon}}(\omega, \boldsymbol{k})$	dielectric dyadic
$\bar{\bar{\mathscr{D}}}(\omega, \boldsymbol{k})$	dispersion dyadic
$\mathscr{D}(\omega, \boldsymbol{k})$	dispersion function
ω	electromagnetic wave frequency
$\gamma(\boldsymbol{k})$	imaginary part (growth rate or damping) of wave frequency
$\boldsymbol{A}_\omega$	normal mode complex amplitude vector
a_i	ith normal mode amplitude
c_{ik}	i–k coupling coefficients
ϕ	phase difference
W	wave energy density

Notation for MHD equations

B_ϕ	toroidal field
B_ϑ	poloidal field
$J_\parallel$	current density component parallel to the magnetic field
R	tori major radius
a	tori minor radius (circular cross section, large R/a)
q	$= rB_\phi/RB_\vartheta$ local magnetic field line winding number (local safety factor)
r_{sm}	minor radius of rational surface where $q = m/n$
$\vec{b}_{mn}$	direction vector of helical magnetic field with pitch m/n
Ψ_{mn}	helical magnetic flux per unit length with pitch m/n
W_{mn}	width of magnetic island of a helical mode m, n
Δ'_{mn}	tearing mode instability parameter for mode m, n

Special Plasma Physics and Thermonuclear Fusion Terminology

Bohm diffusion: a rapid diffusive loss of plasma across magnetic field lines, caused by microinstabilities, with a diffusion coefficient $D_B \propto eT/B$.

Breakeven: the point where the fusion power produced by a reacting plasma balances the input power required to sustain the plasma's high temperature. To produce a net power in a fusion reactor, the 'Lawson criterion' prescribes that a plasma should be constained in steady-state for 1 s at a temperature of $T_e = T_i = 7 \times 10^7$ °C and a density $n_i = 10^{20}$ m^{-3}.

Controlled fusion: a fusion process occurring in a controlled way in a finite (relatively small) volume of high temperature deuterium–tritium or deuterium–deuterium plasma.

Fission: the splitting of a heavy atomic nucleus, such as uranium or plutonium into lighter nuclei, accompanied by the release of a large amount of radiative and kinetic energy of the fission products.

Fusion: the merging of two light atomic nuclei into a heavier nucleus, with a resultant reduction δm of the combined mass, equivalent, according to Einstein relation $\Delta E = \delta mc^2$ to a net release of energy (kinetic) of the fusion products. This process occurs naturally in stars, and in explosive (uncontrolled) fashion in man-made devices used as immensely lethal weapons (hydrogen bomb).

Fusion reactor: a device capable of containing in a finite volume the high-temperature plasma of electrons and nuclei undergoing a series of self-sustaining fusion reactions capable of releasing a net energy output, with a large finite gain (power amplifier mode) or infinite gain (ignited mode).

Gyro–Bohm diffusion: a diffusive mechanism with a diffusion coefficient $D_{\mathrm{gy-B}} \propto (eT/B)(\rho_i/a)$.

H-mode: a regime of operation of tokamaks, particularly if a 'magneic separatrix' boundary is present, attained during high-power auxiliary heating. If the heating power exceeds a threshold, a sudden improvement of the density occurs, and of the stored energy and consequently of the confinement time.

Inertial fusion: jargon for the thermonuclear fusion experiments performed on deuterium–tritium pellets heated by intense laser beams, in which the plasma is confined inertially in a very small finite volume, for a time sufficient to produce sufficient fusion reactions.

L-mode: the normal regime of operation of tokamaks heated Ohmically or with low-power auxiliary heating.

Magnetic fusion: jargon for the thermonuclear fusion experiments performed on plasmas contained in a finite volume by the electrodynamic forces provided by currents and static magnetic field configurations.

Magnetic separatrix: a special isobaric magnetic surface separating closed nested confinement magnetic surfaces from open a region of 'open' field lines. A plasma contained within a magnetic separatrix boundary does not come into contact with any material wall and therefore is generally better insulated thermally.

MHD: magnetohydrodynamics. The branch of physics describing the interaction of low-frequency electrodynamic fields with a continuum conducting medium that can be described as a fluid.

Tokamak: a magnetic confinement device, originally of Soviet design, using a magnetic field resultant of a toroidal and a poloidal component. Lines of force are wound helically on toroidal 'magnetic surfaces' that are isobaric.

Appendix

For the convenience of the reader, we summarize here the basic structure of drift wave theory that appears ubiquitously in magnetized plasma transport problems. In a plasma slab, let the electron and ion densities be represented by a common background and a traveling wave perturbation, associated with an electrostatic perturbation:

$$\begin{aligned} n_{\mathrm{e}}(\boldsymbol{x},t) &= n_0 + \delta n_{\mathrm{e}}\, \mathrm{e}^{\mathrm{i}(\boldsymbol{k}\cdot\boldsymbol{x}-\omega t)} \\ n_{\mathrm{i}}(\boldsymbol{x},t) &= n_0 + \delta n_{\mathrm{i}}\, \mathrm{e}^{\mathrm{i}(\boldsymbol{k}\cdot\boldsymbol{x}-\omega t)} \\ \Phi(\boldsymbol{x},t) &= +\delta\Phi\, \mathrm{e}^{\mathrm{i}(\boldsymbol{k}\cdot\boldsymbol{x}-\omega t)}. \end{aligned} \tag{A.1}$$

The electrons are assumed adiabatic:

$$\delta n_{\mathrm{e}}/n_0 = e\Phi/T_{\mathrm{e}} \tag{A.2}$$

while the ions, carrying the 'mass' of the plasma satisfy a continuity equation:

$$\frac{\partial n_{\mathrm{i}}}{\partial t} + \boldsymbol{v}_{\mathrm{i}}\cdot\nabla n_{\mathrm{i}} = -n_{\mathrm{i}}\nabla\cdot\boldsymbol{v}_{\mathrm{i}} \tag{A.3}$$

and an ion equation of motion:

$$\frac{\partial \boldsymbol{v}_{\mathrm{i}}}{\partial t} = -\frac{e}{m_{\mathrm{i}}}\nabla\Phi + \frac{eB}{m_{\mathrm{i}}c}\boldsymbol{v}_{\mathrm{i}}\times\boldsymbol{b}. \tag{A.4}$$

The latter yields a perpendicular drift velocity

$$\boldsymbol{v}_{\mathrm{i}\perp} = -\mathrm{i}k_y\frac{c\Phi}{B}\boldsymbol{i} + k_y\frac{c\Phi}{B}\frac{\omega}{\omega_{ci}}\boldsymbol{j} \cong -\mathrm{i}k_y\frac{c\Phi}{B}\boldsymbol{i} + O\left(\frac{\omega}{\omega_{\mathrm{ci}}}\right) \tag{A.5}$$

and a parallel streaming velocity:

$$\boldsymbol{b}\cdot\boldsymbol{v} = v_z = \frac{k_\parallel}{\omega}\frac{e\Phi}{m_\mathrm{i}}. \tag{A.6}$$

The above expressions allow the evaluation of the ion velocity compressibility

$$\nabla\cdot\boldsymbol{v}_\mathrm{i} \cong \left[-\mathrm{i}k_y\frac{c\Phi'}{B} + \mathrm{i}k_\parallel\frac{k_\parallel}{\omega}\frac{e\Phi}{m_\mathrm{i}}\right] \tag{A.7}$$

and of the density convection term

$$\boldsymbol{v}_\mathrm{i}\cdot\nabla n = \boldsymbol{v}_\mathrm{i}\cdot\nabla n_0 = -\mathrm{i}k_y\frac{c\Phi}{B}n_0'. \tag{A.8}$$

It is customary and convenient to identify and define the drift frequency:

$$\omega^* = \frac{n_0'}{n_0}\frac{T}{m\omega_\mathrm{c}}k_y \qquad\qquad m_\mathrm{i}\omega_{ci} = m_\mathrm{e}\omega_{ce}.$$

From the steps above, linearizing the ion continuity equation

$$-\mathrm{i}\omega\delta n_\mathrm{i} - \mathrm{i}k_y\frac{c\Phi}{B}n_0' = -n_0\mathrm{i}\left[-k_y\frac{c\Phi'}{B} + k_\parallel\frac{k_\parallel}{\omega}\frac{e\Phi}{m_\mathrm{i}}\right] \tag{A.9}$$

one obtains, with simple algebra, the perturbed ion density

$$\begin{aligned}
\frac{\delta n_\mathrm{i}}{n_0} &= -\frac{k_y}{\omega}\frac{n_0'}{n_0}\frac{e\Phi}{\omega_{ci}m_\mathrm{i}} + \left(\frac{k_\parallel}{\omega}\right)^2\frac{e\Phi}{m_\mathrm{i}} - k_y\frac{c\Phi'}{\omega B} \\
\frac{\delta n_\mathrm{i}}{n_0} &\approx \frac{\omega_\mathrm{e}^*}{\omega}\frac{\delta n_\mathrm{e}}{n_0} + \left(\frac{k_\parallel}{\omega}\right)^2\frac{e\Phi}{m_\mathrm{i}} \\
\frac{\delta n_\mathrm{i}}{n_0} &\approx \left[\frac{\omega_\mathrm{e}^*}{\omega} + \left(\frac{k_\parallel}{\omega}\right)^2\frac{T_\mathrm{e}}{m_\mathrm{i}}\right]\frac{e\Phi}{T_\mathrm{e}}.
\end{aligned} \tag{A.10}$$

Finally imposing the quasineutrality condition

$$\frac{\delta n_\mathrm{i}}{n_0} = \frac{\delta n_\mathrm{e}}{n_0} \tag{A.11}$$

the 'drift waves dispersion relation' is obtained

$$\omega^2 - \omega\omega_\mathrm{e}^* - k_\parallel^2 c_s^2 = 0. \tag{A.12}$$

The ion velocity compressibility and the convective terms appearing in the heat transport equation are then given in terms of the (turbulent) fluctuation of electrostatic potential

$$\nabla \cdot \boldsymbol{v}_{\mathrm{i}} \cong [\omega - \omega_{\mathrm{e}}^{*}] \frac{e\Phi}{T_{\mathrm{e}}} \quad \boldsymbol{v}_{\mathrm{i}} \cdot \nabla n_0 = -\mathrm{i} n_0 \omega_{\mathrm{e}}^{*} \frac{e\Phi}{T_{\mathrm{e}}} \quad \boldsymbol{v}_{\mathrm{i}} \cdot \nabla T \cong -\mathrm{i}\omega^{*} T \eta_{\mathrm{i}} \frac{e\Phi}{T_{\mathrm{e}}}.$$